

**UNIVERSITE DE LA MEDITERRANEE**  
**AIX-MARSEILLE II**

Faculté des Sciences de Luminy  
Ecole Doctorale des Sciences de la Vie et de la Santé

**THESE DE DOCTORAT**  
Pour obtenir le grade de

**DOCTEUR DE L'UNIVERSITE AIX-MARSEILLE II**  
Spécialité : Neurosciences

Présentée et soutenue publiquement par

**Nathalie DEHORTER**

Le 8 novembre 2010

Titre :

**Activités développementales et pathologiques des  
microcircuits GABAergiques du striatum**

Jury :

Pr. André NIEOULLON, président

Pr. James M. TEPPER, rapporteur

Dr. Richard MILES, rapporteur

Dr. Laurent VINAY, examinateur

Dr. Constance HAMMOND, directeur de thèse

*Je dédie cette thèse à ma mère, qui est pour moi un modèle de force morale.*

*Je suis persuadée qu'en science la pugnacité paie toujours!*

## Remerciements

Je souhaiterais en premier lieu exprimer toute ma gratitude aux directeurs de l'INMED, les docteurs Yehezkel Ben-Ari et Alfonso Represa pour m'avoir permis d'intégrer ce laboratoire d'excellence où toutes les conditions furent réunies pour réaliser une recherche de qualité.

Je tiens à remercier très sincèrement le Dr Constance Hammond pour son formidable encadrement de thèse. Dès notre rencontre, j'ai su que j'allais énormément apprendre à vos côtés. Vous êtes non seulement une scientifique de premier ordre qui force l'admiration, mais aussi une femme qui m'a beaucoup touchée par son humanisme, son écoute et son humour ! Pour cela je vous admire énormément. J'ai vraiment eu de la chance de pouvoir travailler avec vous. MERCI MERCI pour ces quatre merveilleuses années à vos côtés. Vous avez toute ma tendresse.

Un grand merci aux membres de l'équipe HAMMOND. Ce projet n'a abouti que grâce au travail d'équipe!

Catherine Lopez, merci pour ton aide précieuse tout au long de cette aventure. J'ai été très heureuse de partager ces années de travail avec toi. François Michel, merci pour tes conseils et tes dépannages de microscope! Diana Ferrari, "la muchacha que linda", thanks for your help and the interesting scientific (or not) discussions. Corinne Brouchoud dite « Boubou », si dynamique et attachante, merci de ton aide dans les manip! Baya Mdzomba dit « Bayou » merci de ta collaboration et merci « Fred » Libersat pour tes nombreux conseils.

Un merci à toute la bande de thésards : Camille Allène, ma première copine du labo, surtout reste comme tu es, petit chat sauvage ; Adriano Cattani, je compte sur toi pour sauver des vies ; Romain Nardou et Thomas Marissal, merci d'avoir été à la fois si amusants et intéressants scientifiquement! Les Minouches (Aurélie et Michel Carabalona-Picardo), notre rencontre dans ce labo a scellé une amitié sincère.

Un grand Merci à toutes les personnes de l'INMED pour leur gentillesse et leur disponibilité, ce fut un réel plaisir de travailler avec vous. Grâce à vous tous, le travail n'en était que plus passionnant !

Papi Alain Ribas et Tahagan Titus, merci pour cette ambiance à l'animalerie !

Merci à Bruno Buisson de NEUROSERVICE et à son équipe pour leur soutien dans ces travaux. Merci également à l'association France Parkinson pour le financement de la dernière année de thèse.

Enfin, merci à mon mari, Foued D. Abbari, qui m'a soutenu dans l'accomplissement de cette thèse. Tu as été, tout au long de ces quatre années un catalyseur, me rappelant sans cesse pourquoi et pour qui je faisais ce métier, et tu as été également un support sur lequel je pouvais compter. Pour tout cela, je te remercie infiniment.

Thanks to Dr James Tepper, Dr Robert Miles, Dr Laurent Vinay and to Pr Nieoullon for accepting to be in my thesis Jury.

## Résumé

Nous avons identifié comment les propriétés fonctionnelles des microcircuits GABAergiques du striatum se mettent en place depuis la période embryonnaire jusqu'à l'adulte, et comment elles sont modifiées dans un modèle adulte pharmacologique (6-hydroxydopamine) ou génétique (PINK1 KO) de la maladie de Parkinson. Les neurones de projection (MSNs) immatures du striatum génèrent une séquence d'activités spontanées : des spikes calciques isolés et des plateaux calciques dans des petites assemblées de neurones connectés par des jonctions gap (E14-P8) puis des bouffées de spikes synchronisées d'origine synaptique (P6-P7). Ensuite les MSNs deviennent silencieux in vitro juste avant l'apparition de la locomotion du fait de l'expression du courant K de la rectification entrante et de la perte de la composante NR2C/D des réponses synaptiques cortico-striatales. Enfin dans les deux modèles murins de Parkinson, les courants synaptiques GABAergiques spontanés des MSNs deviennent géants ou en bouffées du fait du dysfonctionnement d'un seul type d'interneurone GABAergique. Ces résultats montrent l'importance de déterminer l'impact des altérations précoces du système dopaminergique sur le développement des microcircuits GABAergiques du striatum.

## Summary

We investigated how the functional properties of the mouse GABAergic microcircuits of the striatum mature from embryonic to adult stages and how they are altered in a pharmacological (6-OHDA) or genetic (PINK 1 KO) adult model of Parkinson's disease (PD). The dominant population of immature projection neurons, the medium spiny neurons (MSNs) generates a sequence of spontaneous calcium activities: calcium spikes and synchronized gap junction-driven calcium plateaus (E14-P8) followed by synapse-driven synchronized calcium spikes (P6-P7). Then they become silent in vitro (P8-P10) just before the onset of locomotion (P10-P12), because of the parallel expression of the  $K^+$  rectifying current and loss of the NR2C/D component of NMDA receptor-mediated cortico-striatal responses. In addition, we show that the tonic low frequency, spontaneous GABAergic activity of MSNs switches to a gigantic or bursting pattern in both PD models. This switch is due to only one subtype of GABAergic interneuron which entrains the striatal microcircuits in abnormal GABAergic oversynchrony. This study reflects the need for developmental investigations on the impact of early alteration of the dopaminergic system on striatal GABAergic microcircuits.

<b>ABBREVIATIONS</b> .....	<b>12</b>
<b>PREAMBLE</b> .....	<b>16</b>
<b>CHAPTER 1. HOW DOES THE STRIATAL NETWORK BUILD UP DURING DEVELOPMENT?</b> .....	<b>24</b>
1. Striatal neurons originate and migrate from the ganglionic eminences and the preoptic area .....	24
1.1. The fated-projection neurons and the fated-interneurons of the striatum have different temporal and spatial origins. ....	24
1.2. Neurons migrate to the developing striatum in response to intrinsic and extrinsic cues. ....	28
1.2.1. The fated-projection neurons migrate from the LGE to the striatal “anlage” .....	28
1.2.2. GABAergic interneurons of the cortex and the striatum both originate from the MGE: how does the segregation between these two populations occur? .....	34
2. The synaptogenesis in the striatal network follows a sequence.....	40
2.1. Electrical synapses are the first connections present in the developing striatum.....	40
2.2. Feedforward and feedback GABAergic synapses develop sequentially .....	42
2.3. Cholinergic interneurons are early-born neurons that establish synapses with all striatal neuronal types .....	46
2.4. NMDA and non-NMDA receptors-mediated glutamatergic responses do not show the same developmental profile .....	48
2.5. Dopaminergic nigrostriatal projections are present early during development and mature in two waves, one prenatal and one postnatal. ....	54
3. The development of the striatal output is sequential .....	60
<b>Conclusion of chapter 1</b> .....	<b>64</b>
<b>CHAPTER 2. DEVELOPMENTAL ACTIVITIES OF THE GABAERGIC MICROCIRCUITS OF THE STRIATUM</b> .....	<b>66</b>
1. The developing striatal network first generates isolated or gap-junction mediated calcium events at perinatal stages. ....	66
2. The developing striatal network then displays synaptically-driven events at the end of the first postnatal week. ....	68
3. Maturation of the intrinsic membrane properties of the output neurons of the striatum coincides with the disappearance of immature activities. ....	72
<b>Conclusion of chapter 2</b> .....	<b>76</b>
<b>CHAPTER3: IS THERE A FUNCTIONAL SIGNATURE OF PARKINSON’S DISEASE IN THE ADULT STRIATUM?</b> .....	<b>80</b>
1. The animal models of Parkinson’s disease are of two types: pharmacological and genetic. ....	82
1.1. The pharmacological models of Parkinson’s disease are based on the selective killing of central dopaminergic neurons .....	82

1.1.1. The 6-OHDA rodent model allows studying the adult, dopamine-depleted basal ganglia.	84
1.1.2. The chronic MPTP primate model allows studying the presymptomatic phases of the disease	84
1.2. Genetic animal models of Parkinson’s disease show dopaminergic impairments and motor symptoms at old ages.....	86
1.2.1. Alpha-synuclein transgenic mouse models may help to understand molecular mechanisms of early and late stages of PD.	86
1.2.2. The PINK1 mice model is suitable for the study of the earliest changes that might occur in Parkinson’s disease.	90
2. The striatal network is altered by chronic dopamine depletion.....	92
2.1. The morphological characteristics of striatal neurons change in the chronic absence of dopamine.....	92
2.2. The glutamatergic cortico-striatal synapses become overactive in the absence of dopamine. ....	94
2.3. The GABAergic synaptic activity afferent to MSNs is increased and synchronized in the absence of dopamine.....	96
<b>Conclusion of chapter 3.....</b>	<b>100</b>
<b>ARTICLE 1.....</b>	<b>104</b>
<b>ARTICLE 2.....</b>	<b>158</b>
<b>DISCUSSION.....</b>	<b>174</b>
1. What is the origin and functional significance of the immature activities in the striatum?.....	176
1.1. Functional role of the intrinsic and synaptic immature activities in the developing striatum.....	176
1.2. What is the origin of the synchronous synapse-driven events of the striatum?.....	178
2. What are the mechanisms underlying the silencing of the striatal network? ...	182
3. What are the functional roles of the GABAergic interneurons during development and in adult parkinsonian state?.....	184
4. Are the adult pathological oscillations similar as the immature synchronous activities of the developing striatum? .....	186
<b>Conclusion.....</b>	<b>190</b>
<b>REFERENCES.....</b>	<b>194</b>

## Figures Table

Figure 1: The Basal Ganglia are a set of interconnected subcortical nuclei. The striatum represents the input nucleus of the basal ganglia.....	15
<b>Figure 2:</b> The adult striatal network consists of GABAergic microcircuits.....	17
Figure 3: Selection of motor program is under the control of the striatum. ....	19
Figure 4: Development of the rodent striatum: the fated-striatal neurons originate in and migrate from the ganglionic eminences. ....	25
Figure 5: Dlx1-2 genes regulate the migration of late-born striatal precursors of MSNs from the LGE to the striatum.....	29
Figure 6: Striatal compartmentalization of MSNs is regulated by repulsive guidance cues. ....	31
Figure 7: The final destination of the MGE sorting-interneurons is under the control of several molecules.....	33
<b>Figure 8:</b> The specification of the GABAergic and cholinergic striatal interneurons is regulated by Nkx2.1, Lhx6 and Lhx7.....	35
<b>Figure 9:</b> MSNs are preferentially organized in clusters at perinatal stages. ....	39
Figure 10: Tyrosine hydroxylase-positive fibres invade the striatum at E17-19 in the rat and E13-16 in the mouse. ....	55
<b>Figure 11:</b> Birth dating of neurogenesis and synaptogenesis in the rat developing striatum.....	63
Figure 12: 6-OHDA and MPTP toxicity lead to the dopaminergic cell death. ....	83
Figure 13: 6-OHDA intrastriatal injection leads to a progressive deprivation of the dopaminergic afferences in the striatum.....	83
Figure 14: Mutations in the $\alpha$ -synuclein and PINK1 genes induce the pathogenesis of Parkinson' disease. ....	87
Figure 15: PINK1 KO mouse is a suitable model for the pre-symptomatic phase of PD. ....	89
Figure 16: Dopamine depletion induces a reduction in spine density in the D2 but not D1 receptor-expressing MSNs.....	91
Figure 17: Synaptic reorganization between interneurons and projections neurons follows the striatal dopamine denervation. ....	93
Figure 18: Dopamine depletion impairs the cortico-striatal pathway. ....	95
Figure 19: Bursting pattern of the spontaneous GABAergic currents is found in 40-50 % of the 6-OHDA and PINK1 KO MSNs. ....	97
<b>Figure 20:</b> Spontaneous postsynaptic GABAergic currents represent a new electrophysiological signature of Parkinson state in the striatum.....	185

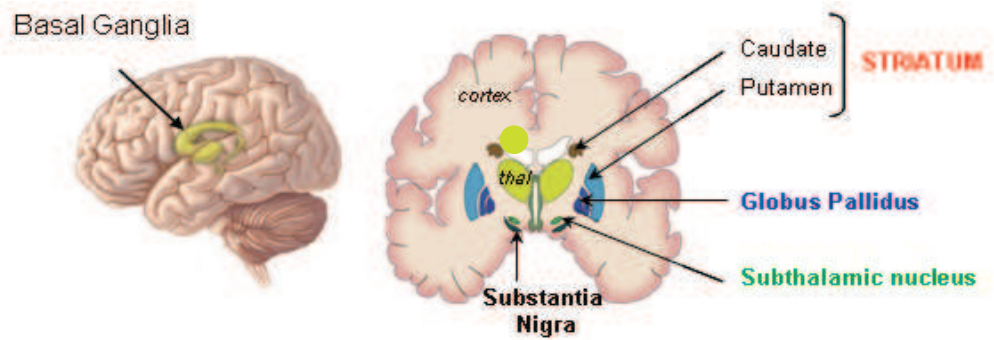
# ABBREVIATIONS

**ACh:** Acetylcholine  
**AEP:** Anterior Entopeduncular Area  
**AMPA:**  $\alpha$ -Amino-3-hydroxy-5-Methylisoxazol-4-Propionic Acid  
**AP-V:** 2-Amino-5-PhosphonoValeric acid  
**CGE:** Caudal Ganglionic Eminence  
**ChAT:** Acetylcholine Transferase  
**CR:** Calretinin, Calcium-binding protein  
**Cx:** Connexin  
**DA:** Dopamine  
**DAT:** Dopamine Transporter  
**DCC:** receptor for Netrin-1  
**Dlx:** Distal-less gene  
**D1, D2:** Dopamine receptor type 1/2  
**EGFP:** Enhanced Green Fluorescent Protein  
**ENK:** Enkephalin  
**EPSC/P:** Excitatory PostSynaptic Current/Potential  
**EX:** Embryonic Day X  
**FS:** Fast Spiking interneurons  
**GABA:** Gamma-Amino Butyric Acid  
**GP:** Globus Pallidus  
**GDP:** Giant Depolarization Potential.  
**GFP:** Green Fluorescent Protein  
**IPSC/P:** Inhibitory PostSynaptic Current/ Potential  
**KA:** Kainic Acid; principal agonist of the glutamate receptor type kainate.  
**KIR:** Potassium Inward Rectifier  
**KO:** Knock-Out  
**LB:** Lewy Bodies  
**LGE:** Lateral Ganglionic Eminence  
**Lhx6/7:** LIM/homeobox protein Lhx6/7 is a protein that in humans is encoded by the LHX6 gene  
**LTS:** Low threshold Spike Interneurons  
**MGE:** Median Ganglionic Eminence  
**MSN:** Medium Spiny Neurons  
**MPP+:** 1-methyl-4-phenylpyridinium  
**MPTP:** 1-methyl-4-phenyl-1,2,3,6-tetrahydropyridine  
**Nkx2.1:** NK2 homeobox 1 (NKX2-1), also known as thyroid transcription factor 1 (TTF-1)  
**NMDA:** N-Methyl-D-Aspartate

**NPY:** Neuropeptide Y  
**NR2C/D:** subunits of the NMDA receptor  
**Nrp:** Neuropilin, receptor for semaphorin  
**6-OHDA:** 6-Hydroxydopamine, enzyme involved in the DA synthesis  
**PX:** Postnatal Day X  
**PINK1:** PTEN-induced kinase 1- associated with Park6 gene  
**POA:** Preoptic Area  
**PD:** Parkinson's Disease  
**PV:** Parvalbumin, calcium-binding protein  
**SNCA:** gene coding for the  $\alpha$ -synuclein protein  
**SNc:** Substantia Nigra pars compacta  
**SNr:** Substantia Nigra pars reticulata  
**SPA:** Small Plateau Assemblies  
**SST:** Somatostatin, calcium-binding protein  
**STN:** Subthalamic nucleus  
**SVZ:** Subventricular Zone  
**TAN:** Tonically Active Neurons  
**TH:** Tyrosine Hydroxylase, enzyme interceding in the dopamine synthesis  
**TTX:** TetrodoToXin  
**VZ:** Ventricular Zone  
**WT:** Wild Type

# **PREAMBLE**

A



B

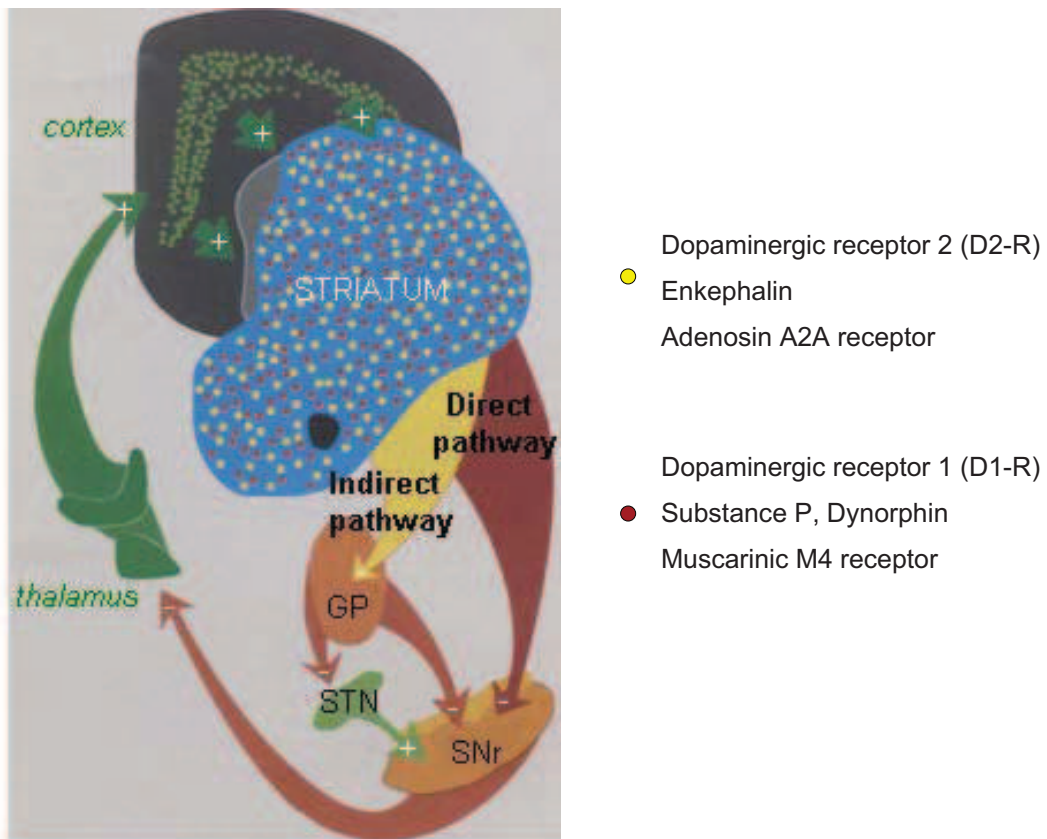


**Figure 1:** The Basal Ganglia are a set of interconnected subcortical nuclei. The striatum represents the input nucleus of the basal ganglia.

**A.** Left, The basal ganglia (BG) are located deep within the cerebral hemispheres in the telencephalon region of the human brain. Right, schematic representation of a coronal section. The BG comprises five interconnected nuclei. *Image Credit: www.pdrhealth.com and www.dana.org (Ellen Davey).*

**B.** The direct and indirect pathways. The rodent striatopallidal (indirect, yellow) and striatonigral (direct, red) projections from the striatum receive excitatory inputs from the cortex (+) and provide inhibitory inputs (-) to the globus pallidus and the substantia nigra, respectively. *Modified from Gerfen, 1992.*

## PREAMBLE

The basal ganglia (BG) consist of five subcortical nuclei, namely the striatum (caudate nucleus and putamen in primates), the globus pallidus (GP, external and internal), the subthalamic nucleus (STN) and the substantia nigra (pars compacta, SNc and pars reticulata, SNr) (fig. 1A). The largest input station of the basal ganglia, the striatum, collects inputs from the entire cortex and sends processed information to the other BG, namely GP and SN. The striatum also receives inputs from the medial thalamus (centromedian and parafascicular nucleus) and from the amygdala. BG are included in a cortico-subcortical loop since the two main output structures of the BG (GPi and SNr) project back to the cortex via the thalamus (and to a lesser extent to the brainstem) (fig. 1B). To process cortical information, the striatum needs two modulators, acetylcholine (ACh) and dopamine (DA) released by local cholinergic interneurons and afferences from the SNc, respectively.

One of the characteristics of the striatum is the absence of intrinsic glutamatergic neurons. Around 98% of the striatal cells are GABAergic, including a large population of principal projection neurons (95%) and a small interneuron population (3%), the remaining 2% are cholinergic. These neurons differ by their morphology, electrophysiological properties, and neurochemical content (Kreitzer 2009). The GABAergic output neurons of the striatum, the so-called Medium Spiny Neurons (MSNs) further divide into two subtypes, on the basis of which types of dopaminergic receptors (D) they express and their target nuclei (Gerfen et al., 1990; For review, Smith et al., 2008) (Fig. 1). The D1 receptor/ substance P/ Dynorphin/ muscarinic M4 receptor expressing MSNs send projections to SNr and GPi (the direct pathway) whereas the D2 receptor/enkephalin/ Adenosin A2A receptor expressing MSNs send projections to GPe (the indirect pathway). This segregation between the direct and indirect pathways is not absolute since some neurons from the direct pathway also send axon collaterals to GPe (Kawaguchi et al., 1990). In addition, single-cell RT-PCR studies have revealed that some MSNs express both D1 and D2 receptors and contain SP together with ENKs (Surmeier et al., 1996). But recent optogenetic studies clearly confirmed the D1/D2 MSNs segregation at least in rodents (Kravitz et al., 2010).

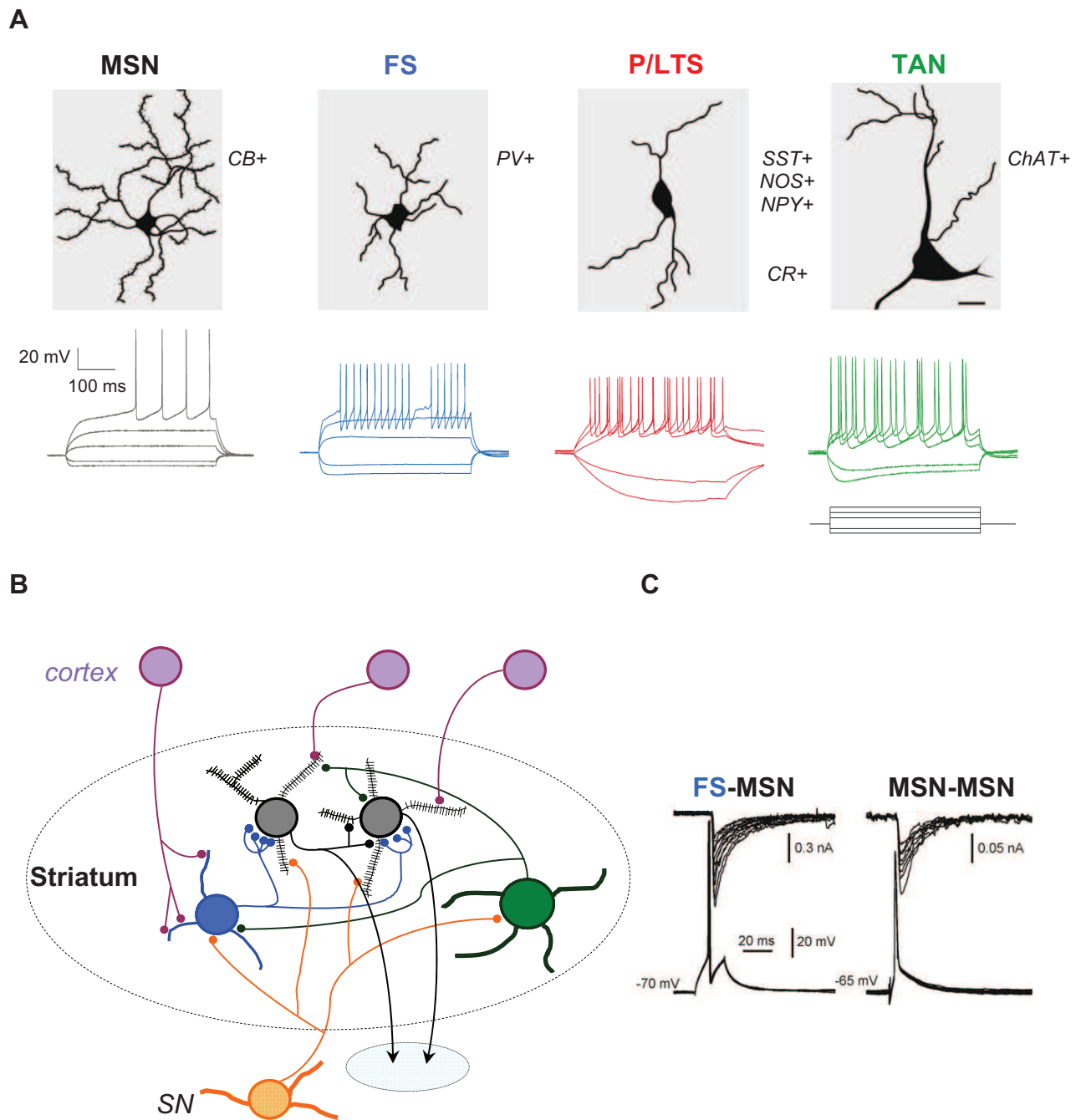


**Figure 2:** The adult striatal network consists of GABAergic microcircuits.

**A.** Top: Morphological characteristics of the adult striatal neurons. Projection neurons of the striatum are Medium Spiny Neurons (MSN) whereas interneurons are aspiny (FS, LTS, TAN). Bottom: Whole-cell current-clamp recordings in vitro showing firing properties of the adult MSN (black), GABAergic interneurons FS and P/LTS (blue and red) and cholinergic interneurons (green). FS: Fast Spiking; P/LTS: Persistent/ Low Threshold Spiking; TAN: Tonic Active Neurons.

**B.** Connections between the different neurons in A that form the microcircuits of the striatum. In grey: MSNs; blue: GABAergic interneurons; green: cholinergic interneurons; purple: cortico-striatal neurons; orange: nigrostriatal dopaminergic neurons.

**C.** Feedforward (FS-MSN) and feedback (MSN-MSN) inhibitions control the MSN response (top traces).

*Modified from Kreitzer, 2009; Tepper and Bolam, 2004; For review, Tepper et al., 2008.*

MSNs are characterized by their high spine density, low input resistance, strong inward rectification, negative resting potential, and long delay to initial spiking (For review, Kreitzer, 2009) (Fig. 2A). GABAergic interneurons are classified according to their neurochemical content (Tepper and Bolam 2004), their electrophysiological and morphological features: (1) GABAergic parvalbumin-expressing interneurons (PV), are fast-spiking (FS) neurons with a characteristic rapid firing pattern and low input resistance; they receive massive cortical innervation (Ramanathan et al 2002) and represent 1.5% of the striatal cells. (2) GABAergic somatostatin (SST), nitric oxide (NO), neuropeptide Y (NPY) expressing-interneurons are persistent low-threshold-spiking (P/LTS) neurons and calretinin (CR) expressing-interneurons which electrophysiological properties have not yet been precisely described. They are characterized by a high input resistance and a sustained plateau potential that persists after the end of current injections. LTS interneurons also display rebound spiking following hyperpolarizations (Kawaguchi et al., 1995; For review, Kawaguchi, 1997). The remaining 2-3% of the cells are the cholinergic interneurons, characterized by a large cell body, a tonic activity in vitro and in vivo (Tonically Active Neurons, TANs), a prominent hyperpolarization-activated current, broad spikes with long after spike hyperpolarization and dense local axonal arborization (Zhou et al., 2002; Bennett and Wilson 1999; Bennett et al., 2000).

GABAergic microcircuits of the striatum consist of powerful GABAergic connections that regulate the synaptic strength of afferent glutamatergic corticostriatal synaptic inputs with high level precision (For review Plenz, 2003). Feedforward and feedback inhibitions function together to precisely control spike timing in MSNs in response to cortical activation. Feedforward inhibition is achieved by FS and LTS interneurons (Koos and Tepper 1999; Tepper et al. 2004, 2008), with each interneuron making synapses with hundreds of MSNs (Fig. 2B, C). Feedback inhibition is exerted by the recurrent collaterals from MSNs to MSNs (Fig. 2B, C). Although such recurrent collaterals bear more synapses than the feedforward circuit, this inhibitory control is much less effective (Fig. 2C, right compared to left), probably due to a more distal synaptic location and a small number of release sites (For review, Wilson, 2007). Only when MSNs generate bursts of action potentials would lateral inhibition become efficient (For review Plenz, 2003).

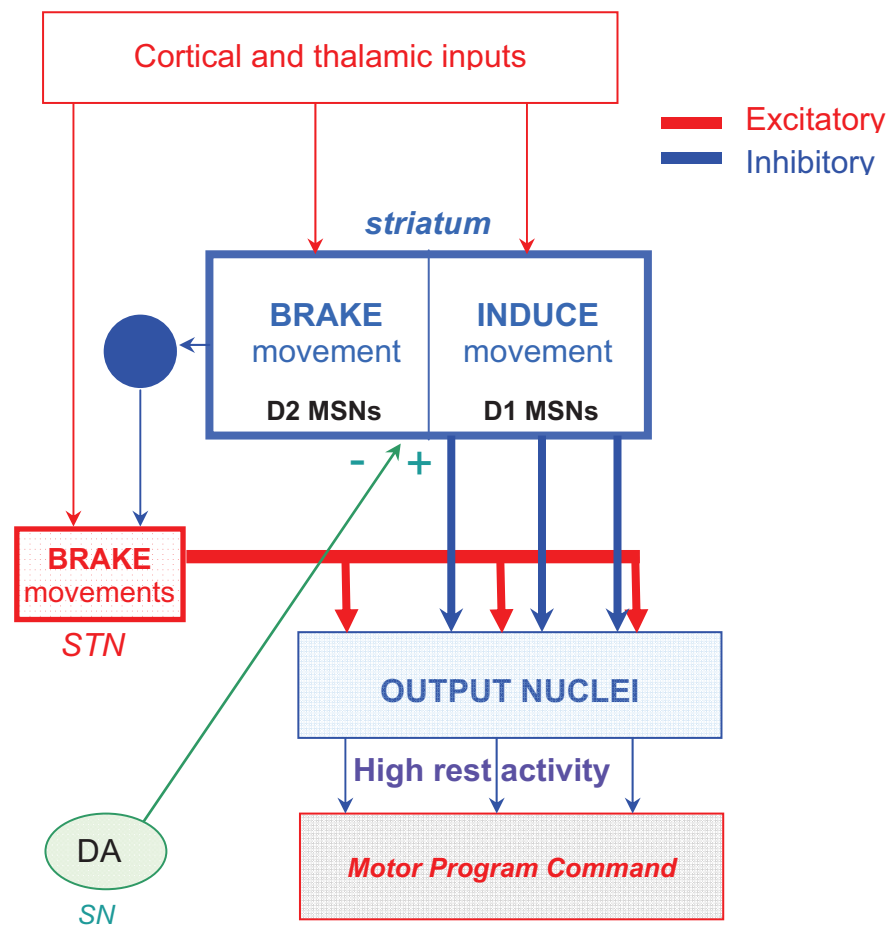


**Figure 3:** Selection of motor program is under the control of the striatum.

Dopamine (DA) acts on the “direct” and “indirect” pathways via subsets of D1 and D2 receptors-expressing MSNs. DA has a repressing effect on the striatopallidal MSNs (-) and a facilitating one in the striatonigral MSNs (+). Under resting conditions, the output nuclei (GP, SNr) project to several motor programs and prevent them being active. If a subgroup of striatal neurons is activated, it provides strong inhibition to pallidal neurons (output nuclei), which have high resting activity and thereby disinhibits target neurons in a motor centre. When the D2 striatal neurons are activated, they inhibit the GP (blue circle) which excites the STN, “hyperdirect” pathway and striatonigral pathway).

From Grillner et al., 2005.

The striatum participates in various motor control tasks such as motor planning, motor sequencing and motor learning of automatized voluntary movements (Fig. 3). It also participates in motor tasks involving motivational, cognitive and emotional drive (For review, Tisch et al 2004; Graybiel et al., 1994). Basal Ganglia are primarily involved in the selection of several possible behaviors to execute at any given time. BG exert an inhibitory influence on thalamo-cortical motor systems, and the release of this inhibition allows the motor system to become active. In pathological conditions, the striatum is involved in several movement disorders, like choreas (e.g Huntington's disease), dyskinesias and Parkinson's disease (For review, Crossman, 2000). Parkinson's disease is characterized by the inability to initiate desired movements (akinesia) and the slowness of movement execution (bradykinesia). This motor disorder results from the degeneration of the dopaminergic neurons of the SNc.

This manuscript describes the development of the GABAergic microcircuits of the striatum and their alteration in adulthood. Understanding how the striatum builds up during development is instrumental to better appreciate how it is altered in adulthood. This information is useful for investigations aiming at understanding whether early genetic or environmental insults alter the developmental sequence and lead to long term deleterious sequels. The introduction is divided in three chapters: the first one describes the early phases of striatal development (neurogenesis, migration); the second concerns the developmental activities of GABAergic microcircuits; the third and last chapter discusses how the activity of adult striatal GABAergic microcircuits is altered in different models of Parkinson's Disease.

# INTRODUCTION

# **CHAPTER 1. How does the striatal network build up during development?**

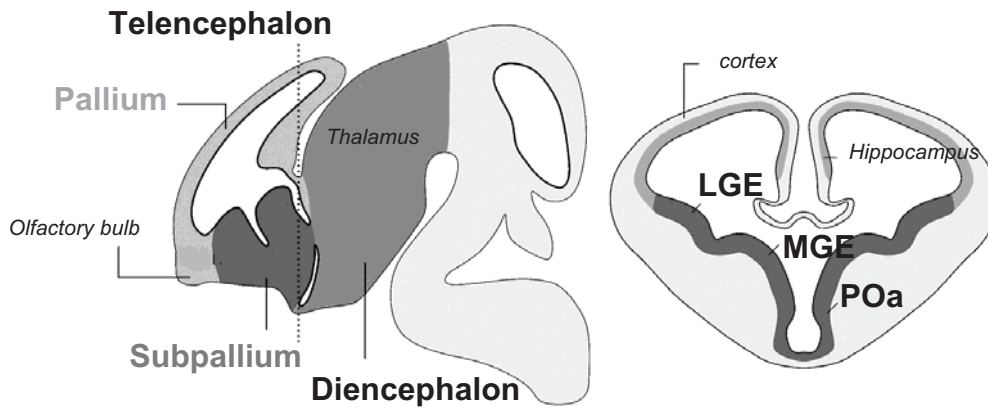
## **1. Striatal neurons originate and migrate from the ganglionic eminences and the preoptic area**

### **1.1. The fated-projection neurons and the fated-interneurons of the striatum have different temporal and spatial origins.**

During vertebrate embryonic development, the prosencephalon, the most anterior of the three vesicles derived from the embryonic neural tube, is further subdivided into the telencephalon and diencephalon at embryonic day 8 (E8) in the mouse. The telencephalon gives rise to two lateral telencephalic vesicles at E9 which will become the left and right cerebral hemispheres. The dorsal telencephalon (pallium) develops into the cerebral cortex and hippocampus, whereas the ventral telencephalon, or subpallium, becomes the basal ganglia (For review, Marin et Rubenstein, 2003). All the different types of striatal neurons originate from the Caudal, Median and Lateral Ganglionic Eminences (CGE, MGE and LGE) transitory brain structures located in the floor of the embryonic ventricles (Fig.4A). Each ganglionic eminence consists of three molecularly distinct cell layers: the ventricular zone (VZ) composed of undifferentiated dividing cells, the subventricular zone (SVZ) a second proliferative zone and the mantle zone formed by postmitotic cells migrating from the proliferative zones. In the mouse, the MGE is distinct at E11 and the LGE at E12 (Smart et al., 1979).

Specific populations of immature neurons spread out from the different germinal progenitor domains and have unique migratory potentials (Wichterle et al., 1999, Flames et al; 2007). On the basis of transplantation studies, it was established that the two populations of GABA-expressing MSNs (D1 and D2), originate in the LGE (Deacon et al., 1994; Olsson et al., 1995, 1998; Campbell et al., 1995) (Fig. 4B).

**A**



**B**

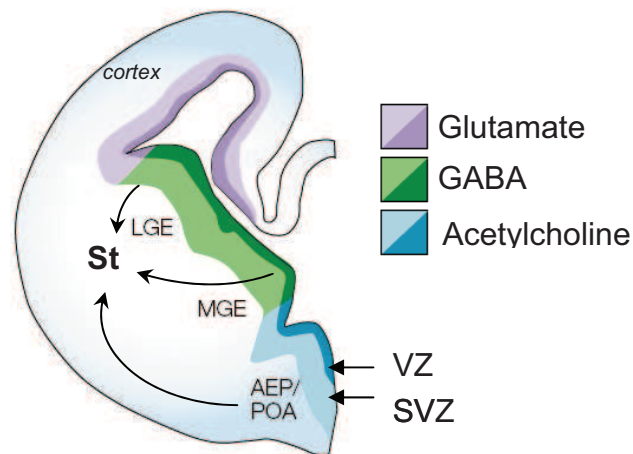


**Figure 4:** Development of the rodent striatum: the fated-striatal neurons originate in and migrate from the ganglionic eminences.

**A.** Ganglionic eminences (LGE, MGE) are located in the ventral part of the telencephalon. Sagittal (left) and coronal (right) views.

**B.** Schematic representation of a coronal section showing that MSNs derive from the LGE whereas the GABAergic striatal interneurons derive from the MGE. Cholinergic interneurons of the striatum derive from the AEP/POA.

LGE: Lateral Ganglionic Eminence, MGE: Medial Ganglionic Eminence; POA: Preoptic area. AEP: anterior entopeduncular area. *Modified from Marin, 2003; Marin and Rubenstein, 2001.*

Early-born MSNs (between E11 and E12 in the mouse (Bhide, 1996; Sturrock, 1980), migrate radially into the developing striatum via radial glial fibers (Kakita and Goldman, 1999) and display a strong ventrolateral to dorsomedial gradient (Fentress et al., 1981). To a lesser extent, MSNs of the posterior striatum may also derive from the CGE (Nery et al., 2002; Sussel et al., 1999; Wichterle et al., 1999).

Striatal GABAergic interneurons mainly originate in the MGE (Marin et al., 2000). Indeed lack of MGE results in the loss of cells migrating to the striatum and cortex. The Somatostatin subtype of GABAergic interneurons (SST/NPY/NOS/NADPH) may originate in the LGE according to Olsson et al. (1998), but this study is still controversial (Marin et al., 2000). Hamasaki and collaborators (Hamasaki et al., 2001) also proposed another source of transient interneurons, the preplate region. These presumably striatal CR-expressing interneurons named SPEG neurons (subcortical preplate early generated neurons) have a peak of birth at P0 and are apparently eliminated by apoptosis in the first postnatal week. Birth-dating of GABAergic interneurons in the differentiating striatum revealed that: PV-expressing interneurons are born between E13 and E20 (max E14-E17) (Sadikot and Sasseville, 1997); CR-expressing interneurons are born between E14 and E17 according to Rymar et al. (2004), with a peak at E15. SST-expressing interneurons are born between E15 and E16 (Semba et al., 1988).

Cholinergic interneurons principally derive from the ventral region of the subpallial telencephalon (Fig. 4B). Progenitor cells in the anterior/ preoptic entopeduncular areas (AEP/POA), a region at the limit between telencephalon and diencephalon, migrate dorsally into the striatum to become the cholinergic interneurons (Marin et al., 2000; Zhao et al., 2003). MGE is also a source of cholinergic interneurons (Fragkouli et al., 2009) which are among the earliest born cells of the striatum (rat: E12-E17, with 75% of them being born between E13 and 15) with a caudal to rostral neurogenesis gradient (Semba et al., 1988; Phelps et al., 1989). Nevertheless, according to Fragkouli and collaborators, less than 20% of the cholinergic interneurons are derived from the MGE (Fragkouli et al., 2009).

## **1.2. Neurons migrate to the developing striatum in response to intrinsic and extrinsic cues.**

Migration of the fated-striatal cells is strongly submitted to molecular cues (For review, Nobrega-Pereira and Marin, 2009). MSNs and interneurons, coming from different spatial origins, migrate differently. Fated-projections neurons of the striatum migrate radially from the LGE and invade the developing striatum following a spatiotemporal distribution. In contrast, fated-striatal interneurons reach their final destination from the MGE via a tangential migration. Two distinct interneuronal populations follow guidance cues: the fated-cortical interneurons, avoiding the striatum and the fated-striatal interneurons entering in the striatum. Numerous molecular cues are involved in the migratory process. Given this, we will focus on the major transcription factors and guidance molecules playing a role in the migration of the striatal neurons.

### **1.2.1. The fated-projection neurons migrate from the LGE to the striatal “anlage”**

The striatum consists of two compartments, patches (or striosomes) and matrix, occupying respectively about 15% and 85% of the striatum (Johnson et al., 1990). Patch/matrix areas differ in their neuronal birthdates, connectivity and neurochemical content. Notably they are delimited by high level of neuropeptides which are all expressed early during development. The patch compartment is characterized by the expression of  $\mu$  opioid receptors, first detected from E15 (Winzer-Serhan et al., 2003; Pert et al., 1976), whereas the matrix compartment is identified via somatostatin and acetylcholinesterase (Gerfen et al., 1987). The compartments are generated by two waves of neurogenesis. The early-born cells (E12-17) are forming the patch, and the late-born cells (from E17 until the early postnatal period) forming the matrix (Van der kooy and Fishell, 1987). Both neuronal populations are first intermixed but then sort out into compartments as the striatum matures postnatally (Krushel et al., 1995).

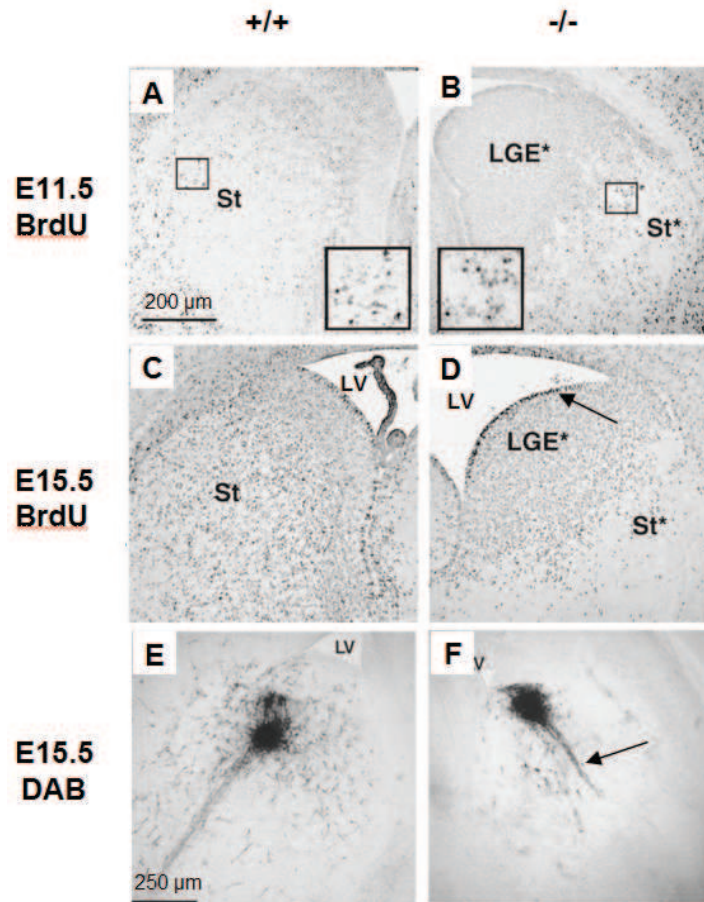


**Figure 5:** *Dlx1-2* genes regulate the migration of late-born striatal precursors of MSNs from the LGE to the striatum.

BrdU injections at early (E11.5, A and B) or late (E15.5, C and D) embryonic stages in pregnant mice and location of the labelled cells at P0. Note that *Dlx1/2* mutation does not affect the migration of the early born cells (A compared to B) whereas late-born cells do not migrate and remain in the LGE in the double mutant *Dlx1-2* (C compared to D). (E, B) At E15.5, cell migration in organotypic slice cultures is altered in the *Dlx1/2* *-/-* mutant (right) compared to the wild type (left). LV: Lateral Ventricule. *From Anderson et al., 1997.*

Neuronal compartmentalization, reminiscent from the developmental stages, is also detected in the adult striatum (see 2.2).

Dlx (Distal-less related, DLX) homeobox genes family encodes for transcription factors required for brain and craniofacial development (Anderson et al., 1997; Qiu et al., 1997). Dlx-1/2 and Dlx-5/6 genes are expressed from E9.5 in the primordium of the mouse striatum, MGE and LGE VZ/SVZ (Liu et al., 1997; Eisenstat et al., 1999). Each of the Dlx genes has a distinct role in striatal differentiation and is necessary for the initiation of GABA synthesis (Stühmer et al., 2002). Dlx1 and Dlx2 are essential for the LGE/MGE differentiation and for the proper migration of the late born neurons from the LGE subventricular zone (Anderson et al., 1997) (Fig. 5). The homozygous mutation for Dlx1-2 is not viable. Indeed loss of function of Dlx1/2 leads to abnormal accumulation of precursors destined to the striatal matrix neurons in the proliferative zone of the LGE. However histogenesis of the early-born (E10-E12) striatal neurons expressing Dlx5/6 appears normal. Dlx1 and 2 could regulate in consequence the expression of Dlx5 and Dlx6 (Anderson et al., 1997; Eisenstat et al., 1999). Single mutants for Dlx1, Dlx2 or Dlx5 gene have almost no detectable defects in the forebrain (Qiu et al., 1997) whereas both Dlx1/2 and Dlx5/6 mutants have abnormalities. Anderson and collaborators (Anderson et al., 1997) suggest that several lineages could be involved to generate neurons of the striatum: One Dlx1-2 independent lineage producing the early-born neurons and one Dlx1-2 dependent lineage producing the late-born neurons. Characterization of the genes regulating Dlx-5 and Dlx-6 expression in the early-born cells of the developing striatum is still under investigation.

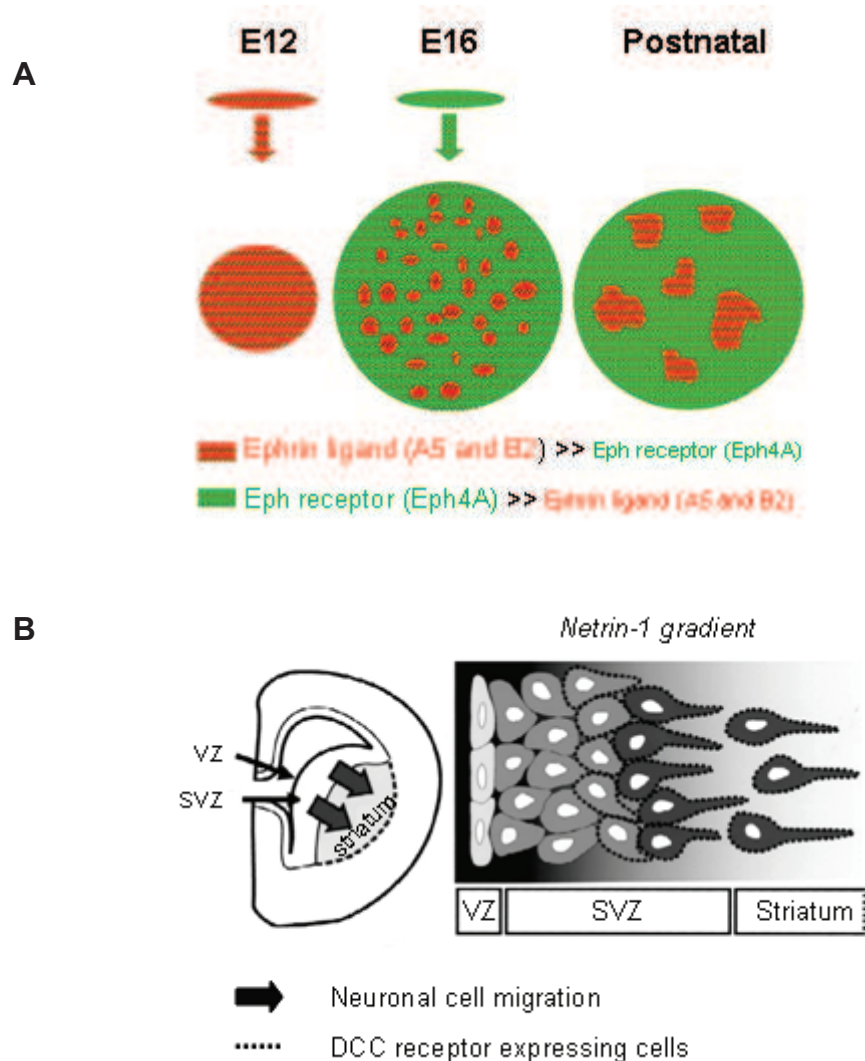


**Figure 6:** Striatal compartmentalization of MSNs is regulated by repulsive guidance cues.

**A.** Early-born cells (from E12 in the LGE) form the striosomes and express high levels of ephrin ligands (red) and low level of Eph receptors (green). Late-born neurons (from E16 in the LGE) generate the matrix compartment, expressing high level of receptors and low level of ligand. Cells in matrix and striosomes are first intermixed, and then partially segregate to form the mature mosaic pattern of the striatum at postnatal stages.

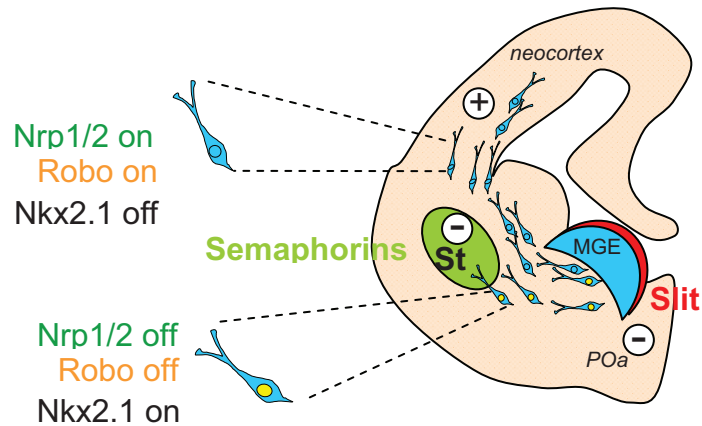
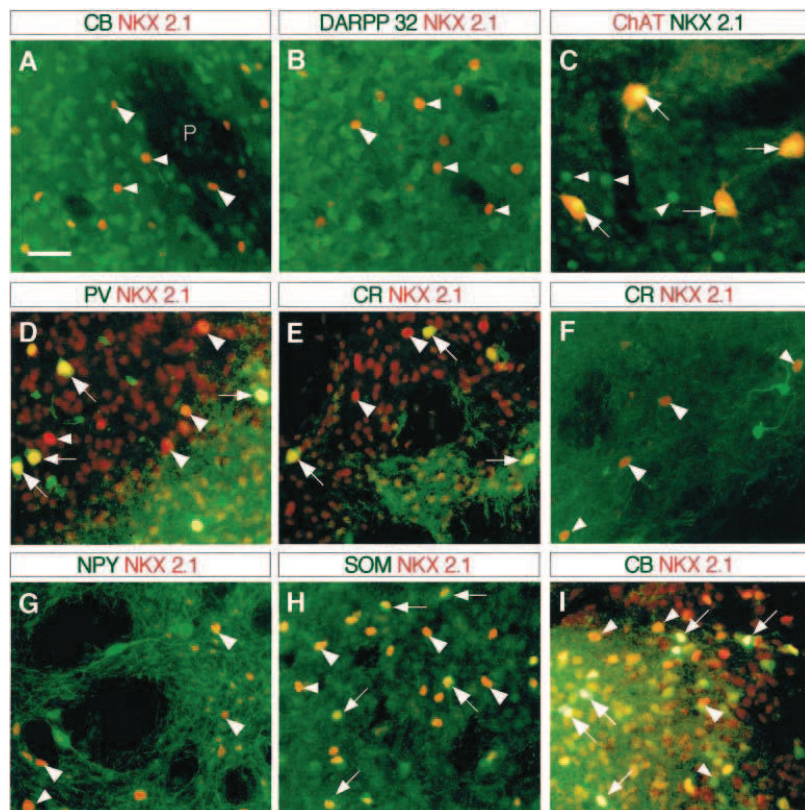
**B.** Netrin-1 signalling regulates the outward migration of the striatal late-born (matrix) neurons. Left, illustration in a coronal slice of the neuronal migration from the LGE to the developing striatum (grey) occurring in a rat at E18. Right, schematic presentation of the expression of Netrin-1. Netrin-1 is strongly expressed in the VZ (ventricular zone, white cells) but not in the SVZ (subventricular zone, dark cells) and thus Netrin-1 extracellular concentration follows a gradient (gray gradient field) from maximal in the VZ to minimal in the SVZ. Its receptor DCC (dots on the cell surface) is expressed on SVZ cells and striatum border. DCC-positive cells exit from the SVZ to the developing striatum due to the repulsive effect of Netrin-1.

*Modified from Passante et al., 2008 and Hamazaki et al., 2003.*

Gradient molecules modulate neuronal migration and therefore are also involved in the initial differentiation of the striatum. For instance, ephrins and Eph receptors are repulsive guidance cues that control the compartmentalization of the mouse striatum into striosomes and matrix (Fig.6 A). Indeed, disruption in the ephrin/ Eph signalling results in the mislocalization of matrix and striosomes neurons (Passante et al., 2008). Ephrin (A5 and B2) ligands and Eph receptor (EphA4) display differential spatiotemporal patterns of expression. More particularly, ephrins are preferentially expressed in early-generated striatal neurons (from E12 LGE), corresponding to striosomal neurons whereas EphA4 receptor is preferentially expressed in later-generated neurons (from E16), corresponding to the matrix neurons (Fishell and Van der Kooy, 1987).

Netrin-1 a diffusible protein expressed in the striatal ventricular zone during the striatal embryogenesis, also serves to guide the large influx of striatal matrix neurons (late born neurons; Van der Kooy and Fishell, 1987) into the striatal primordium by a repulsive chemotropic gradient (Hamasaki et al., 2001; For review, Hamasaki et al., 2003). Its putative receptor DCC, expressed in the striatal SVZ during the neurogenesis of matrix cells in the LGE (from E18), displays complementary expression pattern (Fig.6 B).

Notch receptor/ DSL ligand signalling is required to control cell fate only at early stages of striatal development. More particularly, early removal (E11- E14) of Notch1 in mouse embryos only alters early-born patch neurons, indicating that notch signalling coordinates the patterning of striatal compartments (Mason et al., 2005). The precise underlying mechanisms are still unknown.

**A****B**

**Figure 7:** The final destination of the MGE sorting-interneurons is under the control of several molecules.

**A.** Coronal section at E18 illustrating the migration of the interneurons (generated by the MGE SVZ, blue) in response to the repulsive action of Slit (red). Semaphorins expression within the striatum prevents the fated-cortical interneurons expressing neuropilin (Nrp1/2, semaphorin receptor) and robo (slit receptor) from entering the striatal anlage. Nkx2.1 directly repressing the expression of Nrp2 enables interneurons to invade the striatum. Unidentified repulsive action in the preoptic area (POA) prevents the neuronal migration ventrally whereas attractive cues guide neurons towards the cortex.

**B.** Nkx2.1 is expressed in most striatal interneurons (C-H) but not in projections neurons (A, B, I). Arrowheads indicate cells expressing only Nkx2.1 and arrows show colocalization. CB, Calbindin, marker of the matrix neurons, is also expressed in a small subpopulation of NOS interneurons. DARPP 32: projection neurons marker. ChAT: Acetylcholine Transferase, cholinergic interneurons marker. PV, Parvalbumin; CR, calretinin; NPY, Neuropeptide Y; SOM, somatostatin: markers of the GABAergic interneurons. Scale bar: 40  $\mu$ m, P18 mouse slice, P: patch.

*Modified from Andrews et al., 2007; Nobrega-Pereira and Marin, 2009; Marin et al., 2000.*

### **1.2.2. GABAergic interneurons of the cortex and the striatum both originate from the MGE: how does the segregation between these two populations occur?**

Migration of GABAergic striatal interneurons is particularly submitted to molecular control. Notably, the slit/robo signaling pathway is required to steer neurons into their correct position. Slit protein/ Robo receptor signaling pathway affect cellular migration in vertebrates (For review, Brose and Tessier-Lavigne, 2000). Slits are extracellular molecules which are chemorepulsive to growing axons of the subpallial GABAergic neurons (For review, Marín and Rubenstein, 2001). The ventricular zone of the LGE is repulsive to the fated cortical GABAergic interneurons, via the secretion of the slit protein during the period of interneuronal migration (E13-E17 in rats) (Zhu et al., 1999). Robo1 and 2, receptors for slit, show complementary expression patterns in the subpallium but the Robo2 expression is restricted to the differentiating striatum (Andrews et al., 2007). Robo1 but not robo2 is required for cortical interneurons to avoid the striatum (Fig. 7A): Indeed, loss of Robo1 leads to an increased number of cells entering in the striatum (Andrews et al., 2007). As a result the striatum remains an exclusion zone throughout the period of generation and migration of the fated-cortical interneurons, and slit has a role in streaming these cells to their appropriate tangential routes (Marín and Rubenstein, 2001; Marín and Rubenstein, 2003).

Migration of neurons to their corresponding target territories is highly regulated. In particular, Marín and his colleagues showed in 2001 that the final destination of the tangentially migrating interneurons is determined by the signaling system semaphorin/neuropilin. The striatum expresses semaphorins (3A, 3F) during the interneuronal migration from E12 to E16 in mice. The migrating interneurons enter to the striatum because they lack semaphorins transmembrane receptors, neuropilins 1 and 2, both required for mediating a repulsive effect on semaphorin-expressing axons. On the contrary, the neuropilin-expressing interneurons migrate to the cortex, repelled by the semaphorin-expressing neurons of the striatum (Fig. 7A). Loss of neuropilin function increases the number of interneurons migrating into the striatum and decreases the one reaching the embryonic cortex. Neuropilin 2 is directly regulated by Nkx2.1 transcription factor to enable interneurons to evade the developing striatum (Nobrega-Pereira et al., 2008).

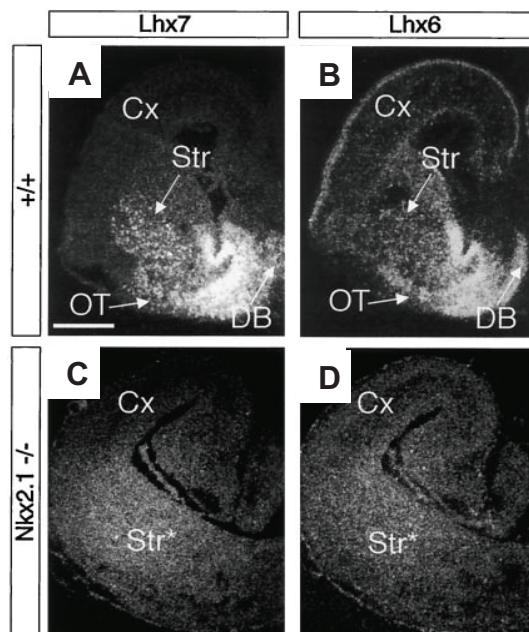
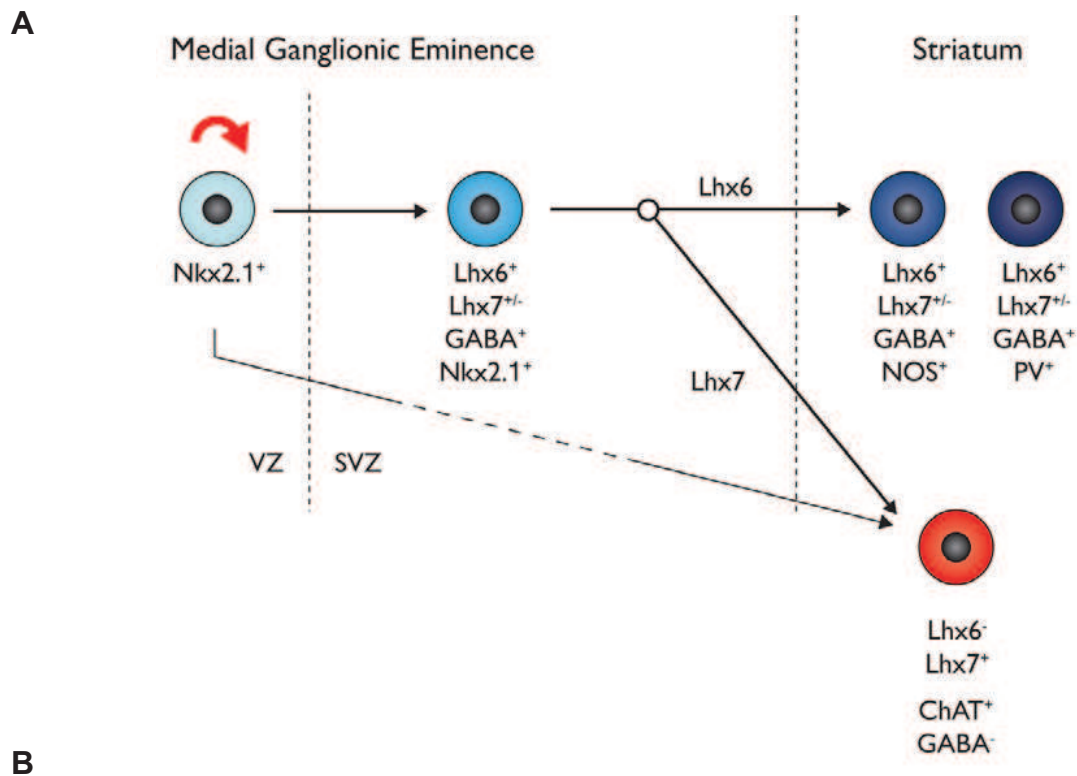


**Figure 8:** The specification of the GABAergic and cholinergic striatal interneurons is regulated by Nkx2.1, Lhx6 and Lhx7.

**A.** Under the continuous activity of Lhx6, many of the precursors (●) differentiate into mature GABAergic interneurons (●●). Activity of Lhx7 downregulates Lhx6 and induces the entrance into the cholinergic interneurons sublineage.

**B.** Expression of Lhx7 and Lhx6 in the striatum (Str) from coronal sections of E18.5 wild type (A and B) and Nkx2.1 mutant (C and D) mice. The absence of Nkx2.1 induces Lhx7 (C) loss and Lhx6 (D) expression. Cx: Cortex. From Fragkouli et al., 2009; Marin et al., 2000.

The homeodomain transcription factor Nkx2.1, expressed from E8 in mouse in the three layers of the MGE, the maturing MGE derivatives and POA (Shimamura et al., 1995) is also necessary for the correct migration of GABAergic interneurons in the striatum. On the contrary, its down regulation is required for the migration of GABAergic interneurons to the cortex (For review, Nobrega-Pereira and Marín, 2009) (Fig. 7A and B). Postmitotic Nkx2.1 directly represses the expression of neuropilin 2 (receptor for Semaphorin 3A) which enables interneurons to avoid the striatum (Nobrega-Pereira et al., 2008). Sussel and colleagues (1999) showed that this transcription factor is crucial for the early born neurons of the striatal primordium (from E8). Indeed, Nkx2.1 mutants (Nkx2.1-/-) lack most striatal interneurons and die at birth (Fig. 8B). This defect is due to molecular re-specification of the ventral MGE and AEP progenitor cells to a dorsal fate, similar to the LGE progenitors (Sussel et al., 1999). Among the same line, removal of the Nkx2.1 gene by conditional loss of function at embryonic stages (E9-E12) also revealed a switch in the neuronal specification as expressed by an increase in the production of striatal projection neurons post-natally (Butt et al., 2008). Nkx2.1 is consequently used as a marker of the striatal interneurons: the majority of the interneurons in the striatum expresses Nkx2.1 and maintains the protein expression into adulthood whereas neither projection neurons (from the LGE) nor the fated cortical interneurons do express Nkx2.1.

Nevertheless some striatal interneurons (NPY/SOM/NOS) appear to down-regulate the expression of Nkx2.1 after leaving the MGE. As a consequence, only 10% of these neurons contain Nkx2.1 at the adult stage (Marin et al 2000). Nkx2.1 expression could be modulated by another transcription factor, sonic hedgehog (Shh), a ventral telencephalic gene (Ericson et al., 1995) and, in turn, Nkx2.1 would modulate the Shh molecule expression.

Lhx 6 and 7 LIM homeobox genes intervene in the striatal differentiation (Fig. 8A and B). Expression of Lhx6 is restricted to the MGE but unlike Nkx2.1, it is also expressed in the cerebral cortex (Fragkouli et al., 2009, Sussel et al., 1999, Marin et al., 2000, Cobos et al., 2006). Lhx6 is induced in Nkx2.1-expressing MGE progenitors as they colonise the SVZ (Flames et al., 2007). Lhx6 acts as effector of Nkx2.1 in the specification of PV and SST expressing-interneurons.

Indeed, the interneuron generation can be rescued in the Nkx2.1 null mice with ectopic expression of Lhx6 (Du et al., 2008, Elias et al., 2008).

Lhx7 is expressed in the ventral forebrain cholinergic neurons only (Zhao et al., 2003). Homozygous mice (Lhx7<sup>-/-</sup>) display a reduced number of the ventral forebrain cholinergic neurons (Mori et al., 2004) suggesting that Lhx7 is required for the specific differentiation of the striatal cholinergic interneurons. Bachy and Retaux (2006) proposed that early inhibitor action of Lhx7 on GABA would preserve a pool of future cholinergic neurons which would have differentiated late during development to become GABAergic. In contrast to Lhx6 which is used as marker of the striatal interneurons (Gittis et al., 2010), Lhx7 represents a specific marker of the cholinergic interneurons of the striatum (Fragkouli et al., 2009).

Interaction between the different transcription factors and the mechanisms underlying the generation of variety of subpallial neuronal populations remain elusive. Flames et al. (2007) emphasized this complexity and proposed that ventricular zone can be divided in different functional domains according to the combinatorial expression of several transcription factors in progenitor cells. Migratory process of the cells occurs as a second step and is controlled by guidance molecules. Representation of the developmental history of each cell or “fate mapping” has become the key tool for neuroscientists to understand the origin of cellular diversity.

It is clear that neuronal subtypes of the striatum can be directly related to their embryonic temporal and spatial origins. Transcriptional process regulates neuronal fate specification while guidance decisions are made downstream to interact during the process of cell migration. Striatal development is governed by plural signalling pathways, each of which being more or less important and compensated if needed by the expression of others proteins with analogous functions.

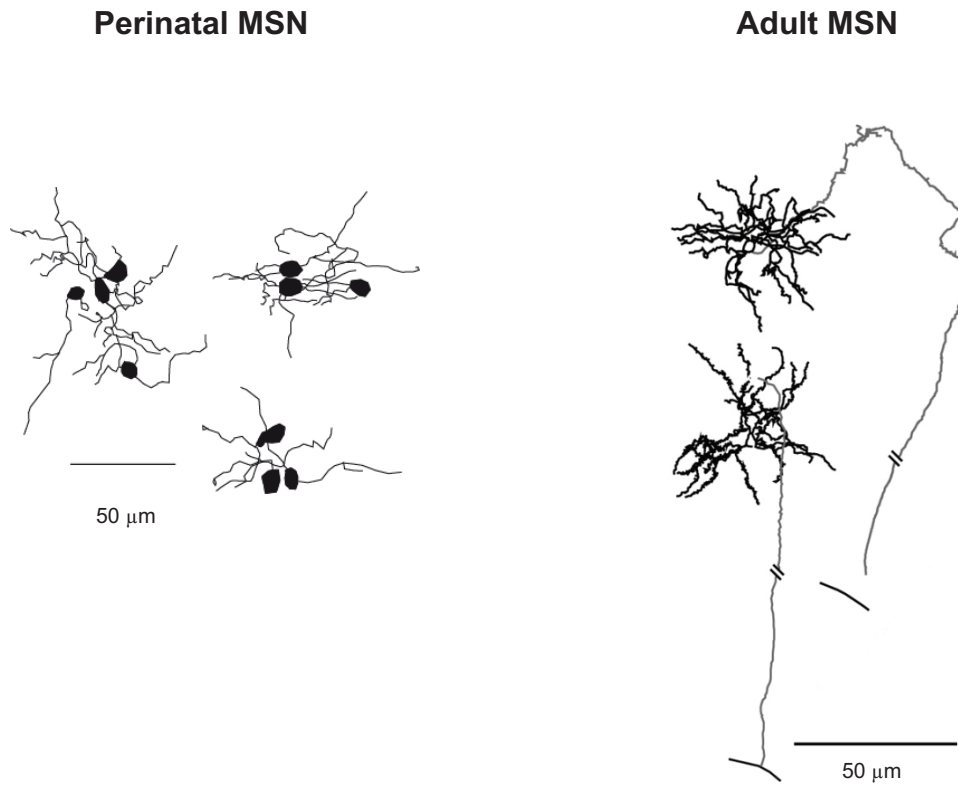


**Figure 9:** MSNs are preferentially organized in clusters at perinatal stages.

Reconstruction of neurobiotin-labelled MSNs in E18 (left) and P30 (adult, right,) mice striatal slices. Clusters of 2-6 MSNs (left) are observed in 60% of the recordings at E16-P2 compared to clusters of 2 MSNs in only 15% of the recordings in the adult striatum (right). *From article 1 Dehorter.*

## **2. The synaptogenesis in the striatal network follows a sequence**

Formation of functional neuronal networks during development is governed by the onset of proper synaptic connections between cells and the expression of numerous pre and postsynaptic receptors.

### **2.1. Electrical synapses are the first connections present in the developing striatum**

Fast signalling in the striatum is achieved by electrical communication through gap junctions before the onset of chemically-mediated synaptic transmission. Each gap junction contains numerous gap junction channels which cross the membranes of both cells to form an electrically conductive link between two neurons. Such channels allow direct passage of various ions and molecules such as second messengers and metabolites, with a weak selectivity. Intercellular channels are formed by two close hemichannels (connexons), each of which composed of six protein subunits (connexins) (For review, Söhl et al., 2005). Electrical synapses represent a low-pass filter which assures rapid transmission (around 0.2 ms). These characteristics allow electrically-connected neurons to fire synchronously (For review, Bennet and Zukin, 2004; Gibson et al., 2004; for review, Söhl et al, 2005).

Gap junctions are commonly found in the striatum (For reviews, Galaretta and Hestrin, 2001; Vandecasteele et al., 2007) where several connexin mRNAs are expressed during development: Cx47, Cx31.1, Cx36 and Cx32 (Venance et al., 2004). Expression of gap junctions within the striatum is specifically distributed.

MSNs and interneurons populations correspond to two distinct electrically-coupled networks (Koos and tepper, 1999; Venance et al., 2004). MSNs are mainly organized in clusters at early stages (E14-P2; Fig.9) and display synchronized network activity (Article 1 Dehorter). FS GABAergic interneurons connected by functional electrical synapses also display synchronous activity in the adult. Electrical coupling is observed in 33% of the GABAergic interneurons (FS) and 24% of the MSNs pairs in juveniles (P17-21) (Koos and Tepper, 1999).

Coupling occurrence is high at P5, representing 60% of the MSNs pairs and then decreases in the adulthood (9-15%) (Venance et al., 2004; article 1 Dehorter) (Fig. 9). The decrease of dye coupling is associated with a decrease of gap junction permeability during maturation (Cepeda et al., 1991). Endogenous substances, such as dopamine, modulate gap junctions (Onn and Grace, 1999; Cummings et al., 2008). Activation of D1 receptors decreases dye coupling whereas activation of D2 receptors enhances coupling. Degeneration of the adult nigro-striatal dopaminergic system, leads to a 4-fold increase in dye coupling between cells in vivo (Onn and Grace, 1999).

## **2.2. Feedforward and feedback GABAergic synapses develop sequentially**

In parallel to electrical signaling, neurotransmitter-releasing chemical communication develops in the striatum during maturation. Although most synapses of the adult striatum are glutamatergic, GABAergic synaptic inhibition plays a key role in the modulation of striatal outputs (For review, Wilson 2007). Yet, little is known about the onset of GABAergic synapses maturation in the striatum at embryonic and perinatal periods. GABAergic symmetric synapses mature before the excitatory glutamatergic ones (Misgeld et al., 1986).

Axons of adult MSNs give rise to extensive local axon collaterals (Wilson and Groves, 1980) connecting to other MSNs and generating feedback (lateral) inhibition (Tunstall et al., 2002). There are more synapses involved in the feedback circuit than in the feedforward circuit and there is 50-100 times more convergence from MSNs to MSNs than from FS interneurons to MSNs (For review, Tepper et al., 2004). However, lateral inhibition between MSNs is much less efficient than feedforward inhibition (Jaeger et al., 1994), probably due to the more distal synaptic location and the low number of release sites with high failure rate at the MSN-MSN synapses. Thus, they play a role in the control of neighbouring synapses and synaptic plasticity (Carter and Sabatini, 2004 and for review, Tepper et al., 2008). In embryonic and early postnatal stages, feedback inhibition would be even weaker. The dendritic and axonal arborizations of MSNs are limited (Article 1, Dehorter) and the probability of a synaptic connection among pairs of immature MSNs is low or null before P11. It increases to around 16% at P11-P14 to reach adult level at P15 in the rat striatum i.e. 33% of the recorded MSNs pairs are connected (Koos et al., 2004).

During the two first postnatal weeks, the proportion of GABAergic synapses to the total synapses population is larger than in the adult because only a few glutamatergic synapses are present and spontaneously active (Tepper et al., 1998; article 1 Dehorter). Around P5, all the MSNs generate spontaneous GABAergic postsynaptic currents, but their frequency represents only one third of the adult one, indicating that GABAergic transmission is still not yet mature. The frequency of spontaneous GABAergic activity reaches the adult level around P17 in mice (Article 1 Dehorter). FS interneuron–MSNs synapses reach near-maximum numbers by P14 (Uryu et al., 1999), and stimulation of FS interneurons evoke IPSPs in MSNs already at P14 in rats (Tepper et al., 1998). FS interneuron-mediated feed-forward inhibition may thus be present when the striatum is still undergoing major changes of morphology, physiological properties, synaptogenesis and receptor composition. Consequently, GABAergic synaptic activity recorded in the MSNs may principally originate from GABAergic interneurons during the perinatal period. Starting at the third postnatal week, GABAergic synaptic activity would result from both local interneurons and neighbouring MSNs.

### **2.3. Cholinergic interneurons are early-born neurons that establish synapses with all striatal neuronal types**

In the adult striatum, cholinergic neurons form symmetrical synapses with dendritic spines necks or distal branches of MSNs (Wilson, 1980; Aznavour et al., 2003) and contact also the GABAergic interneurons (Chang and Kita, 1992). A number of presynaptic and postsynaptic neuronal mechanisms are controlled by nicotinic and muscarinic acetylcholine receptors in the striatum (Koos and Tepper, 2002; Pakhotin and Bracci, 2007). The striatal cholinergic neurons express D5 and D2 receptors which activation decreases ACh release via inhibition of N-type Calcium current (Yan et al., 1997).

Cholinergic neurons are among the first cells appearing in the developing striatum. Born between E11 and E18, cholinergic interneurons are detected in the lateral part of the developing striatum at birth (Aznavour et al., 2003). Choline acetyltransferase staining (ChAT, the enzyme for ACh synthesis) is first detected at E13 in rats (Kessler, 1986). ChAT is strongly expressed in the matrix compartment at early stages (Graybiel et al., 1981). At P8, cholinergic axons fill the entire striatal region and starting at P16, they represent a dense network in the striatum (Aznavour et al., 2003). At early stages, we can assume that before MSNs become spiny, cholinergic neurons would form synapses with dendrites of the projection neurons.

Nicotinic binding sites have been detected in the striatum by autoradiography from E16 in rat (Naeff et al., 1992), nicotinic receptors and vesicular acetylcholine transport sites at E20 (Aubert et al., 1996). Muscarinic (M1, M2 and M3) receptors are weakly detected at E16 and the adult level is reached from the third (M1, M3) and the fifth (M2) postnatal weeks (Aubert et al., 1996). Functional muscarinic post-synaptic receptors have been first detected at E17 on rat (De Vries et al., 1992). Consequently, an important role can be presumed for acetylcholine during the striatal development.

## **2.4. NMDA and non-NMDA receptors-mediated glutamatergic responses do not show the same developmental profile**

Glutamate, the principal excitatory transmitter in the mammalian brain plays a crucial role in the physiology of the striatum for movement regulation. Striatum receive glutamatergic afferents from many parts of the primary motor cortex, somatosensory cortex, premotor cortex and supplementary motor area (For review, Tisch et al., 2004). The cortical pyramidal neurons projecting to the striatum are located in layers II-VI, most of which coming from the deep layer V. Distribution of glutamatergic inputs is compartmentalized. In the adult, layers II-III and superior layer V of the motor cortex project to the matrix compartment (Gerfen, 1989), whereas deep parts of layers V-VI of the neocortex project to the patch compartment (Christensen et al., 1999). Cortico-striatal fibers terminate on the dendritic shafts of GABA interneurons and on MSNs dendritic spines (asymmetric axospinous synapses) (Kemp and Powell, 1971; Sharpe et al., 1998). Each MSN receives convergent inputs from multiple cortical areas (Gerfen, 1989) and their firing requires cortical synchronization (For review, Mahon et al., 2004). Intralaminar (centro median – parafascicular nuclei) and ventral motor nuclei are the main sources of thalamic inputs to the striatum. Thalamo-striatal neurons make direct synaptic contact with the dendritic shafts of spiny neurons (For review, Smith et al., 2004; Lapper and Bolam, 1992).

Cortico-striatal fibers arrive at E16 and follow a progressive postnatal development (Christensen, 1999; article 1 Dehorter). The majority of glutamatergic synaptic contacts are established during the third postnatal week, between P15 and P21 in the rat (Sharpe and Tepper, 1998; Uryu et al., 1999). Before P12, MSNs are mostly aspiny with varicose dendrites (Tepper and Trent, 1993), in contrast with the highly spiny adult MSNs dendrites (Wilson et al., 1983). Due to the absence of dendritic spines, cortical inputs in the developing striatum first terminate on MSNs dendritic shafts.

Most excitatory responses are mediated by two classes of ionotropic glutamate receptors: N-methyl-D-aspartate (NMDA) and non-NMDA receptors,  $\alpha$ -amino-3-hydroxy-5-méthylisoazol-4-propionate (AMPA) and kainate (KA). According to Nansen and collaborators, glutamate receptors are present at birth in the striatum, the non-NMDA receptors KA and AMPA receptors are the first to mature, followed by NMDA receptors (Nansen et al., 2000). More precisely, AMPA receptors GluR1, GluR2/3 subunits staining are first observed at P0 and are distributed in the striatal patches until P3. After P7, staining becomes homogenous and from P15, GluR1 and GluR2 non-NMDA components are the predominant receptors expressed within the somatic and proximal dendritic membrane of MSNs in rat (Nansen et al., 2000). AMPA GluR1-2 and 3 develop throughout the second week of life (Hurst et al., 2001). Electron microscopy revealed that GluR1 subunit is mainly distributed in the dendrites and spines (Bernard et al., 1997), GluR3 is found in the substance P and enkephalin expressing-neurons whereas GluR4 is detected in interneurons (Stefani et al., 1998). AMPA-mediated spontaneous postsynaptic excitatory currents (AMPA-EPSCs) gradually develop from E16 to P7 and from P17 the frequency of AMPA-sEPSCs reaches the adult level (Article 1 Dehorter).

Adult distribution of the KA receptor (GluR5/6 and KA1/2, cation channels permeable to  $\text{Na}^+$ /  $\text{K}^+$ ), expression is observed by P3 in the striatum (Nansen et al., 2000; Wüllner et al., 1997). KA2 and GluR6 mRNA are abundant but GluR7 is weak at P1, and GluR6 expression decreases between P1-P4 and P10-P20 in rats (Wüllner et al., 1997). Functionally, the frequency of the spontaneous KA-mediated postsynaptic currents is mature at P17 (Article 1 Dehorter).

NMDA receptors are glutamate-activated cationic ( $\text{Ca}^{2+}/\text{Na}^+/\text{K}^+$ ) channels which require both glutamate and membrane depolarisation to open. NR1, NR2 (A and B) NMDA-subunits are predominantly expressed in the adult striatum (Albers et al., 1999; Nansen et al., 2000). While NR1 is expressed ubiquitously throughout the brain, NR2 subunits are submitted to temporal and spatial regulation (Monyer et al., 1994) inducing a different processing of glutamatergic inputs in the ventromedial (limbic) and dorsolateral (sensorimotor) regions of the striatum (Chapman et al., 2002).

Expression levels of NR2A and NR2D mRNA are high at P7-P14 and decrease to moderate level in adult whereas NR2B and NR2C expression is low at P1 but increases at P7 until adulthood (Lau et al., 2003; Wenzel et al., 1997). Immunodetection of the NR2C and D subunits in the striatum is difficult: NR2D subunit is barely detectable at the maximal level in perinatal rat striatum (E14-P7). The protein level decreases by twofold throughout the brain from the peak of expression at P7 until adulthood (Dunah et al., 1996; Monyer et al., 1994).

We first detected functional synaptic NMDA receptors at E16 in 20% of the MSNs, At P5-P7 100% of the MSNs generate spontaneous NMDA synaptic currents, in contrast to 33% of adult MSNs (Article 1 Dehorter). Decay times of the NMDA-mediated EPSCs also largely decrease from the second postnatal week in the dorsal striatum (Hurst et al., 2001; article 1 Dehorter) as shown in the accumbens (Zhang and Warren, 2008). Based on these observations, Logan and collaborators hypothesized a possible incorporation of the NR2D subunit into heterotrimeric complex (NR1/NR2B/NR2D) after the first postnatal week in mice (Logan et al., 2007) and both NR2C and NR2D could have a role in shaping the perinatal synaptic NMDA response (Logan et al., 2007; Standaert et al., 1994; article 1 Dehorter).

Decrease in the receptor subunits expression and decay times both suggest that functional properties of the NMDA receptors shift during the second postnatal week in the striatum. This shift could probably correspond to a change in the ability to experience plasticity as function of time, between high plastic periods of the early stages (E14-P12) and low plastic period in adult (Partridge et al., 2000; Schramm et al., 2002). A role in synaptogenesis is also attributed to NMDA receptors in the developing striatum: they would reshape the corticostriatal connections during the third postnatal week (Butler et al., 1999). Activation of NMDA receptors could prevent the premature synaptic maturation; only punctuated bursts of activity could lead to the induction of functional synapses (Adesnik et al., 2008).

Precise developmental pattern of the glutamate receptors in striatal interneurons is poorly known. Striatal interneurons, like the FS ones, are submitted to a strong cortical control. Their cortical innervation consists of convergent synapses from somatosensory and motor corticostriatal afferences (Ramanathan et al., 2002).

Striatal interneurons receive a massive glutamatergic innervation from P15 (Tepper and Trent, 1993; Tepper et al., 1998) and mature considerably between P12 and P19 in the rat striatum (Chesselet et al., 2007). In the adult rat, cortical inputs form asymmetric synapses on the soma and proximal dendrites of FS interneurons (Bennett & Bolam, 1994). Cholinergic neurons receive a prominent direct synaptic input from thalamus in the distal dendritic regions (Lapper and Bolam, 1992) and to a lesser extent from the cortex (Thomas et al., 2000). Adult interneurons express KA receptors (GluR5/6/7) (Stefani et al., 1998), AMPA receptors (GluR1-2-3) and different NMDA receptor subunits (NR1, NR2). Double immunofluorescence studies reveal that during development FS PV+ neurons display a high level of NR1 and NR2A at P14 but not NR2B which is only expressed in adult. On the contrary, cholinergic interneurons express the three of them from P14 to adulthood (Lau et al., 2003).

### **2.5. Dopaminergic nigrostriatal projections are present early during development and mature in two waves, one prenatal and one postnatal.**

In the adult striatum, nigro-striatal dopaminergic terminals form symmetric synaptic contacts with necks of MSNs dendritic spines (For review, Bolam et al., 2000) and control GABAergic and glutamatergic synaptic transmissions (Delgado et al., 2000; Centonze et al., 2004; Surmeier et al., 2007). Dopamine is also supposed to play a role in the development of the striatum. It is therefore crucial to birth date dopaminergic neurogenesis and nigro-striatal synapse formation. Bromodeoxyuridine (BrdU) administration and immunohistochemical studies for tyrosine hydroxylase (TH, enzyme involved in the dopamine synthesis) distribution in rats determined that dopaminergic cells are born between E11 and E14, with a peak at E12 when almost 80% of the dopaminergic cells are generated (Gates et al., 2004; Gates et al., 2006) in the most ventral surface of the mesencephalic flexure.

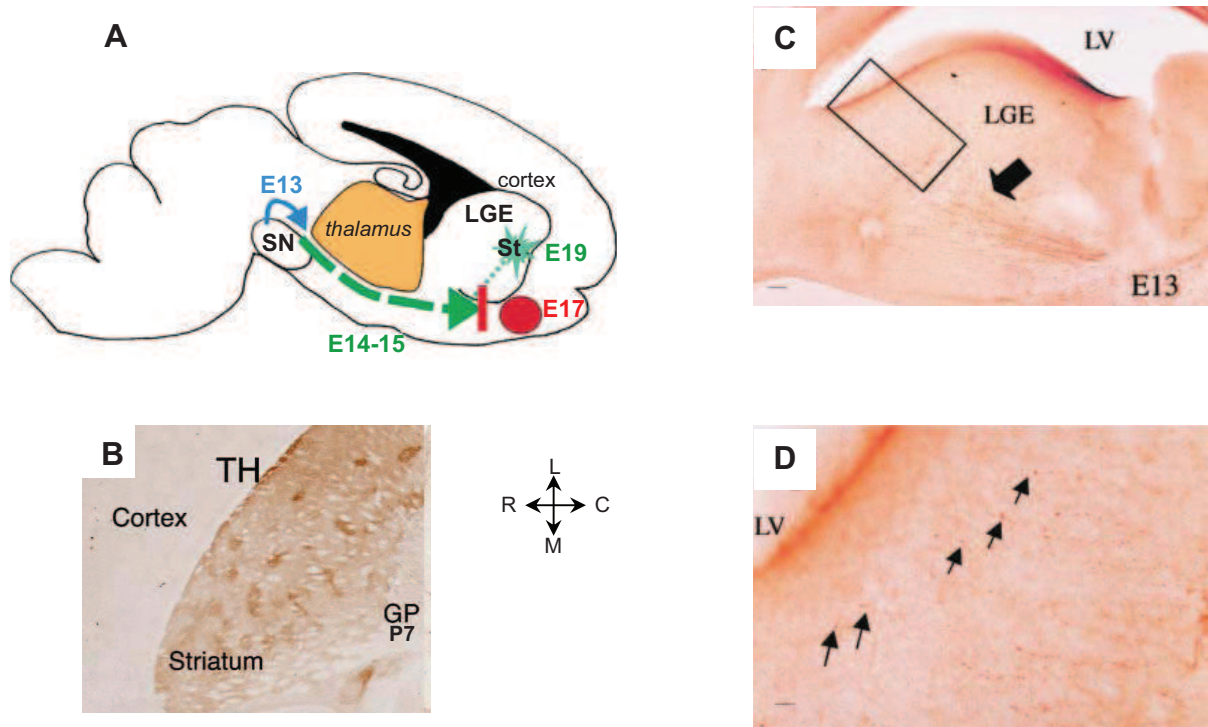


**Figure 10:** Tyrosine hydroxylase-positive fibres invade the striatum at E17-19 in the rat and E13-16 in the mouse.

**A.** Illustration of the timing of the dopaminergic nigro-striatal innervation (sagittal view). Majority of dopaminergic neurons are born at E12 in the fated-SN in rats. Between E17 and E19 dopaminergic fibres start innervating the latero-ventral part of the striatum.

**B.** Tyrosine Hydroxylase (TH) immunoreactivity of horizontal section from a P7 mouse. Dopaminergic afferences innervate the whole surface of the striatum and follow the striosome/matrix distribution at P7.

**C.** Immunohistochemistry for TH reveals positive axons in the striatum at E13 in the mouse (arrow).

**D.** Higher magnification from the boxed area (in C). Arrows show growing tips of TH-positive fibers.

Scale: A, 50  $\mu$ m and B, 10  $\mu$ m. From Ohtani et al., 2003; Gates et al., 2004, Miura et al., 2007.

Dopaminergic TH-positive fibres and terminals begin to innervate the emerging striatum between E17 (Goffin et al., 2010) and E19 (Gates et al., 2004) in the rat. By P4, the whole striatal surface is immaturely innervated (Gates et al., 2004). Coincident TH-positive axons arrival has also been detected by immunohistochemistry at E13-E14 in the latero-ventral part of the mouse striatum (Ohtani et al., 2003; Ferrari et al., in prep) (Fig. 10). Mouse embryonic basal forebrain is enriched in dopamine D1-like and D2-like binding sites that are first detected in the LGE by E13 and are heterogeneously distributed. The first receptor-mRNAs are expressed at E12 in the ganglionic eminences, with D2R mRNAs higher expressed than the D1 ones, and largely superior to D4R and D5R (Araki et al., 2007).

Genesis of striatal neurons in the striosomes coincides with the arrival of the first nigro-striatal dopaminergic fibres at E14. Dopaminergic innervation and patch-matrix compartments distribution both follow a ventro-lateral to dorso-medial gradient (Fishell and Van der Kooy, 1991). The patch MSNs are mainly innervated by DA neurons of the SNr, prior to MSNs of the matrix that will be innervated by DA neurons of SNc (Gerfen et al., 1987). The rich dopaminergic innervation of the striatum that arises from the SNc intimately and equally interacts with the dense local cholinergic innervation of the striatum.

Dopaminergic projections develop in two waves of innervation. First the afferences homogeneously innervate the striatum from E14. Matrix dopaminergic innervation only starts postnatally (from P0 to P16), revealing clusters of dopaminergic fibres in patches (Moon Edley, 1984; Popolo et al., 2004). Mature level of innervation is reached by P16 and until adulthood, dopamine distribution appears diffuse and homogeneous. This would suggest that DA innervation influence the onset of the patch/matrix organization in the striatum during embryonic and postnatal periods (Snyder-keller et al., 2008, Goffin et al., 2010). But it has been shown that DA is not crucial for this compartmentalization since neither in utero and prenatal 6-OHDA depletions (Snyder-keller, 1991; Van der Kooy and Fishell, 1992) nor homozygous null mutation (Kim et al., 2002) have an effect on the appearance of patch/matrix organization.

Exogenously applied dopamine controls cell proliferation, with D1 receptor activation reducing and D2 receptor activation promoting cell cycle in the LGE (Ohtani et al., 2003). It also acts on the progenitor cell type specification in the LGE with differential antimitogen effects.

Activation of D1 receptors favours the presumptive neuronal precursors in the VZ whereas activation of the D2 receptors promotes the presumptive glial precursor cells in the SVZ (Popolo et al., 2004). Migration of the GABAergic neurons from the MGE and LGE to the cortex is also controlled by exogenously applied dopamine. Activation of D1 receptors promotes whereas that of D2 receptors decreases neuronal migration (Crandall et al., 2007). Dopamine consequently acts on neuronal proliferation, specification and migration via opposite effects of D1 and D2 receptors activation. Nevertheless, dopaminergic receptors can play a united role as well during development. For instance, activation of both D1 and D2 receptors influences the GABAergic synaptogenesis by decreasing the number of functional GABAergic synaptic contacts between embryonic precursors of MSNs (Goffin et al., 2010).

However, all these data do not take into account the time when dopamine starts being spontaneously released (Popolo et al., 2004; Goffin et al., 2010; Gates et al., 2006). Roles of dopamine on migration and neurogenesis described by Crandall, Othani and Popolo have been observed in response to the application of exogenous dopamine. Some precautions have to be taken concerning the physiological relevance of these results. The presence of dopamine receptors does not imply that they are activated by synaptically-released dopamine. From E14 to P0 in mice, TH –labelled fibres are mainly present in the latero-ventral part of the striatum, where the early-born (older) neurons are located. Besides evoked spontaneous dopamine release is first detected in amperometry at E18 (Ferrari et al., in prep.). This distribution suggests, in contrast to the above studies, a role of synaptic dopamine on late stages of development like synaptogenesis.

### **3. The development of the striatal output is sequential**

The main function of the striatum is to collect the excitatory inputs from the cortex and to send the information processed by the GABAergic microcircuits to the other basal ganglia nuclei. How does the striatal output develop?

Early striatal projections from MSNs to the substantia nigra follow the segregation patch/matrix. Fluorescent anterograde axonal labeling in rats revealed that the majority of patch neurons sends the first striatonigral projections at E18 whereas a majority of matrix neurons do not form an efferent connection to the substantia nigra until the first postnatal week (Fishell and Van der Kooy, 1987 and 1989). In other words, MSNs in patches at embryonic stages transiently send projections to the dopamine enriched-cell pars compacta (Gerfen, 1984 and 1985).

A vast majority of the patch and matrix projections then innervate the substantia nigra reticulata from P2 until adulthood. Nevertheless, it remains still possible that patch MSNs selectively form synapses with dopaminergic dendrites of the pars compacta that extend into the pars reticulata (Fishell and Van der Kooy, 1989). In adult, the reminiscent matrix and patch compartments, distinguished by immunocytochemistry (see 2.4) both contain enkephalin and subP-expressing neurons and consequently have heterogeneous efferent projections to the GPe and to the SN respectively (Kawaguchi et al., 1990; Tokuno et al., 2002). Only dendritic fields of the MSNs in the patch and matrix are confined in the compartments whereas dendritic fields of the interneurons convey information between the compartments (Kawaguchi et al., 1989).

The developing striatum displays a unique mosaic organization based on neuronal segregation in two compartments (patch and matrix) which distinct function is still poorly understood. This organization in three dimensions appears extraordinarily complex and has to be taken into account in the study of the striatal development. The development of the direct and indirect pathways and how MSNs segregate into these two pathways is also poorly understood.

In the adult, cortical information processed by the output neurons of the striatum is targeted to SNr and GPi (direct pathway) and GPe (indirect pathway). MSNs of the “direct” pathway inhibit the activity of SNr and GPi neurons via GABAergic synapses and finally disinhibit thalamo-cortical neurons. On the contrary, MSNs of the “indirect” pathway projecting to SNr/GPi via GPe and STN (Fig. 1B) finally inhibit the activity of thalamo-cortical neurons. Thus, the “direct” and “indirect” pathways have opposite effects. In other words, activation of the “direct” pathway leads to the cortical excitation whereas activation of the “indirect” pathway causes cortical inhibition (For review, Deniau et al., 2007).

The two populations of MSNs are randomly distributed in the striatum (Shuen et al., 2008) (Kawaguchi et al., 1990). They are characterized by their neuropeptide content. MSNs from the “direct” pathway preferentially express substance P, dynorphin and neurokinin A whereas neurons from the “indirect” striatopallidal pathway preferentially express enkephalin and neurokinin B. D1 and D2 dopamine receptors are also preferentially segregated in the direct and indirect MSNs, respectively (Gerfen et al., 1990; Bolam et al., 2000). DARPP-32 (dopamine-associated receptor phosphoprotein) expressed in a postmitotic postmigrational manner from E14 in the rat developing striatum (Foster et al., 1987) is used as marker to identify D1-expressing striatal medium-sized spiny neurons of the “direct” pathway (Anderson and Reiner, 1991).

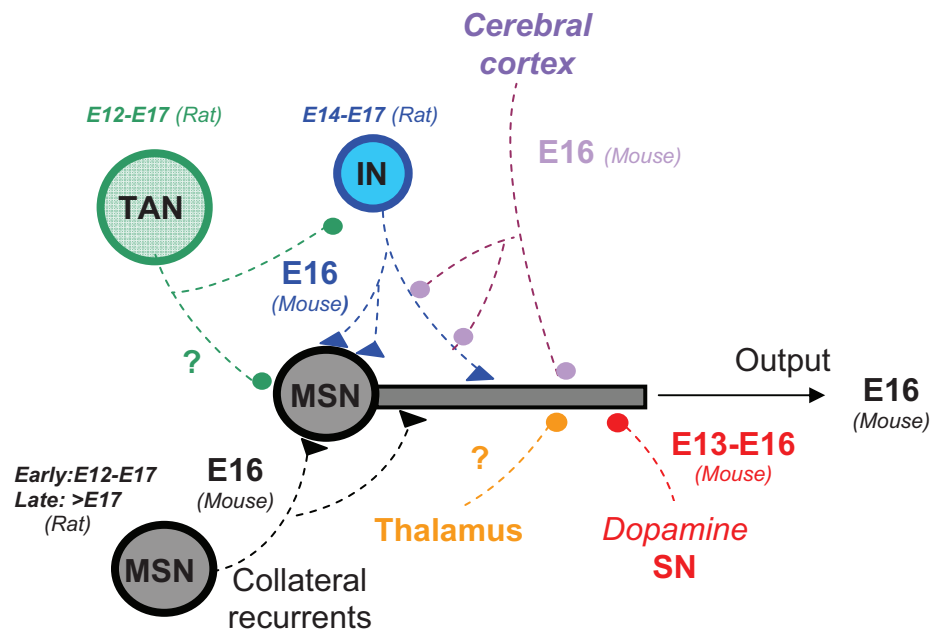


**Figure 11:** Birth dating of neurogenesis and synaptogenesis in the rat developing striatum.

Birth dating of the striatal neurons, MSNs (black), GABAergic (blue) and cholinergic (green) interneurons and functional synapse formation with intrinsic (black, blue, green) and extrinsic (from cortex (purple), thalamus (orange) and SN (red)).

## **Conclusion of chapter 1**

The striatum undergoes a long developmental process, starting from the embryonic day 8 in the mouse. Cell proliferation from the primordium of the striatum, the ganglionic eminences of the subpallium, generates a large number of MSNs and interneurons. Neuronal migration achieves the final location of the fated-striatal cells to the developing striatum. Then, differentiation, including the maturation of transmitter specification and outgrowth of axons and dendrites, enables synapse formation (Fig. 11). Consequently, by the end of the first postnatal week all the MSNs are synaptically connected. But it is only from the fourth postnatal week that the maturation of the striatum is achieved. At this time, MSNs display adult morphology, membrane properties and activity.

## **CHAPTER 2. Developmental activities of the GABAergic microcircuits of the striatum**

Early cellular activity is presumed to be a required partner to genetic programs at different stages of development such as neuronal proliferation, migration and differentiation (For review, Spitzer 2006). Maturation of neuronal networks starts from non-synaptically connected neuronal populations, displaying scattered spontaneous activity, to neuronal microcircuits communicating through thousands of synapses. This precise onset generates specific patterns of activity which leads to functional neuronal network. Features of the neuronal activity in the striatal network have been extensively studied after the first postnatal week in vitro and in vivo (Vergara et al., 2003; Carrillo-Reid et al., 2008; Mahon et al., 2003), but little is known about this network activity at perinatal stages. In this chapter we try to bring some clues based on our original study (see article 1 Dehorter) to characterize the type and timing of the immature network activities generated in the striatum at embryonic and perinatal stages?

### **1. The developing striatal network first generates isolated or gap-junction mediated calcium events at perinatal stages.**

Electrical recordings and intracellular calcium imaging at embryonic or perinatal stages revealed that cells communicate even before the presence of synapses, notably through paracrine signalling (Platel et al., 2005). Gap junctions might be used as a paracrine route to spread factors that modulate the fate of the surrounding cells (For review, Krysko et al., 2005) making up inaugural microcircuit (Crépel et al., 2007). During the embryonic period, immature striatum displays spontaneous activities consisting of intrinsic non-synaptic voltage-gated calcium currents (see article 1). Voltage-gated calcium channels, activated at depolarized membrane potentials, directly promote calcium entry. Calcium influx couples neuronal activity to metabolic processes. Both MSNs and interneurons display spontaneous asynchronous calcium spikes recorded from E14 with a peak around birth (Article 1 Dehorter).

Nifedipine, a L-type calcium channel blocker, and TTX, the Na<sup>+</sup> channel blocker, fully block spontaneous calcium spikes, suggesting that spontaneous calcium activity is strongly dependent on the extracellular calcium influx. Uncorrelated calcium spikes represent the dominant pattern between E14 and P10. Synchronous calcium plateaus in cell assemblies (SPAs), restricted to gap junction interconnected MSNs, progressively develop between E14 and P4 (see chapter 1- 2.1). SPAs are voltage dependent events that disappear when the cell is hyperpolarized (e.g -80 mV). Therefore, micro networks of intrinsically active neurons generate synchronized recurrent bursts during the perinatal period and form the earliest pattern of correlated activity in the striatum.

## **2. The developing striatal network then displays synaptically-driven events at the end of the first postnatal week.**

Initially restricted to few neurons, spontaneous activity follows synapse formation and becomes more complex, involving larger ensembles of neurons as the network matures and the density of functional synapses increases (Owens and Kriegstein, 1998). Spontaneous synchronous neuronal activity is a feature of the developing brain and has been observed in a wide range of peripheral and central structures such as the retina, cortex and hippocampus (Meister et al., 1991; Syed et al., 2004; Crépel et al., 2006; Allène et al., 2009). These synchronous events are described as Giant Depolarizing Potentials (GDP) and are generated by GABA and glutamate synapses. The exact mechanisms by which GDPs are generated and in particular the proportion of GABA to glutamate synapses needed is controversial notably in neonatal rat hippocampal slices. GABAergic depolarization would promote voltage-dependent bursting activity and glutamatergic inputs would trigger GDPs (Sipilä et al. 2005). This spontaneous coordinated activity is believed to control the formation of region-specific synaptic connections (Colin-Le Brun et al., 2004; Garaschuk et al., 2000; Kasyanov et al., 2004).

In the striatum, MSNs generate synchronous synapse-driven events during a narrow time window (P5-P7). This seems to be directly correlated to the increase of synaptic inputs to MSNs. Striatal network indeed displays synchronous global events/GDPs, when all MSNs receive glutamatergic and GABAergic afferents. In the same period, changes occur in the intrinsic membrane properties of MSNs.

The action of GABA and the characterization of the membrane potential of MSNs have been extensively studied at early and adult stages with different electrophysiological techniques like gramicidin-perforated patch (Bracci et al., 2006; Gustafson et al., 2006) or cell-attached recordings (Article 1 Dehorter; Dehorter et al., 2009). At resting membrane potential (around -70 mV at P2 and -80 mV in adult), GABA is depolarizing but not excitatory. GABA reversal potential is around -55 mV in the young (P2) and -65 mV in the adult MSNs, and both values are far from the threshold potential for spikes (around -35 mV; Dehorter et al., 2009, Fino et al., 2007). GABA-induced depolarization attenuates the voltage-dependent magnesium block of NMDA channels (Ben-Ari et al., 2007 for review). NMDA channels are highly permeable to calcium and prolonged NMDA EPSCs lead to sodium and calcium entry which in turn depolarize the MSNs membrane.

Based on that, it is clear that GABA alone is not sufficient to trigger action potentials in MSNs. Generation of spikes in neostriatal neurons are thus influenced by the combined action of both GABA and glutamatergic inputs, notably NMDA (Kita 1996; Bracci et al., 2006; article 1 Dehorter). During early development, MSNs do not express any inward rectification via KIR channels and, consequently have a depolarized resting membrane potential. They also display a high input resistance, mainly due to the lack of potassium channels (Tepper et al., 1998; Belleau and Warren, 2000; article 1 Dehorter). Hence, MSNs generate calcium activities between E14 and P8 because their membrane properties largely differ from the more mature ones, enabling immature MSNs to fire more easily compared to the adult MSNs.

### **3. Maturation of the intrinsic membrane properties of the output neurons of the striatum coincides with the disappearance of immature activities.**

Young and adult MSNs are likely to integrate excitatory synaptic inputs differently during development because of their differences in their membrane and firing properties. Intrinsic membrane properties of the MSNs rapidly mature (Tepper et al., 1998; Belleau and Warren, 2000 and article 1 Dehorter). From the beginning of the second postnatal week, resting membrane potential hyperpolarizes, input membrane resistance decreases and inward rectification develops in the MSNs. Notably, disappearance of the immature oscillations at P8-P10 in the MSNs is correlated to a hyperpolarised resting membrane potential, a decrease of input membrane resistance and increase of inward rectification (Article 1 Dehorter). Taken together these data mean that the output neurons of the striatum become less likely to spontaneously generate action potentials from the second postnatal week in vitro. Along those lines, calcium imaging recordings of striatal neuronal populations reveal sporadic, asynchronous activities in rat (P14-29) and mice (P12) striatal slices, involving only 4% of the cells (Carrillo-reid et al., 2008; article 1 Dehorter).

Discrete up and down states described in adult rat MSNs in vivo (Tseng et al., 2001; Wilson and Kawaguchi, 1996) are absent in young animals until P15. Down states are mainly due to an inwardly rectifying potassium conductance, dominating the membrane conductance at rest; the up states result from complex interaction between excitatory synaptic inputs and voltage-dependent outward K<sup>+</sup> conductances, activated below spike threshold. In young MSNs, such K<sup>+</sup> conductances are absent (Tepper et al., 1998; Belleau and Warren, 2000; article 1 Dehorter) and the tonic excitatory input from cortex and thalamus is low. In fact even if functional corticostriatal and thalamostriatal connections are present earlier, neurons have a low probability of spontaneous activity (Tepper et al., 1998; article 1 Dehorter).

Feedforward and feedback inhibitions regulate synaptic strength of the corticostriatal synaptic inputs in the adult MSNs with high level precision (For review, Plenz, 2003). Individual interneurons are responsible for feedforward inhibition and exert powerful IPSPs that can prevent or delay action potentials in MSNs (Gustafson et al., 2006; Koos and Tepper, 1999). MSNs control feedback inhibition via their reciprocal connectivity (Tunstall et al., 2002). Precise onset of feedforward and feedback inhibitions during the first postnatal week still remains unknown. The only available data concern the process of maturation of the GABAergic interneurons in the striatum which precedes the maturation of the MSNs. For instance, electrophysiological properties are more mature in striatal FS interneurons than projection neurons at P12–14 (Plotkins et al., 2005), and interneurons are already under continuous cortical influence by the end of the second postnatal week. GABAergic synaptic connectivity progressively increases during the first postnatal week and thus feedback inhibition is presumably weak at this time point (see chapter 1-2.2).

## Conclusion of chapter 2

Cerebral cortex is responsible for the initiation of any goal-directed behaviour, whereas subcortical structures determine when a given motor program should be selected and engaged. Changes in the intrinsic membrane properties and synaptic connectivity of the MSNs occur at the beginning of the second postnatal week. Interestingly, though corticostriatal spontaneous activities already appear at E16, movements are not generated because of the developmental retardation in the formation of functional cortico-spinal pathways (Gianino et al., 1999; For review, Vinay et al., 2002). In rodents, corticospinal tract progressively grows during the first postnatal week of life. The axons are located above the distal cervical region at P2, the distal thoracic region at P7 and the distal lumbar region at P9. All levels of the spinal cord are innervated at P11 (Gianino et al., 1999). Onset of goal oriented locomotor behavior is observed around P10 in mice (Article 1 Dehorter).

Walking Gait fully matures during the third postnatal week by P24 (Clarke and Still, 2001), which could correspond to the maturation of the motor units like the striatum (Article 1 Dehorter; For review, Grillner et al., 2005). The immature striatal network thus generates developmental activities and then shuts down before the largest increase of glutamatergic synapses occurs (from P15) and the corticospinal pathway becomes functional (from P11-P13).

GABAergic microcircuits of the striatum follow a developmental sequence consisting of a succession of intrinsic network activities similar to those described in the cortex and hippocampus where the principal neurons are glutamatergic (Crépel et al. 2007; Allène et al., 2009). This interesting data suggests that a conserved activity-dependent pattern of maturation exists for the developing networks. Nevertheless, striatum has a particular feature compared to the other structures cortex and hippocampus. The main output neurons (MSNs) exhibit very little spontaneous activity at rest in adult, and are activated only during goal directed movements. Adult striatal neurons are electrically silent because of a strong hyperpolarized resting membrane potential, powerful potassium currents and a synaptic control of the GABAergic interneurons. This silence is interrupted by converging cortical stimuli relying on the high

signal noise ratio that enable to generate an output signal associated with goal-directed movements.

In other words, coordinated sequence of events occurs in the cortico-striatal ensemble such as during transient developmental period ( $< P8$ ), high level of network activity is generated but with no external manifestations. Then developmental oscillations silence to avoid producing uncoordinated movements once the outputs of the basal ganglia are mature.

## **CHAPTER3: Is there a functional signature of Parkinson's disease in the adult striatum?**

Subcortical structures constitute key elements for motor planning. In particular, the striatum, the input nucleus of the basal ganglia, is instrumental for selection and initiation of motor behavior (For review, Graybiel et al., 1994) (see Fig. 3). Parkinson's disease (PD) is a neurodegenerative disorder characterized by the progressive loss of the dopaminergic neurons of the substantia nigra pars compacta. Reduced dopamine innervation of the striatum results in hypokinesia with difficulties to initiate motor tasks. The identification of early functional dysfunctions of the striatum in animal models reproducing the PD pathological features is decisive to find new therapeutic strategies to delay the onset of motor signs. In this chapter we focus on the impact of dopaminergic denervation on the activity of GABAergic microcircuits of the striatum in different models of PD and ask whether a common signature can be found.

Although PD aetiology is not fully understood, major biochemical processes involved in DA neurons death such as oxidative stress and mitochondrial inhibition have been identified (Dawson and Dawson, 2003). Decrease of the number of SNc dopaminergic neurons and the presence of intra-cytoplasmic inclusions (also called Lewy's bodies) containing alpha-synuclein, ubiquitin and parkin proteins (Schlossmacher *et al.*, 2002), are the cellular hallmarks of the disease. It is generally admitted that the first parkinsonian signs appear when DA neuronal death exceeds 80% of nigro-striatal terminals.

## **1. The animal models of Parkinson's disease are of two types: pharmacological and genetic.**

What would be a “realistic” rodent model of PD (Dawson et al., 2010)? It should be age-dependent and progressive. The motor dysfunction should include slowness of movements. Lewy bodies that contain alpha-synuclein and ubiquitin-proteosomal proteins should be present and the loss of DA neurons should be progressive (Chesselet, 2008). These requirements imply that rodent dopaminergic neurons have the same sensitivity as human ones to toxic and/or genetic factors which are still to be demonstrated. Both may have common genetic factors or compensatory mechanisms that protect their DA neurons. If true, conditional approaches that enable deletion or expression of mutated forms in adult animals must be the best option.

Although none of the current models recapitulates accurately key clinical and neuropathological features of PD, the use and constant improvement of both phenotypic and genetic models can significantly speed up progress toward understanding the pathophysiology of PD and finding innovative cures.

### **1.1. The pharmacological models of Parkinson's disease are based on the selective killing of central dopaminergic neurons**

The main chronic animal models of PD are based on toxins that specifically target the dopaminergic neurons. These include the 6-hydroxydopamine (6-OHDA) model in rodents (rats and mice) and the 1-methyl-4-phenyl-1,2,3,6-tetrahydropyridine ( $\alpha$ -MPTP) model in mice and primates (For review, Blum *et al.*, 2001; Blandini et al., 2008).

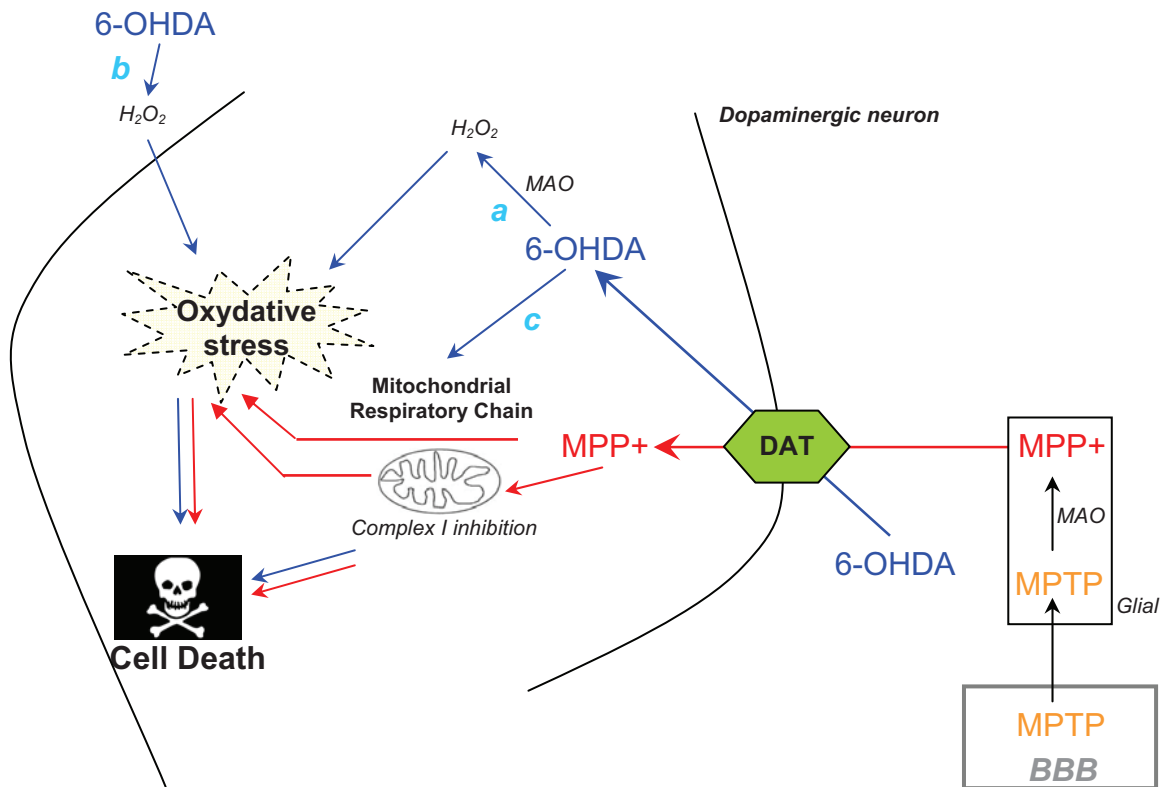


**Figure 12:** 6-OHDA and MPTP toxicity lead to the dopaminergic cell death.

6-OHDA (blue) enters the dopaminergic neuron via the dopamine transporter (DAT). Intracellular hydrogen peroxide formation ( $H_2O_2$ ) induced by MAO activity (a), extracellular auto-oxidation (b) and direct inhibition of the mitochondrial respiratory chain (c) lead to strong oxidative stress causing the cell death. MPTP (orange) injected peripherally, crosses the blood–brain barrier (BBB) and is transformed by glial enzyme MAO into the active compound MPP+ (red). The latter crosses the neuronal membrane by a specific uptake mechanism. Once inside the cells, MPP+ leads to a major inhibition of the respiratory chain but also to oxidative stress, both triggering cell death. *Modified from Blum et al., 2001.*

### TH immunostaining of the striatum

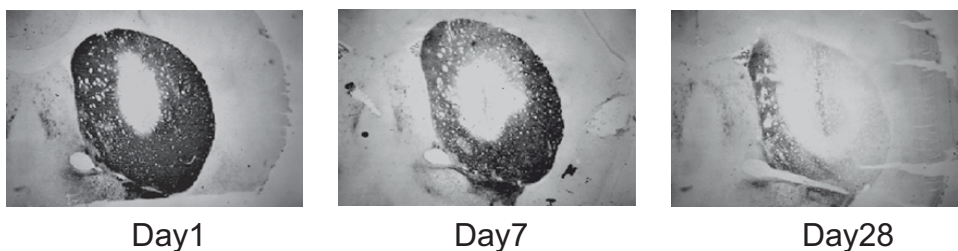


**Figure 13:** 6-OHDA intrastriatal injection leads to a progressive deprivation of the dopaminergic afferences in the striatum.

Immunohistochemical stainings for Tyrosine Hydroxylase (TH, dark staining) in the striatum at 1, 7 and 28 days post-lesion in adult rats. *From Blandini et al., 2008.*

### **1.1.1. The 6-OHDA rodent model allows studying the adult, dopamine-depleted basal ganglia.**

Among the specific neurotoxins targeting the catecholaminergic neurons, 6-OHDA is the most common tool for the selective destruction of the SNc dopaminergic neurons (For review, Blum *et al.*, 2001, Blandini *et al.*, 2008). Since it does not cross the blood brain barrier, 6-OHDA is directly injected by stereotaxy in deep cerebral structures such as the SNc, median forebrain bundle (MFB) or striatum, the latter for retrograde degeneration. The neurotoxin is specifically up-taken by the dopamine transporter (DAT), enters the dopaminergic neurons and induces an oxidative stress by inhibition of the mitochondrial respiratory chain (possibly by inhibition of the activity of complex I and IV). This process, amplified by the cytoplasmic calcium increase and the cellular ATP decrease, induces the degeneration of dopaminergic neurons (Dawson and Dawson, 2003) (Fig. 12, 13).

Versatility is a characteristic of the 6-OHDA model (For review, Blandini *et al.*, 2008). 6-OHDA intrastriatal injections induce the delayed and progressive retrograde degeneration of DA cells and provide an excellent tool for testing innovative treatments (e.g neuroprotection). On the contrary, direct injection in the SN or MFB can induce complete and immediate lesion. In this case, immediate consequences of the dopaminergic loss in the striatum can be studied. Therefore, the 6-OHDA model is suitable for studies during the symptomatic phase of the disease, when DA cell loss is still in progress.

### **1.1.2. The chronic MPTP primate model allows studying the presymptomatic phases of the disease**

MPTP has been discovered in the 80s for its toxicity on human dopaminergic neurons (Bradbury *et al.*, 1986). This neurotoxin which easily crosses the blood brain barrier is now largely used to obtain primates and mice models of PD. Inside the brain, MPTP is metabolised in MPP<sup>+</sup> (1-methyl-4-phenylpyridinium), a compound toxic for the dopaminergic neurons. MPP<sup>+</sup> is specifically uptaken by dopaminergic neurons by the

dopamine transporter (DAT) (For review, Storch et al., 2004) and interferes with the respiratory chain complex I leading to neuronal cell death and accumulation of free radicals (Fig. 12). MPTP also induces “parkinsonian” signs in mice but at much higher doses. Since the MPTP chronic model reproduces the evolution of the major motor symptoms of PD in primates and is reversed by L-dopa (Levodopa, a dopamine precursor) treatment (Langston et al., 1984), it became the main model for the study of the pre-symptomatic phases of the disease (For review, Blum *et al.*, 2001 and Bezard et al., 2003).

## **1.2. Genetic animal models of Parkinson’s disease show dopaminergic impairments and motor symptoms at old ages.**

Although the majority of human PD cases are sporadic, a small percentage (around 10%) is familial. Several loci and mutations in genes involved in the pathogenesis of familial PD have been described and some of them may be susceptible factors in the sporadic forms (For review, Dawson et al., 2002). Alternative to the toxic models, “physiological” models (transgenic mice) have been engineered. They enable to tackle the neurodegenerative process observed in the familial cases of PD. We will focus on two mouse models,  $\alpha$ -synuclein mutated and PINK1 KO (For review, Chesselet, 2008; Dawson et al., 2010).

### **1.2.1. Alpha-synuclein transgenic mouse models may help to understand molecular mechanisms of early and late stages of PD.**

Alpha-synuclein is a presynaptic protein encoded by the SNCA gene that has a role in neurotransmitter release. Alpha-synuclein is a soluble, natively unfolded 17 kDa protein, which acquires an anti-parallel conformation after binding to phospholipid surfaces. Its abundant expression in neurons and the selective localization to nerve terminals point to an important role for signaling and synaptic maintenance. Evidences implicate alpha-synuclein in synaptic vesicle recycling and neurotransmitter release in interaction with the vesicle co-chaperone cysteine-string protein- $\alpha$  (CSP $\alpha$ ) (Chandra et al., 2005).

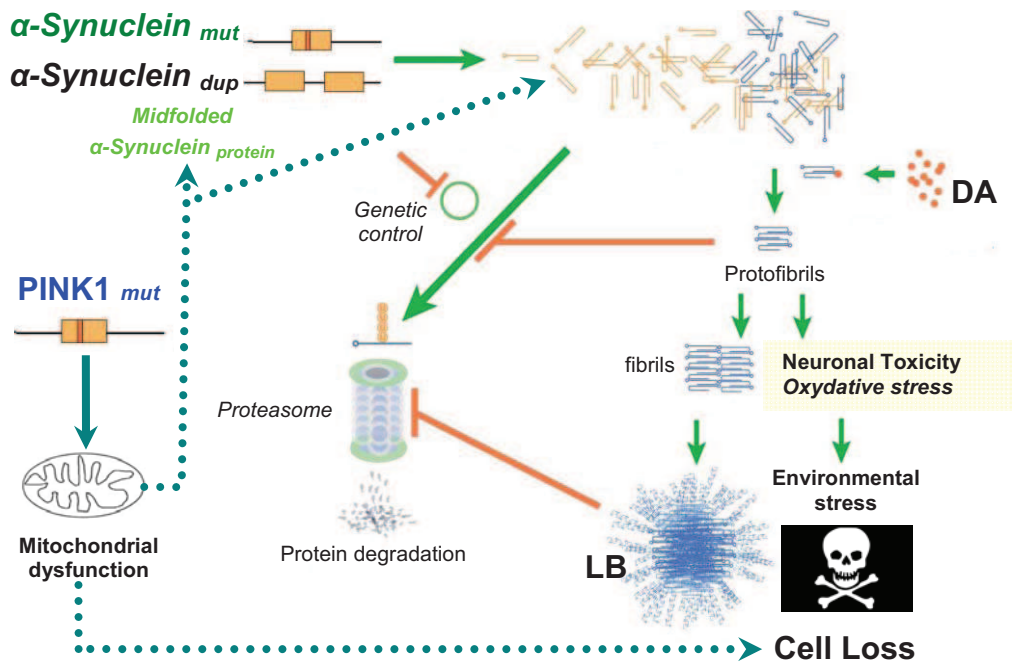


**Figure 14:** Mutations in the  $\alpha$ -synuclein and PINK1 genes induce the pathogenesis of Parkinson' disease.

Mutation (*mut*) or duplication (*dup*) in the  $\alpha$ -synuclein gene result in excessive intracellular accumulation of  $\alpha$ -synuclein leading to the formation of Lewy Bodies (LB). Two mechanisms potentiate the aggregation of LB: The degradation process of  $\alpha$ -synuclein in the proteasome, genetically controlled and inhibited by both the protofibrils and LB. Dopamine (DA) may also form stable products with protofibrils, inducing a neuronal stress which, combined to environmental stress, leads to neuronal loss. Mutation (*mut*) in the PINK1 gene induces mitochondrial dysfunction which would render DA neurons more vulnerable to injury. It could also trigger misfolded proteins formation that may contribute to neurodegeneration. Precise underlying mechanisms are unknown. *Modified from Eriksen et al., 2003 and Vila and Przedborski, 2004*

More particularly it has been recently shown that synucleins may function to sustain normal SNARE-complex assembly in a presynaptic terminal during aging (Burré et al., 2010). The rare missense mutations in the SNCA gene (A53T, A30P and E46K), duplication and triplication of the gene are responsible for autosomal dominant variants of PD with particularly early manifestation and full (100%) penetrance (Polymeropoulos et al., 1998).  $\alpha$ -synuclein is the major component of the Lewy body; it aggregates, assembles into fibrils and is supposed to be involved in neuroprotection (For review, Dawson, 2000), e.g. after oxidative stress (Kowall et al., 2000) (Fig. 14).

To mimic the human pathology,  $\alpha$ -synuclein knock-out (KO) or transgenic mice expressing high levels of human wild-type or mutated SNCA have been generated (Dawson et al., 2002). The KO or deficient mice for  $\alpha$ -synuclein do not show lesions of the nigral pathway but display impaired dopaminergic neurotransmission (Abeliovich et al., 2000). In contrast, in 3 to 4 month-old transgenic mice expressing wild-type human  $\alpha$ -synuclein there are cytoplasmic inclusions in several cerebral structures including SNc (Masliah et al., 2000). At the age of 12 months these mice show reduced tyrosine hydroxylase (TH) activity and DA content in the striatum and progressive behavioural deficits (Masliah et al., 2000). This suggests the requirement of a critical threshold of  $\alpha$ -synuclein accumulation to detect dopaminergic and behavioural deficits (Masliah et al., 2000). However, only transgenic mice expressing A53T alpha-synuclein under control of the mouse prion promoter (Giasson et al., 2002) exhibit alpha-synuclein aggregation, fibrils and truncation, and progressive age-dependent degeneration (For review, Fleming et al., 2005; Chesselet, 2008; Dawson et al., 2010). They exhibit altered DA content and elevated DA receptors in the striatum, together with a reduced postsynaptic transcriptional response to DA and impaired spontaneous locomotor activity by the advanced age of 18 months, features highly similar to early PD stages (Kurz et al., 2010). Progressively altered striatal levels of the endocannabinoid receptor CB1 and the mGluR-interactor Homer1 together with the loss of LTD indicate a relevant pathology of corticostriatal plasticity in these mice (Kurz et al., 2010).

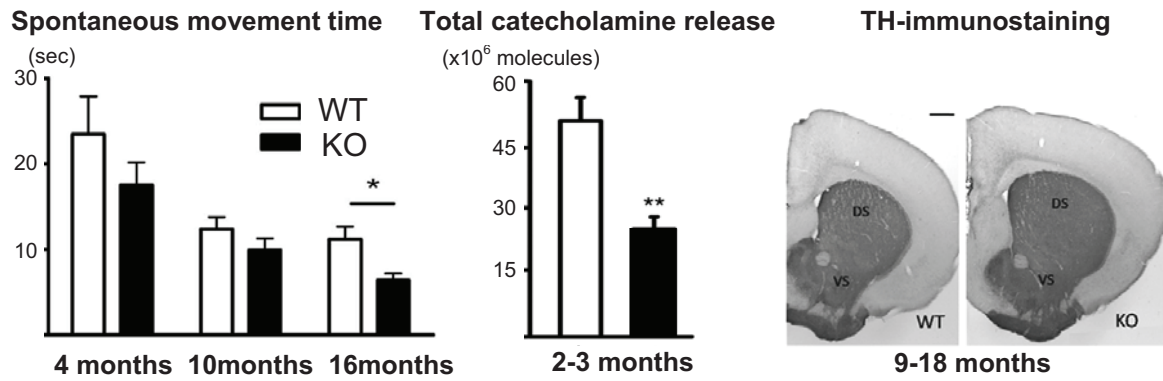


**Figure 15:** PINK1 KO mouse is a suitable model for the pre-symptomatic phase of PD.

PINK1 KO mice model show a progressive reduction of spontaneous movement (**left**). Such a motor deficit is associated with impaired dopamine release (**middle**) without detectable striatal dopaminergic denervation (**right**). Abbreviations: DS: Dorsal Striatum, VS: Ventral Striatum, WT: Wild Type, KO: Knock Out. Scale: 500  $\mu$ m; From Kitada *et al.*, 2007 and Gispert *et al.*, 2009.

### **1.2.2. The PINK1 mice model is suitable for the study of the earliest changes that might occur in Parkinson's disease.**

PINK1 (PTEN-induced kinase 1) is a ubiquitously expressed protein with a serine-threonine kinase domain and an N-terminal mitochondrial targeting motif. PINK1 is localized to the mitochondrial inter membrane space and membranes of the mitochondria (Silvestri et al., 2005). The kinase domain is supposed to face the cytosol suggesting that physiological substrates may reside in the cytosol. PINK1 gene activity is required for cell survival, and plays a role in DA neurotransmission and/or mitochondrial function (For review, Shen and Cookson, 2004). Mutations in the mitochondrial protein PINK1 cause autosomal recessive PD, with particularly early onset and mild progression (Valente et al., 2004; Gispert et al., 2009). G309D-PINK1 mutation of patients has been inserted into the orthologous mouse locus to generate PINK deficient mice (Gispert et al., 2009).

PINK1 KO mice already display significant reduction in weight at 1 year of age that suggests altered bioenergetics and mitochondrial dysfunction. They also show progressive and late motor impairments with no detectable reduction of locomotor activity until the age of 16 months (Fig. 15, left). These locomotor impairments in the aged PINK1 deficient mice might be caused by impaired dopaminergic transmission but not by dopaminergic neurodegeneration. Indeed, 2-3 months-old PINK1 KO mice already show a decrease in the evoked DA release recorded by amperometry in the striatum (Fig.15, middle), inducing an impaired synaptic plasticity at the corticostriatal synapses in the MSNs (Kitada et al., 2007). On the contrary, any reduction in the optical density of TH-positive terminals has been detected in the striatum of 9 and 18 months-old mice (Gispert et al., 2009) (Fig.15, right). Along the same line, nigral cell loss and Lewy bodies are not detectable in these mice even after 18 months (Gispert et al., 2009). Thus, although neurodegeneration is not detectable within transgenic mice lifespan and their life time remains unchanged, alterations suggest an accompanying pre-synaptic pathology which might model early stages of PD.

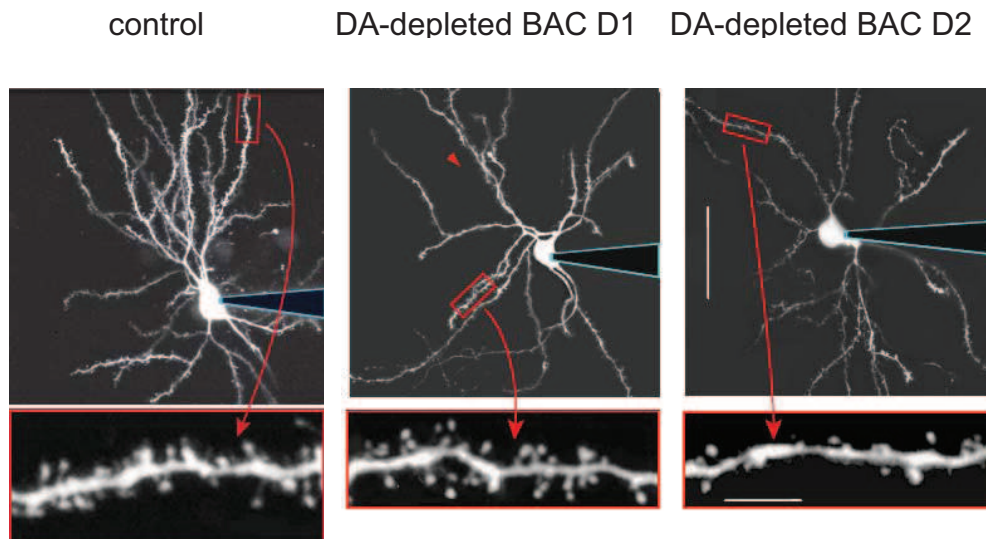


**Figure 16:** Dopamine depletion induces a reduction in spine density in the D2 but not D1 receptor-expressing MSNs

Labelling of MSNs with Alexa Fluor 594 in P17-25 mice in control (left) and 6-OHDA-treated slices (DA-depleted, middle and right). Note the decrease in spine density in the DA-depleted BAC D2 MSNs (right) compared to the control (left) or DA-depleted BAC D1 MSNs.

Scale: 40  $\mu\text{m}$ , magnification: 5  $\mu\text{m}$ . *Modified from Day et al., 2006*

## **2. The striatal network is altered by chronic dopamine depletion**

Dopaminergic neurons massively innervate the principal neurons of the striatum and dopamine assures the proper function of the striatal network (see Fig.3), Therefore dysfunction or degeneration of the dopaminergic system should lead to profound changes of this network.

### **2.1.The morphological characteristics of striatal neurons change in the chronic absence of dopamine.**

Loss of striatal dopaminergic innervation results in morphological changes in striato-fugal neurons. Indeed there is a significant loss of dendritic spines of MSNs in MPTP-treated monkeys (Smith and Villalba, 2008). In 6-OHDA-treated rats, spine loss is correlated to the decreased number of afferent glutamatergic synapses (see below) (Solis et al., 2007; Ingham et al., 1998). In vitro imaging studies in D1/D2-EGFP reserpinized mice and electronic microscopy of immunoreactive spines in 6-OHDA adult rats, have characterized more precisely this alteration. D2-containing striatopallidal neurons are selectively affected by spine loss (Fig. 16). L-type voltage gated calcium channels (LVGCC) may be involved in this process since genetic deletion or pharmacologic blockade of LVGCC in DA-depleted MSNs totally block spine loss (Day et al., 2006).

The absence of dopamine in the striatum also leads to compensatory mechanism in cell composition. Dye coupling between MSNs and between aspiny interneurons increases in DA-depleted rat striatum (Onn and Grace, 1999). Coupling allows the transfer of excitatory signals among clusters of neurons underlying synchronous activity among connected cells. The density of intrastriatal dopaminergic neurons, described in rat, monkey and human striatum (For review, Smith and Kieval, 2000; Cossette et al., 2005; Ibanez-Sandoval et al., 2010) increases after DA depletion.

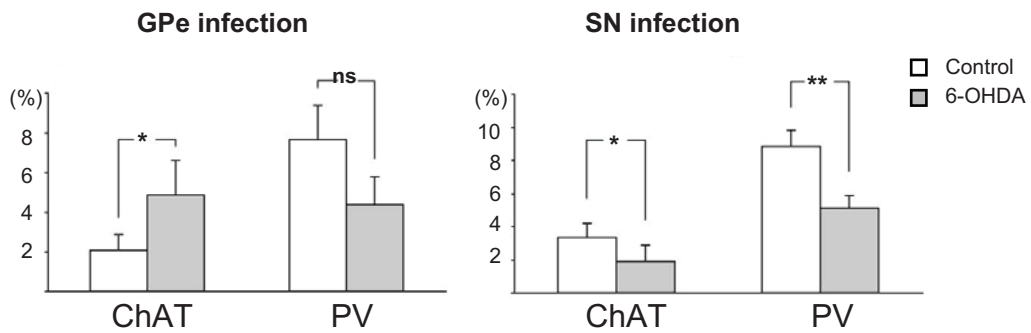


**Figure 17:** Synaptic reorganization between interneurons and projections neurons follows the striatal dopamine denervation.

Interneurons are trans-synaptically-labelled following rabbiies virus infection of the GPe or SNr in control and in 6-OHDA treated rats to determine the number of connected interneurons to the MSNs of the “indirect” and “direct” pathway. The population of cholinergic interneurons (ChAT) increases in the “indirect pathway” MSNs and decreased in the “direct” one. In contrast, the population of GABAergic PV-positive interneurons is reduced in the SNr-projecting MSNs only. *From Salin et al., 2009.*

Such an increase in cell density may underly a compensatory mechanism for the progressive DA loss (Bezard et al., 2003). The functional role of these striatal DA neurons intrinsic to the striatum is still under investigation.

Neuronal reorganization is reported in the 6-OHDA-treated rat striatum (Salin et al., 2009) (Fig. 17). The number of cholinergic interneurons innervating the striatopallidal MSNs increases whereas that innervating the striatonigral MSNs decreases. Moreover, the number of PV-expressing GABAergic interneurons decreases.

## **2.2. The glutamatergic cortico-striatal synapses become overactive in the absence of dopamine.**

Striatal dopaminergic depletion increases the excitability of MSNs *in vivo* (Tseng et al., 2001) and *in vitro*, in chronic (Azdad et al., 2009) and acute animal models (Fino et al., 2007). MSNs excitability is primarily due to the decrease of the rapidly inactivating A-type potassium current ( $I_A$ ) (Azdad et al., 2009). Intrinsic membrane properties such as resting membrane potential, input resistance or action of GABA in the MSNs are not changed after dopamine-depletion (Calabresi et al., 1993; Centonze et al., 2005, Azdad et al., 2009; Dehorter et al., 2009) suggesting a key role of the synaptic inputs for the excitability of the MSNs. Notably, excitatory inputs from the thalamus and cortex are increased in the DA-depleted striatum (Aymerich et al., 2006; Pang et al., 2001; Picconi et al., 2004; Centonze et al., 2006) (Fig.18A). Dopamine depletion acts on the glutamatergic signalling at the post-synaptic level in the MSNs by reducing the number of the excitatory synapses, which follows spines loss (see 2.1 and Fig. 18B). The remaining synapses are presumed to have enhanced responsiveness and consequently an increase in the dendritic excitability of the striatal neurons (Day et al., 2006). Since dopamine depletion slightly decrease the mean discharge rate of the cortico-striatal neurons (Mallet et al., 2006; Ballion et al., 2008), the enhanced excitatory inputs afferent to the MSNs should be due to a sprouting of the cortical afferents.

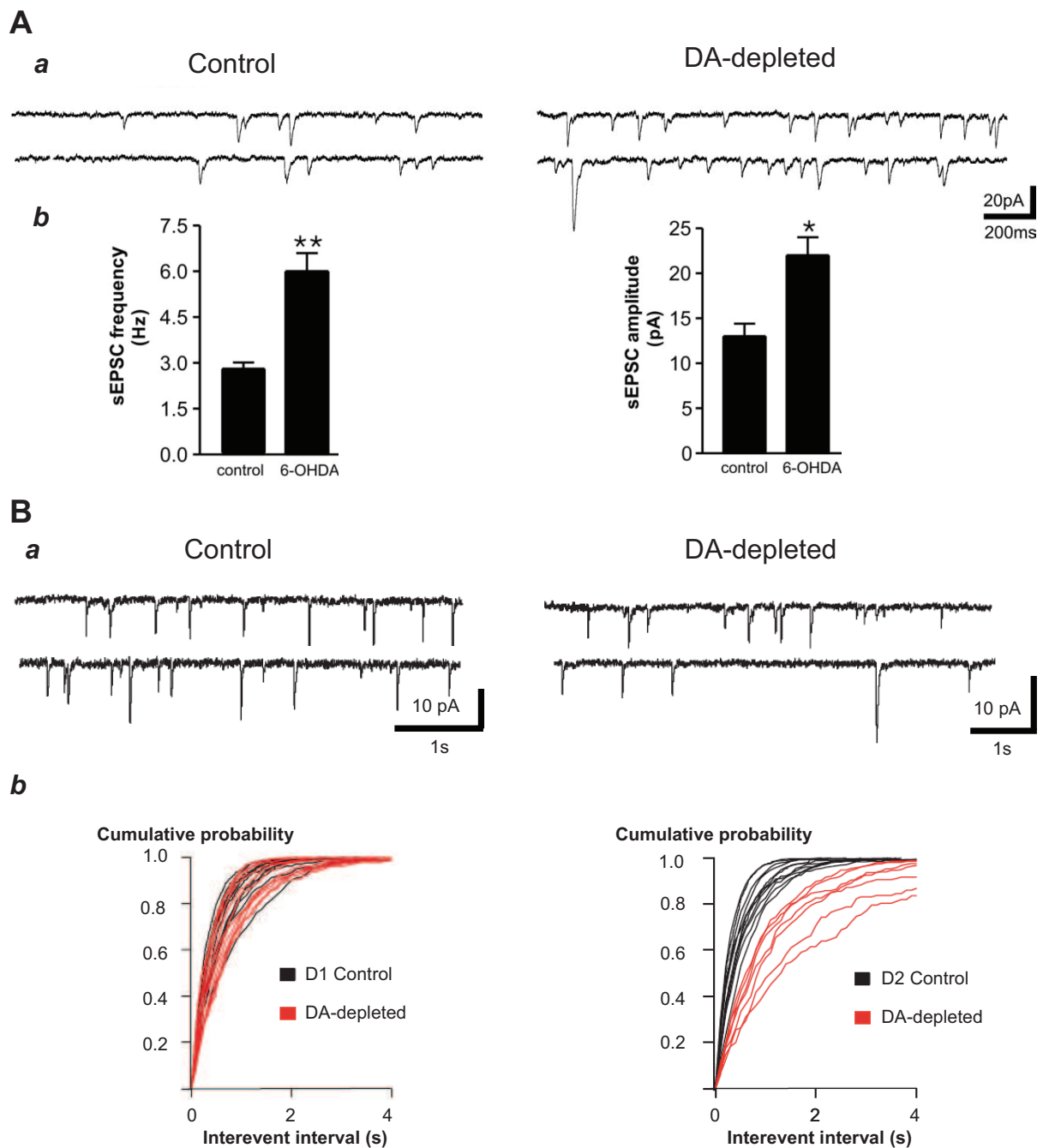


**Figure 18:** Dopamine depletion impairs the cortico-striatal pathway.

**A.** Traces of spontaneous excitatory synaptic currents (sEPSCs) in MSNs, recorded in voltage clamp at -80 mV in control (a, left traces) and SN/MFB-injected 6-OHDA (a, right traces) adult rat slices. Both sEPSC frequency (b, left) and amplitude (b, right) increase in the absence of dopamine.

**B.** Traces of miniature events (mEPSCs) recorded in D1 and D2 MSNs in voltage clamp at -60 mV in control (a, left traces) and 6-OHDA (a, right traces) conditions from P17-25 transgenic mice. Frequency of the mEPSCs is unchanged in the D1-expressing MSNs in absence of dopamine (a, top traces). On the contrary, D2-expressing MSNs display reduced mEPSCs frequency (a, bottom traces). Cumulative probability plots illustrate the invariance in the inter-event interval of mEPSCs between the control and the dopamine-depleted D1 MSNs (b, left) and an increase in the inter-event interval between the control and the dopamine-depleted D1 MSNs (b, right). *Modified from Centonze et al., 2006 and Day et al., 2006.*

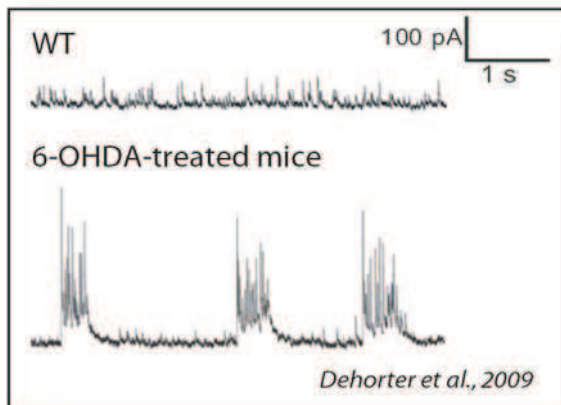
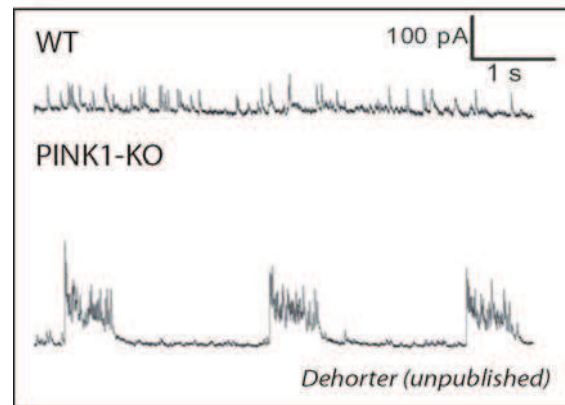
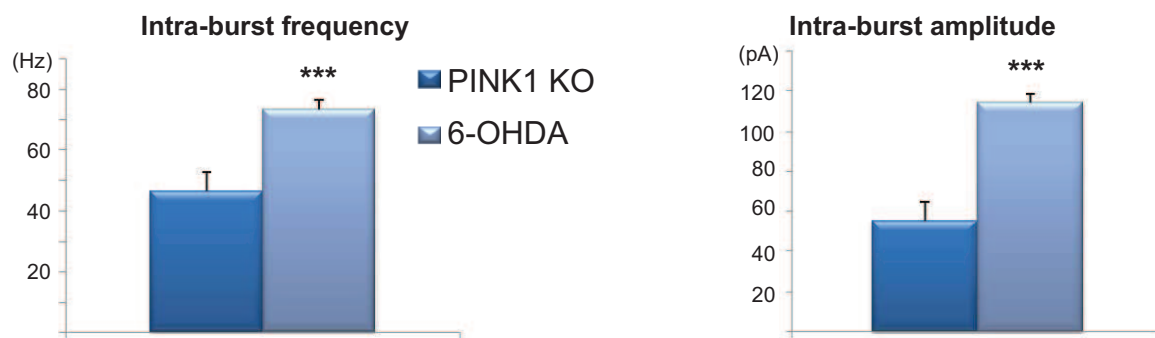
## **2.3. The GABAergic synaptic activity afferent to MSNs is increased and synchronized in the absence of dopamine.**

### **2.3.1 Dopamine depletion imbalances the direct and indirect striatofugal GABAergic pathways.**

Many studies have reported an imbalance between the direct and indirect pathways in parkinsonian state (Gerfen et al., 1990; For review, Surmeier et al., 2007). In vivo specific activation of the MSNs involved in the direct pathway via channel rhodopsin activation in transgenic D1R-GFP mice, fully rescues motor deficits induced by 6-OHDA-treatment (Kravitz et al., 2010). This clearly demonstrates that the indirect pathway is overactive in the absence of dopamine compared to the direct pathway. D1 receptor activation increases inwardly rectifying potassium current ( $I_{KIR}$ ) in MSNs and should serve to suppress activity evoked at membrane potentials close to the potassium equilibrium potential (For review, Nicola et al., 2000). Besides, D2-EGFP but not D1-EGFP MSNs display reduces opening of Kir2 potassium channels via a signalling through M1 muscarinic receptors in 6-OHDA-treated mice (Shen et al., 2007). This modulation leads to an increased dendritic excitability and synaptic integration of the striatopallidal neurons in parkinsonian state.

Secondary mechanisms might contribute to the imbalance observed in the DA-depleted striatum. Notably, feedforward inhibition worsens the D1/D2 imbalance by differentially regulating the time window of responses to cortical inputs for the two pathways in 6-OHDA-treated rats. Cortically evoked responses are narrower for striatonigral neurons and wider for striatopallidal neurons (Mallet et al., 2006). This striatal imbalance results from intrinsic mechanisms rather than cortico-striatal imbalance (Ballion et al., 2008). D2-expressing MSNs are more excitable to cortico-striatal stimulation than the D1-expressing MSNs in control, and DA-depletion increases this disparity (Flores-Barrera et al., 2010).

Lateral (feedback) inhibition is also disrupted in PD models. Synaptic connections between MSNs, differentially coupling the D1 and D2 MSNs are dramatically attenuated in 6-OHDA treated-rats (Tecuapetla et al., 2009; Taverna et al., 2008).

**A****B****C**

**Figure 19:** Bursting pattern of the spontaneous GABAergic currents is found in 40-50 % of the 6-OHDA and PINK1 KO MSNs.

Spontaneous GABAergic activity afferent to the MSNs in 19-month old PINK1 KO (**A**) and 2 month-old 6-OHDA mice (**B**) recorded in voltage-clamp at +10mV. Note the similarity in the pattern of activity in both conditions (bottom), compared to the control (WT: Wild type; top). **C.** Intra-burst frequency (left) and amplitude (right) of the spontaneous GABAergic events are significantly higher in 6-OHDA than in PINK1 KO MSNs. *Unpublished data from Dehorter et al..*

This impairment in the GABAergic connectivity would contribute to alter the strength in the glutamatergic connection of the DA-depleted MSNs.

### **2.3.2 GABAergic synaptic activity afferent to MSNs is increased and synchronized in the absence of dopamine.**

In vitro, the spontaneous GABAergic postsynaptic currents (IPSCs) afferent to the MSNs have a tonic, low frequency pattern. This pattern switches from tonic to bursting in 50% of the DA-depleted MSNs (Dehorter et al., 2009) (Fig. 19A). This switch is due to the shift of activity of a subtype of GABAergic interneurons, the LTS, in the chronic absence of DA. In contrast, after acute dopaminergic depletion with  $\alpha$ -MTP, Fino and collaborators did not show any difference of GABAergic interneurons activity compared to control (Fino et al., 2007). These data suggest that changes occurring in LTS interneurons occur in chronic DA-depleted conditions only.

In our preliminary study in the striatum of 19 months-old PINK1 KO (Gispert et al., 2009) or A53T-SNCA  $\alpha$ -synuclein surexpressing mice (Kurz et al., 2010), we also recorded the bursting and synchronized GABAergic pattern from 40 to 50% of the MSNs. This pattern is similar to that previously observed in 6-OHDA-treated mice (Dehorter et al., 2009) (Fig. 19B). Emergence of the bursting pattern of the spontaneous GABAergic inputs afferent to the MSNs could be directly related to the progressive alteration of the dopaminergic innervation in the striatum. Different intra-burst frequency and amplitude observed between the two models (Fig. 19C) could be attributable to different alteration of the dopaminergic system. Indeed, compared to the 6-OHDA toxin-based model that fully depletes the striatal dopaminergic innervation, genetic models displays deficient dopaminergic transmission (For review, Blandini et al., 2008; Gispert et al., 2009). Compensatory mechanisms in the 19 months-old PINK1 null mutants could have decreased the impact of deleterious effects on the dopaminergic system. Examining the progression of the pathological phenotypes in the MSNs of the transgenic mice, PINK1 and surexpressing  $\alpha$ -synuclein, should provide insights into the age-related progression of DA neurodegeneration.

### **Conclusion of chapter 3**

PD is a complex disorder requiring the investigation of good models recapitulating the major symptoms of the disease, namely the motor signs -rigidity, akinesia, resting tremor- and DA degeneration. Toxic-based and genetic models in primates and rodents both suggest that dopaminergic denervation alters the activity of the GABAergic microcircuits of the striatum. Striatal network undergoes profound physiological reorganization already from the early phase of the disease. Physiology of the neurons in the developing striatum from genetic models of PD is currently unknown. Investigating this should further our understanding of the time-course of the pre-symptomatic compensatory mechanisms which precede the dopaminergic cell loss.

# Article 1

*In preparation*

## **The Immature Activities of the Striatum Resume Before the Mouse Pup Walks**

Nathalie Dehorter, François Michel, Thomas Marissal, Yann Rotrou, Catherine Lopez, Marat Minlebaev, Roustem Khazipov, Yehezkel Ben-Ari and Constance Hammond

# Article 1

Déterminer comment le réseau immature du striatum génère des activités développementales est fondamental pour la compréhension de sa mise en place. Or si les propriétés électrophysiologiques des neurones de sortie du striatum, les neurones épineux de taille moyenne (MSNs), ont été largement étudiées après la première semaine de vie postnatale, peu de données concernaient l'activité de ces neurones, et plus largement l'activité de réseau du striatum, aux stades embryonnaires et lors de la première semaine de vie postnatale.

En utilisant une imagerie calcique ultra rapide (2-photons) et l'électrophysiologie de patch clamp sur des tranches immatures de souris transgéniques Nkx2.1 GFP (E14-P12) afin de différencier les MSNs (GFP négatifs) des interneurones (GFP-positifs), nous montrons que les MSNs génèrent trois types d'activités immatures spontanées : 1) Des pics calciques correspondants à des potentiels d'action calciques et générés par des canaux voltage-sensibles intrinsèques aux MSNs (dès E14 et maximum à P0). 2) Des plateaux calciques synchrones restreints à de petits groupes de MSNs interconnectés par des jonctions communicantes (de type gap), et générés par des canaux calciques voltage-sensibles (SPAs, dès E14 et maximum à P4). 3) Des activités synaptiques synchrones, médiées par les courants GABA et glutamate (P5-P7). Puis les MSNs deviennent silencieux in vitro comme dans les tranches adultes.

Entre E14 et P8, les propriétés membranaires des MSNs, sont très différentes de celles de l'adulte ce qui leur permet de générer spontanément les pics et plateaux calciques : leur résistance membranaire est forte et leur potentiel de repos est dépolarisé, essentiellement du fait de l'absence du courant potassique de la rectification entrante. L'apparition des événements synaptiques synchrones entre P5 et P7 correspond à la période où 100% des MSNs génèrent des courants glutamatergiques et GABergiques spontanés. C'est aussi la période où les courants glutamate de type NMDA sont fortement exprimés avant de décliner.

C'est seulement vers P8 que les synapses corticostriatales augmentent en densité et que les propriétés membranaires intrinsèques aux MSNs changent. Un comportement locomoteur dirigé se met en place à ce moment.

# The Immature Activities of the Striatum Resume before the Mouse Pup Walks

*Dehorter et al in preparation*

## **Abstract**

Immature networks initially generate primitive patterns required to modulate the formation of functional entities followed by specific oscillations signalling the emergence of coordinated behaviour. What are the mechanisms involved in this shift? The Basal Ganglia are particularly suitable to investigate these changes as striatal output medium spiny neurons (MSNs) must be silent to integrate cortical inputs and generate coordinated motor behaviour. Here using dynamic imaging, we report that voltage and synapse synchronised activities that engage large populations of embryonic and early neonatal MSNs are silenced around P10 when coordinated gait is first identified in pups. Using embryonic and neonatal MSN recordings, we show that this is mediated by activation of a  $K^+$  current that shifts the resting membrane potential to negative values and down regulation of the NR2CD-mediated component of corticostriatal responses. Our results demonstrate how immature activities stop in a central motor network precisely when the corticostriatal system is ready to generate coordinated locomotion. The sequence and mechanisms described here may provide information relevant to genetic motor disorders involving basal ganglia.

## **Results**

Using an imaging device, we quantitatively determined the maturation of pup locomotor behavior relying on belly contact with the platform, dynamic of paw contacts and vectorial displacement of the pup in an open field (24 x 16 cm) during one-minute tests.

P2 pups spent most of their time on the belly ( $35.3 \pm 4.9\%$ ,  $n = 16$ ) and barely moved in the field; Pivoting and crawling predominated in P3-P6 pups whereas P7-P8 pups have lifted their belly ( $2.9 \pm 0.7\%$  of time contact compared to  $17.8 \pm 1.6\%$  at P3-P6,  $n = 16$ ) and started walking but to a limited extent. Spontaneous quadruped walking with the ventral surface of the body off the floor was first observed at P10. Then the fraction of time during which the mice walked following a straight line significantly increased at P9-P10 ( $13.1 \pm 2.6\%$ , top) compared to P7-P8 ( $3.3 \pm 1.0\%$ ) ( $n = 14$ ) (**Fig. 1A, B, S1**).

Spontaneous calcium activities of the striatal network recorded in embryonic and postnatal brain slices using multibeam two photons imaging (a total of 260 movies covering 115 188 neurons) revealed a striking parallel change of activity during the same time window. The fraction of striatal neurons generating spontaneous immature activities in the field ( $444 \times 336 \mu\text{m}$ ) shifted from  $17.5 \pm 1.0\%$  at P0-P2 ( $58 \pm 4$  out of  $337 \pm 16$  fura 2-loaded cells,  $n = 51$  fields) and  $14.4 \pm 1.1\%$  at P3-P6 ( $34 \pm 3$  out of  $244 \pm 34$ ,  $n = 26$  fields) to  $4.2 \pm 0.8$  at P9-P10 ( $6 \pm 1$  out of  $148 \pm 12$ ,  $n = 15$  fields). At least half of the remaining activity at P10 and after was generated by interneurons (1) identified as GFP-positive neurons in slices from Nkx2.1-GFP mice (2) (**Fig. 1C, D and S2**). Before silencing, embryonic (E14-E18) and postnatal (P0-P8) MSNs exhibited a three phase sequence that parallels that reported for cortical networks: isolated  $\text{Ca}^{2+}$  spikes, correlated  $\text{Ca}^{2+}$  plateaus synchronized in small cell assemblies (SPAs) and synchronized synapse-driven network events similar to the Giant Depolarising Potential (GDPs, (3, 4) (**Fig. 2A, B**).

$\text{Ca}^{2+}$  spikes predominated from E14 ( $93.0 \pm 0.8\%$  of active cells,  $11.5 \pm 4.3\%$  of total fura-2 loaded cells,  $0.2\%$  cell pairs significantly correlated, 4 fields, 2268 cells) to P6 ( $88.9 \pm 4.1\%$  of active cells,  $10.2 \pm 2.1\%$  of total cells,  $0.6\%$  cell pairs significantly correlated, 12 fields, 3143 cells) and decreased to  $4.2 \pm 0.8\%$  of total cells at P10 ( $0\%$  cell pairs significantly correlated, 15 fields, 2357 cells) (**Fig. 2C, 5A**).

They had a mean frequency of  $0.021 \pm 0.002$  Hz (E14-E16) and their time to peak was of longer duration at E14-E18 ( $1.31 \pm 0.08$  s, 777 events, 18 fields) compared to P0-P5 ( $0.92 \pm 0.07$  ms; 207 events, 7 fields,  $p < 0.01$ ).

SPAs were rare at E14 ( $14.7 \pm 2.4\%$  of active cells, 6% cell pairs significantly correlated, 4 fields, 2268 cells), peaked at P4 ( $36.3 \pm 8.0\%$  of active cells, 5% cell pairs significantly correlated, 5 fields, 1166 cells) and were virtually absent at P9-P12 ( $0.2 \pm 0.1\%$ , 21 fields, 2862 cells). They had a similar mean frequency at E18 and P4 ( $0.014 \pm 0.003$  Hz vs  $0.017 \pm 0.002$  Hz,  $p = 0.8$ ) and a similar mean duration ( $14.4 \pm 1.9$  s vs  $14.5 \pm 0.8$  s,  $p = 0.1$ ) (107 and 89 events, 10 and 5 fields).  $\text{Ca}^{2+}$  spikes and SPAs were intrinsic, non synaptic, voltage-gated currents insensitive to ionotropic GABA and glutamate receptors antagonists (decreased by  $9.0 \pm 1.3\%$ ,  $p = 0.79$  and  $3.4 \pm 0.6\%$ ,  $p = 0.08$ , respectively; **Fig. 2D, E P2**) that differed in duration ( $1.31 \pm 0.08$  s vs  $16.46 \pm 2.01$  s at E14-E18,  $p < 0.001$ ).

Also, SPAs were likely to be generated by gap junction-connected cells since multiple labelling of 2-7 MSNs was observed after intracellular labelling of only one MSN (**Fig. S3, 5C**). These gap junctions were not specifically sensitive to carbenoxolone ( $100 \mu\text{M}$ ) or mefloquine ( $25 \mu\text{M}$ ). GDPs were absent before P5, appeared at P5-P7 (10 % of the recordings,  $n = 4$  out of 40 fields,  $13 \pm 4\%$  of the total imaged neurons (24 % cell pairs significantly correlated, 4 fields, 823 cells) and disappeared subsequently. They involved  $80.1 \pm 12.6\%$  of the active cells, had a mean frequency of  $0.06 \pm 0.02$  Hz and a mean duration of  $0.75 \pm 0.13$  s (81 events, 4 fields). They were synapse-driven events totally abolished by the antagonists of ionotropic glutamate and GABA receptors (**Fig. 2E P6**). They were present during the transition phase (P5 to P7) that preceded the expression of coordinated locomotion.

Targeted patch clamp recordings from 519 identified MSNs in striatal slices revealed that both the frequency of GABA<sub>A</sub> receptors-mediated spontaneous postsynaptic currents (sPSCs) and the percentage of MSNs generating GABA<sub>A</sub> sPSCs (n = 38) increased monotonously from E14 to P30 whereas the amplitude or kinetics of GABA<sub>A</sub> sPSCs did not significantly change from E16 to P30 (**Fig. S4, 5D**).

The resting membrane potential ( $V_{rest}$ ) determined from current–voltage (I–V) relationships of single NMDA channel recordings (5) progressively and significantly hyperpolarized by circa 10 mV from P2–P6 to P10 with no further change afterward (6) (**Fig. S5A**). The Driving Force of GABA ( $DF_{GABA}$ ) determined with single GABA channels was not significantly different between P2 and P30 (6) (**Fig. S5B**). The estimated values of  $E_{GABA}$  ( $DF_{GABA} - V_{rest}$ ) was however 15–20 mV more depolarised at P2 than P30 ( $E_{GABAA} = -55 \pm 5$  mV at P2 and  $-64 \pm 3$  mV at P30) (**Fig. S5C**). In spite of this depolarisation, focal application of the GABA<sub>A</sub> receptor agonist isoguvacine failed to generate action potentials in cell-attached recorded MSNs at P2 (n = 6, **Fig. S5D**) or P5 (n = 7, data not shown) reflecting the need for additional currents to generate them.

We therefore examined glutamatergic EPSCs and particularly NMDA receptor-mediated currents that could act with depolarising GABA to generate immature patterns and play an important role in developmental processes. With specific antagonists, the isolated AMPA and KA receptor-mediated sEPSCs revealed a monotonous increase of the fraction of MSNs generating AMPA or KA receptor-mediated sEPSCs as well as the mean frequency of AMPA and kainate receptor mediated sEPSCs suggesting that they are not involved in the transition phase. In striking contrast, the fraction of MSNs generating NMDA receptor-mediated sEPSCs shifted from less than 40% at P0, to more than 80% at P5–7 and decreased thereafter to 30% at P30, suggesting an abrupt increased contribution of NMDA receptor mediated signals prior to MSNs silencing (n= 12 at P0, 18 at P5–7 and 12 at P30; **Fig. S6, 5E**).

Cortico-striatal synapses provide most of the glutamatergic synapses to MSNs and are essential for motor coordination. Already at E16, Dil labelling (n = 5) of cortical fibers revealed staining in the striatum (**Fig. 3A**) and intrastriatal stimulation (500  $\mu$ s, 50 ms) in the presence of gabazine (10  $\mu$ M) evoked glutamatergic EPSCs in 10 % (n= 2/18) of the recorded MSNs.

The percentage of responding MSNs shifted to 76% (n = 10/13) at birth and remained stable subsequently (75% at P5-P7, n = 9/12; 78% at P30, n = 7/9). At P5-P7 but not at P10 or P30, single cortical stimulation evoked long lasting EPSCs ( $455 \pm 23$  ms, n = 7- vs  $51 \pm 1$  ms, n = 7;  $p < 0.001$ ) associated with a burst of action potentials (2-4 spikes, n = 10) (**Fig. 3B**). These EPSPs were strongly reduced by the NMDA receptor antagonist APV (by 46%, n = 5;  $p < 0.001$ ) but not by the AMPA/kainate receptor antagonist and GABA antagonist (NBQX 10  $\mu$ M and Gabazine 5  $\mu$ M, by 10%, n = 4;  $p = 0.46$ ). PPDA, the specific antagonist of the NR2CD subtype of NMDA receptors significantly reduced the gabazine-NBQX-resistant EPSCs by 52% at P6 (n = 5) and only by 2% at P10 (n = 5) (**Fig 3C**) suggesting a preferential role of these NR2 subunits. NR2CD subunits confer a reduced voltage-dependent magnesium blockade and longer kinetics to NMDA receptor signalling thereby facilitating the generation of NMDA receptor mediated events at resting membrane potential (7, 8). Therefore, evoked cortico-striatal stimuli generate at P5-P7 large EPSCs associated with bursts (**Fig. 3B**) and spontaneous GDPs (**Fig. 2A**) when a large NR2CD-mediated NMDA component is present (**Fig. 3C**). This suggests that NMDA receptors are tuned (via NR2CD subunits) to generate maximal activity during the transition phase before silencing of MSNs (9, 10).

Other intrinsic parameters including  $V_{rest}$ , the input membrane resistance ( $R_m$ ), the threshold potential for spike ( $V_{threshold}$ ), the delay of firing due to the early D-type  $K^+$  current ( $I_D$ ) and the inward rectifier  $K^+$  current ( $I_{K_{IR}}$ ) are instrumental in setting the cellular response of neurons to their synaptic inputs (**Fig. 4A, B**) (11).

The mean input resistance of MSNs was 4 times higher during the first postnatal week ( $1061 \pm 88 \text{ M}\Omega$ , P2-P6,  $n = 42$ ) than P10 ( $243 \pm 16 \text{ M}\Omega$ ,  $n = 8$ ) and P30 ( $83 \pm 6 \text{ M}\Omega$ ,  $n = 6$ ; **Fig. 4C**) but neither the spike threshold nor the delay to fire changed between P2 and P10 (**Fig. 4B, D, E**). The fraction of MSNs expressing  $I_{K_{IR}}$  was small until the end of the first postnatal week as shown with the linear I-V relationship evoked by hyperpolarizing steps between E16 and P6 ( $n = 41/44$ ) but not after ( $n = 8/8$  at P10 and  $n = 6/6$  at P30, **Fig. 4F**).

This shift and the parallel decrease of  $V_{rest}$  (**Fig. 4G**) will enhance the depolarisation needed to generate an action potential ( $V_{threshold} - V_{rest} = 34 \pm 3 \text{ mV}$  at P10 and  $46 \pm 1 \text{ mV}$  at P10  $n = 10$ ;  $p = 0.03$ ). Therefore, the expression of  $I_{Kir}$  and the decrease of  $R_m$  coincide with striatal silencing and elimination of immature network patterns at P10 (**Fig. 1B, 5B**).

## Discussion

The present results demonstrate that the in vitro mouse striatal network spontaneously generates immature activities as early as embryonic day 14 and is silenced at the beginning of the second postnatal week when all MSNs express  $I_{K_{IR}}$  and have reduced  $I_{NMDA}$  expression. This silencing happens just before the animal generates the first form of walking and thus immature activities do not interfere with coordinated locomotion.

We have identified two phases in the maturation process of striatal output neurons, striatal network and coordinated locomotion, the immature and the adult-like phases (**Fig.5**). During the immature phase (from E 14 to P8) the striatal network is active with a pattern of voltage-gated and synapse-driven immature activities. MSNs are more excitable than adults because they lack the typical  $K^+$  currents ( $I_{K_{IR}}$  and  $I_D$ ), have a high input resistance and express the NR2CD component of NMDA currents. Pups at that stage generate crawling movements only. Then, quite abruptly, between P8 and P10 the adult-like phase begins.

MSNs immature activities disappear and are replaced in vitro by the adult silence. The triggering mechanism includes the general expression in all MSNs of  $I_{K_{IR}}$  associated with a drop of membrane resistance, hyperpolarization of  $V_{rest}$  and  $E_{GABA_A}$  and a loss of NR2CD-mediated current leading to a much reduced contribution of NMDA signals to corticostriatal EPSPs because of the stronger voltage-dependent  $Mg^{2+}$  block of adult NMDA receptor subunits (12, 13). At the same period pups begin to walk in a coordinated manner.

During the following three-four weeks, until the adult stage, quantitative (but not qualitative) changes take place in MSNs including development of intrinsic membrane properties and spine acquisition (14, 15), increased number of glutamatergic and GABAergic synapse (16), acquisition of the capacity to fire only in response to precisely synchronized excitatory inputs (For review, (17, 18)).

Our recordings of embryonic and early postnatal MSNs thanks to their clear identification as Nkx-GFP negative neurons in transgenic mice have enabled to identify the early transient developmental stage (immature stage) that has not been observed previously. In parallel, the converging single channel recordings essential to correctly determine  $V_{rest}$  in immature neurons and dynamic two photons imaging technique needed to record large neuronal ensembles provided direct evidence of the coordinated maturation of cellular and network patterns.

In a more global perspective, the motoneurons (19), and upper centers (4) mature first and lastly the descending pathways (P9-P11) (20-22). How this entire system is coordinated is not known. Present results suggest that corticostriatal NMDA-driven ongoing currents play a role in the transition from immature to adult-like MSNs. The nigro-striatal dopaminergic pathway may also play a role since the second wave of innervation begins just during the same transition phase. This should also help to birth date the onset of dysfunction of the striatum in genetic diseases like Huntington's or familial forms of Parkinson's disease.

## **Methods**

### **Gait development analysis**

Gait development was assessed in Swiss newborn mice (n=16) from two different litters (Janvier SAS, Le Genest Saint Isle, France) from postnatal day 2 (PND 2, day of birth: PND 0) to PND 12. Each pup was tested twice a day, with a 20 minutes delay between the two tests. We recorded the mouse locomotion with two cameras simultaneously recording the pup in the visible and the infrared. We acquired the contact points of the paws with the surface depicted by brightly illuminated areas, based on the FTIR principle (Frustrate Total Internal Reflexion) of the light. The enhanced contrasts between contact and non contact areas enabled to perform the automatic detection of the mouse contacts with custom-made software (NeoGAIT). Each contact was semi-automatically tagged as: right or left forelimb, right or left hindlimb, tail, head, belly or unspecified. Distribution of the tagged contacts as a function of time gives variables for the displacement (travelled distance and duration of the gait) and the locomotion (stance time: duration of a contact and swing time: duration without any contact).

### **Embryonic and postnatal slice preparation**

Experiments were performed in wild type C57BL/6 mice (Janvier, France) or Nkx2.1-GFP mice obtained by crossing Nkx2.1-CRE C57BL/6 mice (Jackson lab) and a reporter strain (kindly provided by G. Fishell lab). Slices were obtained from embryos at embryonic day E14, E16 and E18 (E0 being the morning after detection of the vaginal plug). Pregnant mice were decapitated under xylazine (Rompun 2%; used at 0.05%) and ketamine (Imalgene 1000; used at 50g/L) anesthesia (Volume injected: 0.2 mL/g). Embryos were excised from the uterus and kept in ice-cold oxygenated solution containing (in mM): 110 choline, 2.5 KCl, 1.25 NaH<sub>2</sub>PO<sub>4</sub>, 7 MgCl<sub>2</sub>, 0.5 CaCl<sub>2</sub>, 25 NaHCO<sub>3</sub>, 7 glucose.

Postnatal C57BL/6 mice (P0-P45) were killed by decapitation under isoflurane anaesthesia. Coronal, or oblique parasagittal slices (400  $\mu\text{m}$  thick) were cut in the ice-cold oxygenated choline solution. During the recovery period, all types of slices were placed at room temperature with standard artificial cerebrospinal fluid (ACSF) saturated with 95%  $\text{O}_2$ /5%  $\text{CO}_2$  and containing the following (in mM): 126 NaCl, 3.5 KCl, 1.2  $\text{NaH}_2\text{PO}_4$ , 1.3  $\text{MgCl}_2$ , 2  $\text{CaCl}_2$ , 25  $\text{NaHCO}_3$ , 11 glucose.

### **Patch clamp recordings**

We performed all recordings at 32°C. Cells were visualized with infrared-differential interference optics (Axioskop2; Zeiss). For whole-cell voltage-clamp recordings of postsynaptic  $\text{GABA}_A$  and glutamatergic currents, the pipette (6–10  $\text{M}\Omega$ ) contained the following (in mM): 120 Cs-gluconate, 13 CsCl, 1  $\text{CaCl}_2$ , 10 HEPES, 10 EGTA, pH 7.2–7.4 (275–285 mOsm). We used the CsGlu solution to record spontaneous IPSCs ( $\text{GABA}_A$  currents) at the reversal potential of the glutamatergic events (+10mV). For glutamatergic EPSCs, recordings were performed in the continuous presence of bicuculline (10  $\mu\text{M}$ ), a  $\text{GABA}_A$  antagonist, at -80 mV and +40 mV to separately detect AMPA and NMDA sEPSCs, respectively (23).

Because sEPSCs recorded at + 40 mV may consist of both AMPA and NMDA components the NMDA component was estimated thanks to their kinetics (the NMDA decay time is longer than the AMPA one) or to its sensitivity to the AMPA receptor antagonist, NBQX (10 $\mu\text{M}$ ). The kainate component was estimated at -80 mV in the continuous presence of APV (40 $\mu\text{M}$ ), the selective NMDA receptor antagonist and NBQX (1 $\mu\text{M}$ ), the preferential antagonist of AMPA receptors.

Spontaneous postsynaptic currents (sPSCs) analysis was based on recordings of 180 sec duration at a given membrane potential. Recordings were transferred into the Mini-Analysis Program (version 5.1.4; Synaptosoft, Decatur, GA). All events visually judged as PSCs were manually indicated for additional analysis in Mini-Analysis 5.1 and fully characterized by the following parameters: rise time (10%–90%), amplitude, and decay time ( $\tau$ ). To discriminate mixed AMPA/Kainate events in the absence of specific receptor antagonists, the standard deviation given by the fit of each event was used to determine whether one or two exponentials best fitted the decays (24). Recorded cells were identified as MSNs from their morphological characteristics (axon, dendritic tree...) after the first postnatal week. At embryonic and perinatal stages, when these characteristics are absent, we used Nkx2.1-GFP mice where striatal interneurons (Nkx2.1 positive) express GFP but MSNs (Nkx2.1 negative) do not (25).

For current clamp recordings, the pipette contained (in mM): 15 KCl, 5 NaCl, 125 KMeSO<sub>4</sub>, 10 HEPES, 2.5 Mg-ATP, 0.3 Na-GTP. For single channels recordings (6) the pipette (4–5 M $\Omega$ ) contained the following (in mM): 120 NaCl, 20 TEA-Cl (tetraethylammonium chloride), 5 KCl, 5 4-aminopyridine, 0.1 CaCl<sub>2</sub>, 10 MgCl<sub>2</sub>, 10 glucose, 5 GABA, 5 isoguvacine, 3 CsCl, 10 HEPES-NaOH buffered to pH 7.2–7.3; osmolality of 300–320 mosmol.

For single NMDA channels, pipettes were filled with nominally magnesium-free ACSF containing the following (in mM): 140 NaCl, 3.5 KCl, 1.8 CaCl<sub>2</sub>, 10 HEPES, 10 NMDA, 10 glycine, 1 strychnine buffered to pH 7.43; osmolality of 300–320 mosmol. To identify the morphology of neurons recorded in cell-attached configuration, we repatched them with a conventional whole-cell electrode containing neurobiotin (Abcys). The single-channel currents were filtered at 1 kHz (GABA<sub>A</sub> channels) or 3 kHz (NMDA channels) and digitized at 10 kHz.

Multilevel and short (2 ms) openings were discarded during analysis.  $I-V$  relationships were performed by measuring amplitude of unitary GABA and NMDA currents evoked by steps from -120 to +40 mV. Histograms of cursor-measured amplitudes allowed determination of the mean unitary current amplitude at each voltage tested.

Series resistance ( $R_s$ ), membrane capacitance ( $C_m$ ), and input resistance ( $R_{input}$ ) were determined by on-line fitting analysis of the transient currents in response to a + 5 mV pulse at -70 mV. Criteria for considering a recording included  $R_{input} > 100 \text{ M}\Omega$ ,  $R_s < 25 \text{ M}\Omega$ , with  $R_s < 30\%$  change. Average values are presented as means SEM and statistical comparisons were performed with the Student's  $t$  test (SigmaStat 3.1, Origin 5.0), Mann-Whitney rank sum test (SigmaStat 3.1) or one-way anova (Tukey's Test as post hoc test; SigmaStat 3.1). The level of significance was set as  $P = 0.05$ . Set of datas without any statistical differences were grouped as follow: P2 (P0-P2), P6 (P3-P6), P8 (P7-P8), P10 (P9-P10) and P12 (P11-P12) except for figures 2C, 3, 4G and supplemental figures s4, s5 and s6.

For current-voltage (I-V) curve analysis, we measured voltages at the end of each current step episode of hyperpolarization (950 ms). The inward rectification (IKIR) is detected when the I-V relationship below -90 mV is far from linearity up to -120 mV. To compare immature and adult MSNs adaptation, corresponding to the delayed inward current ( $I_D$ ), we measured the first interspike interval of the depolarizing steps. We then pooled the slopes values of the linear regression lines and compare their distribution as function of time.

The threshold potential for  $\text{Na}^+$  spikes was estimated in whole-cell (current clamp) recordings by applying successive depolarizing steps (duration 250 ms, 950 ms) or by evoking spikes by cortical stimulation, both from the value of  $V_{rest}$  (-70 mV from E16-P7 and -80 mV for the adult).

## Calcium Imaging

Slices were incubated in the dark with fura-2 AM for 30 minutes in a chamber containing 2.5 ml of oxygenated and warmed up ACSF (35°–37°C) with 25µL of a fura-2 AM solution (1 mM, in 100% DMSO; Molecular Probes). Imaging was performed with a multibeam two-photon laser scanning system (Triscope-LaVision Biotec) coupled to an Olympus microscope. Slices were imaged using a high-numerical-aperture objective (20X, NA 0.95, Olympus). Images (4 x 4 binning) were acquired via a CCD camera (La Vision Imager 3QE) with a time resolution of 115 to 147 ms. Size of the scan field (500 x 400 µm) and duration of the movies (1000-3000 images) were unchanged.

Patch clamp recordings were coupled to imaging to correlate calcium signal to electrical activity of a particular neuron. Fura pentapotassium salt (30 µM; Invitrogen) was added to the pipette solution to keep cell fluorescent during electrophysiological recordings. Analysis of the calcium activity was performed with custom-made software (3) written in Matlab (MathWorks). The contour of each loaded cell is semi-automatically detected and its fluorescence is measured as a function of time. Active cells are neurons exhibiting at least one calcium event of at least 5% deflection within the period of recording. We considered an event with a minimal duration of 30 frames as a 'calcium plateau'. In slices from Nkx2.1-GFP mice, we first took images of the GFP-expressing neurons (laser at 910 nm) before acquiring spontaneous fura-2 fluorescence changes. During the analysis, GFP-expressing neurons are identified by superposing the two fields.

## **Drugs.**

Drugs were prepared as concentrated stock solutions and diluted in ACSF for bath application: bicuculline 20  $\mu$ M, Gabazine 5  $\mu$ M, GABA<sub>A</sub> receptor antagonists; D-amino pyruvate (D-APV) 40 $\mu$ M, a NMDA receptor antagonist and (+/-)-cis-1-(phenanthren-2-yl-carbonyl)-piperazine-2,3-dicarboxylic acid (PPDA) 100 nM, a NR2C/D subunits antagonist; 6-cyano-7-nitroquinoxaline 2,3-dione (CNQX) 10 $\mu$ M, and 2,3-dihydroxy-6-nitro-7-sulfamoyl-benzo[f]quinoxaline (NBQX) 1-10 $\mu$ M, the AMPA/ kainate receptor antagonists. Isoguvacine 100 $\mu$ M, a GABA<sub>A</sub> receptor agonist, was locally applied. All drugs were purchased from Sigma (St Louis, MO, USA).

## **Immunocytochemistry.**

To visualize the morphology and identify the recorded cells we revealed the neurobiotin injected during whole cell recordings. After 12h in paraformaldehyde (3%) at 4°C, the sections were rinsed in PBS, left 12h in PB-sucrose 20% and then at -80°C for at least 2h. They were thawed at room temperature, rinsed in PB and incubated 30 min in 1% H<sub>2</sub>O<sub>2</sub> in PB. Slices were washed with PB and KPBS and incubated for 12h in ABC complex at a dilution of 1: 100 in KPBS + 0.3% triton (Abcys).

They were rinsed in KPBS and incubated for approximately 10 min in 3,3' diaminobenzidine (DAB 0.7 mg/ml) with peroxide (0.2 mg/ml) (Sigma Fast), rinsed, mounted in Crystal/Mount (Electron Microscopy Sciences), coverslipped and examined. Dendritic and axonal fields were reconstructed for morphological analysis using the Neurolucida system (MicroBrightField Inc., Colchester, VT).

For double immunocytochemistry Neurobiotin-Nkx2.1, slices were cryoprotected in PB with 20% sucrose, freeze-thawed in isopentane and rinsed in PB. Slices were then incubated in PBS Triton 0.3% normal goat serum (NGS, 2%) for 1 hour and then in Nkx2.1 antibody (1:10) for 4 days at room temperature (RT).

After thorough rinsing, slices were incubated for 90 min at RT in alexa-488 goat anti-mouse (1:300; Molecular Probes, Leiden, the Netherlands) in PBS and NGS 2% overnight. After thorough rinsing, slices were again incubated in PBS and Cy3 streptavidine antibody(1:300), rinsed again and incubated with secondary antibody for 1 hour to label the recorded cell. After thorough rinsing, slices were mounted in fluoromount, coverslipped and examined with a confocal microscope (Zeiss LSM 510).

## Reference List

1. L. Carrillo-Reid *et al.*, *J. Neurophysiol.* **99**, 1435 (2008).
2. S. Nobrega-Pereira *et al.*, *Neuron* **59**, 733 (2008).
3. V. Crepel *et al.*, *Neuron* **54**, 105 (2007).
4. C. Allene *et al.*, *J. Neurosci.* **28**, 12851 (2008).
5. R. Tyzio *et al.*, *J. Neurophysiol.* **90**, 2964 (2003).
6. N. Dehorter *et al.*, *J. Neurosci.* **29**, 7776 (2009).
7. S. S. Kumar, J. R. Huguenard, *J. Neurosci.* **23**, 10074 (2003).
8. A. M. Binshtok, I. A. Fleidervish, R. Sprengel, M. J. Gutnick, *J. Neurosci.* **26**, 708 (2006).
9. S. M. Logan, J. G. Partridge, J. A. Matta, A. Buonanno, S. Vicini, *J. Neurophysiol.* **98**, 2693 (2007).
10. W. K. Lau, P. W. Lui, C. K. Wong, Y. S. Chan, K. K. Yung, *Neurochem. Int.* **43**, 47 (2003).
11. E. S. Nisenbaum, C. J. Wilson, *J. Neurosci.* **15**, 4449 (1995).
12. H. Monyer, N. Burnashev, D. J. Laurie, B. Sakmann, P. H. Seeburg, *Neuron* **12**, 529 (1994).
13. A. W. Dunah *et al.*, *J. Neurochem.* **67**, 2335 (1996).
14. M. L. Belleau, R. A. Warren, *J. Neurophysiol.* **84**, 2204 (2000).
15. J. M. Tepper, N. A. Sharpe, T. Z. Koos, F. Trent, *Dev. Neurosci.* **20**, 125 (1998).
16. N. A. Sharpe, J. M. Tepper, *Neuroscience* **84**, 1163 (1998).
17. C. J. Wilson, *Prog. Brain Res.* **99**, 277 (1993).
18. S. Charpier *et al.*, *Neuropharmacology* **38**, 1699 (1999).
19. K. D. Walton, R. Navarrete, *J. Physiol* **433**, 283 (1991).
20. S. Gianino *et al.*, *Brain Res. Dev. Brain Res.* **112**, 189 (1999).

21. F. Clarac, E. Pearlstein, J. F. Pflieger, L. Vinay, *J. Comp Physiol A Neuroethol. Sens. Neural Behav. Physiol* **190**, 343 (2004).
22. S. Chakrabarty, J. H. Martin, *J. Neurosci.* **30**, 2277 (2010).
23. L. Groc, B. Gustafsson, E. Hanse, *J. Neurosci.* **22**, 5552 (2002).
24. J. Epsztein, A. Represa, I. Jorquera, Y. Ben-Ari, V. Crepel, *J. Neurosci.* **25**, 8229 (2005).
25. O. Marin, A. Yaron, A. Bagri, M. Tessier-Lavigne, J. L. Rubenstein, *Science* **293**, 872 (2001).

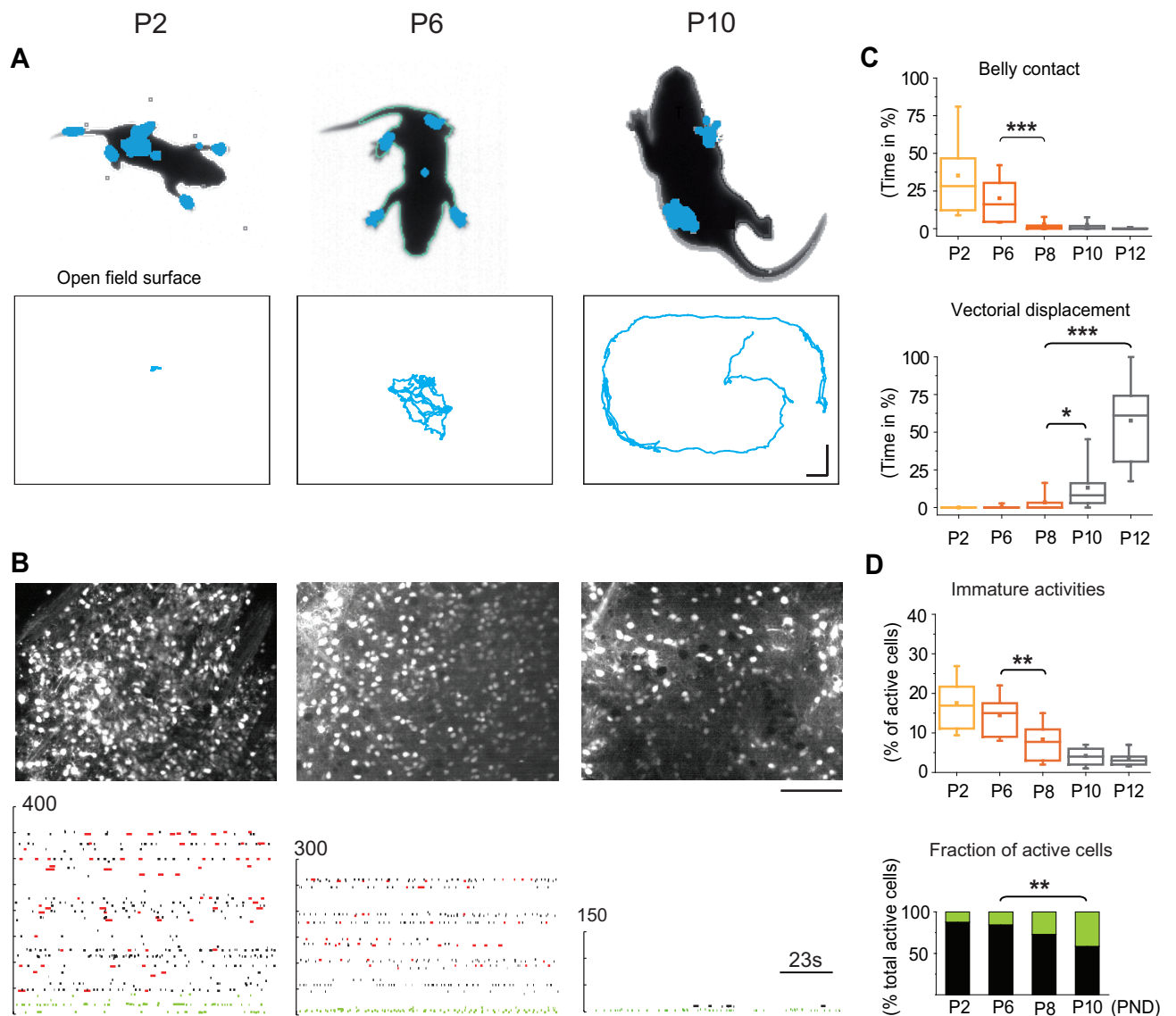


**Figure 1: Maturation of the striatal output precedes the acquisition of coordinated locomotion.**

**(A)** (top) Photos of representative postnatal mice from below showing the number and extent of pressure points (in blue) at the indicated ages. (Bottom) displacement in the field (same mice) during a 1 min test.

**(B)** Mean percentage ( $\pm$  SEM) of belly contact time ( $n = 16$ , top) and vectorial walking ( $n = 14$ , bottom) as a function of postnatal age. Boxes represent the median and interquartile range, the top and bottom vertical bars denote the 90<sup>th</sup> and 10<sup>th</sup> percentile.

**(C)** Calcium fluorescence images of the striatum from Nkx-GFP mice slices (top) and corresponding raster plots of the calcium activities (bottom) generated by GFP+ cells (interneurons, green dots) and non-GFP cells (MSNs, black and red dots).

**(D)** (top) Mean percentage ( $\pm$  SEM) of all active cells as a function of age. Relative fraction of active GFP-positive neurons (interneurons, green) and MSNs (black) as a function of age.

\* $P < 0.05$ ; \*\*  $P < 0.01$ ; \*\*\* $P < 0.001$ : one-way ANOVA for B and D.

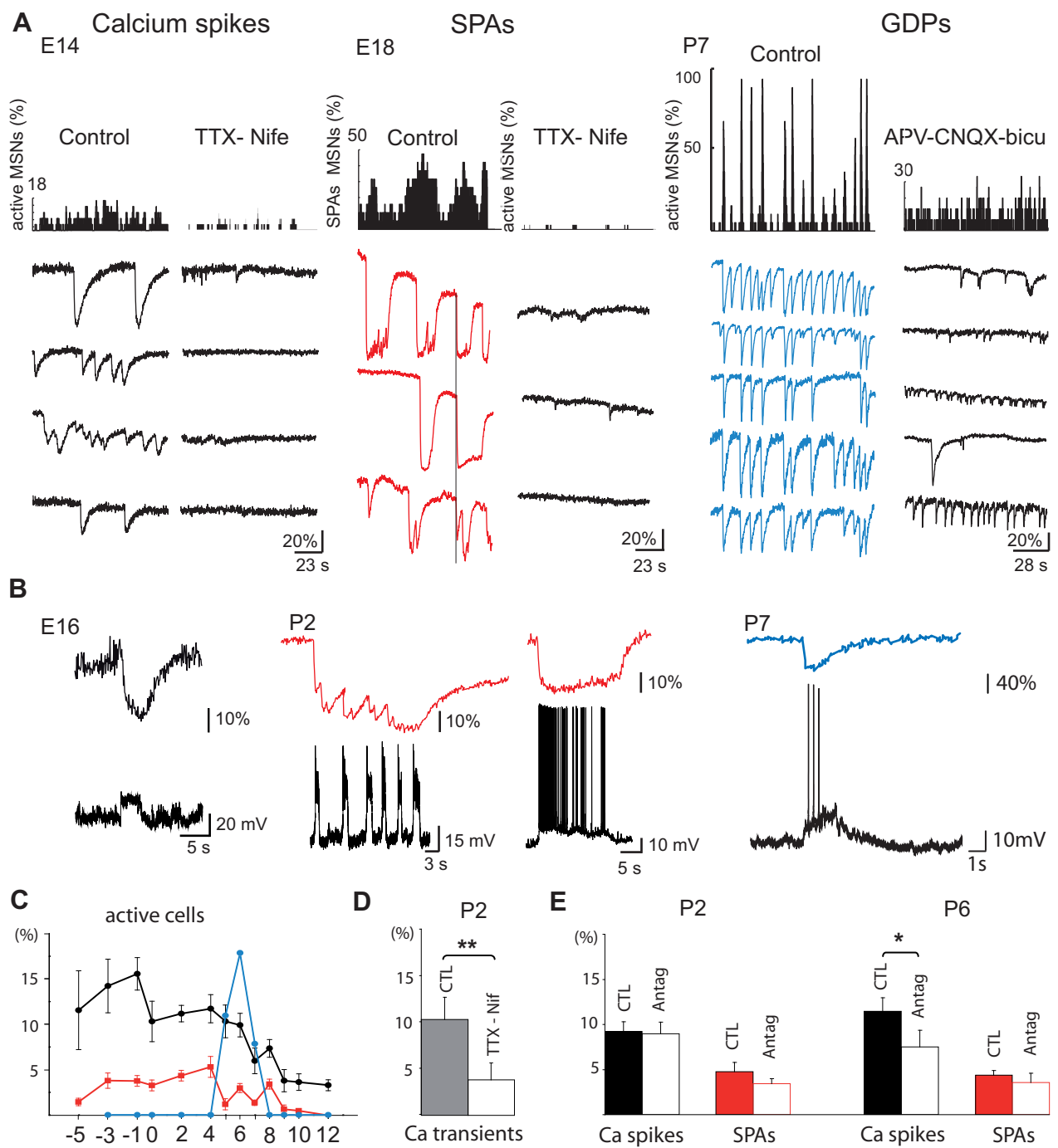


**Figure 2:** Immature activities generated by MSNs follow three main maturation steps.

(A) Representative histograms (top) indicating the fraction of imaged MSNs detected as being active (left and right) or evoking SPAs (middle left) and representative calcium fluorescence traces (Ca<sup>2+</sup> spikes in black, SPAs in red and GDPs in blue) from MSNs (bottom) in control ACSF or in the presence of blockers of voltage-gated Na<sup>+</sup> and Ca<sup>2+</sup> channels (TTX 1 μM- Nifedipin 10 μM, left and middle) or of ionotropic glutamate and GABA receptors (APV 40 μM-CNQX 10 μM-Bicuculline 10 μM, right). SPAs (red) were temporally correlated in control ACSF (vertical line).

(B) Simultaneous optical (top) and current clamp (bottom) recordings of calcium spikes (Vm = -70 mV, left), SPAs (Vm = -50 mV, middle) and GDPs (Vm = -60 mV, right).

(C) Mean percentage (± SEM) of fura-2 loaded cells evoking at least one Ca<sup>2+</sup> spike (black) or one SPA (red) or GDPs (blue) as a function of age (-5 = E14; -3 = E16; -1 = E18; 0 = E19 or P0, 4-12 = P4-P12).

(D) Mean percentage (± SEM) of fura-2 loaded cells evoking at least one Ca<sup>2+</sup> spike in control ACSF (black) and in the presence of TTX-Nifedipin (white). (E) Mean percentage (± SEM) of fura-2 loaded cells evoking at least one Ca<sup>2+</sup> spike (black) and one SPA (red) in control ACSF and in the presence of synaptic blockers (Antag, white) at P2 and P6.

\*P < 0.05; \*\* P < 0.01: paired Student t test for D and E).

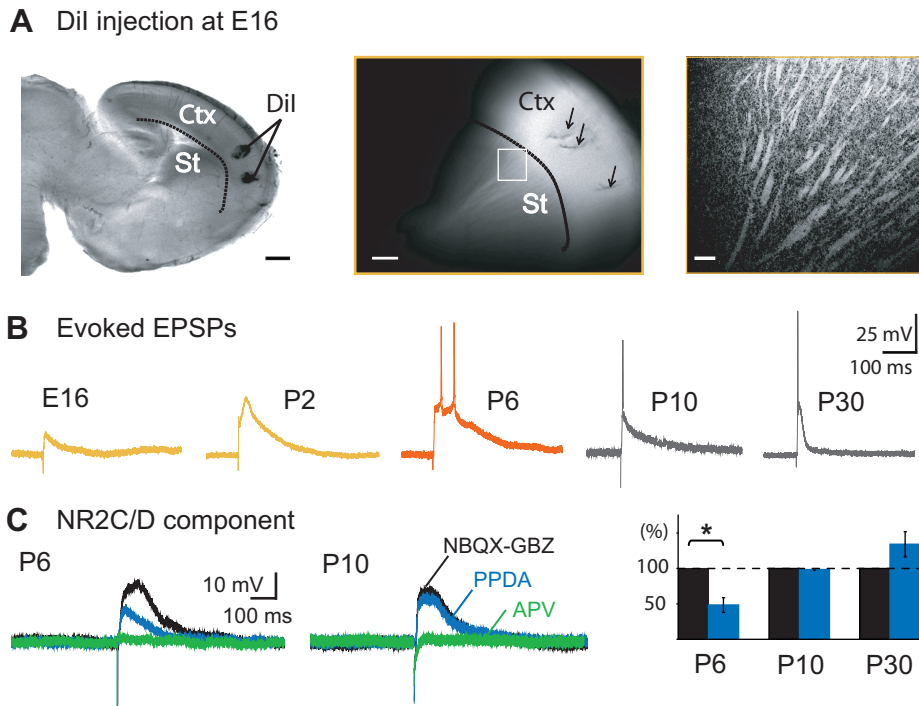


**Fig. 3:** Early embryonic cortico-striatal EPSPs and postnatal transient expression of the NR2CD-mediated NMDA component.

**(A)** (left) Dil injections in the neocortex in a E16 formalin-treated sagittal slice. After 15 days of incubation, Dil-labelled cortical fibres were observed in the striatum as shown in the confocal image (right) of the region indicated by a square (middle). Scale bars: 500, 200 and 50  $\mu$ m.

**(B)** Whole cell current clamp responses of embryonic and postnatal MSNs to intra-cortical stimulation in absence of synaptic blockers. At P6, the response was ten times longer than at P30 \*\*\* $P < 0.001$  (Student t test).

**(C)** The Gabazine (GBZ 10  $\mu$ M)-NBQX (10  $\mu$ M)-resistant whole cell EPSP was decreased by  $52 \pm 10\%$  at P6 ( $n = 5$ ),  $2 \pm 1\%$  at P10 ( $n = 5$ ) by the selective NR2CD antagonist PPDA (100nM, 15 min) (blue traces; \* $P < 0.05$ : paired Student t test) and was entirely abolished by APV (40  $\mu$ M) at all ages.

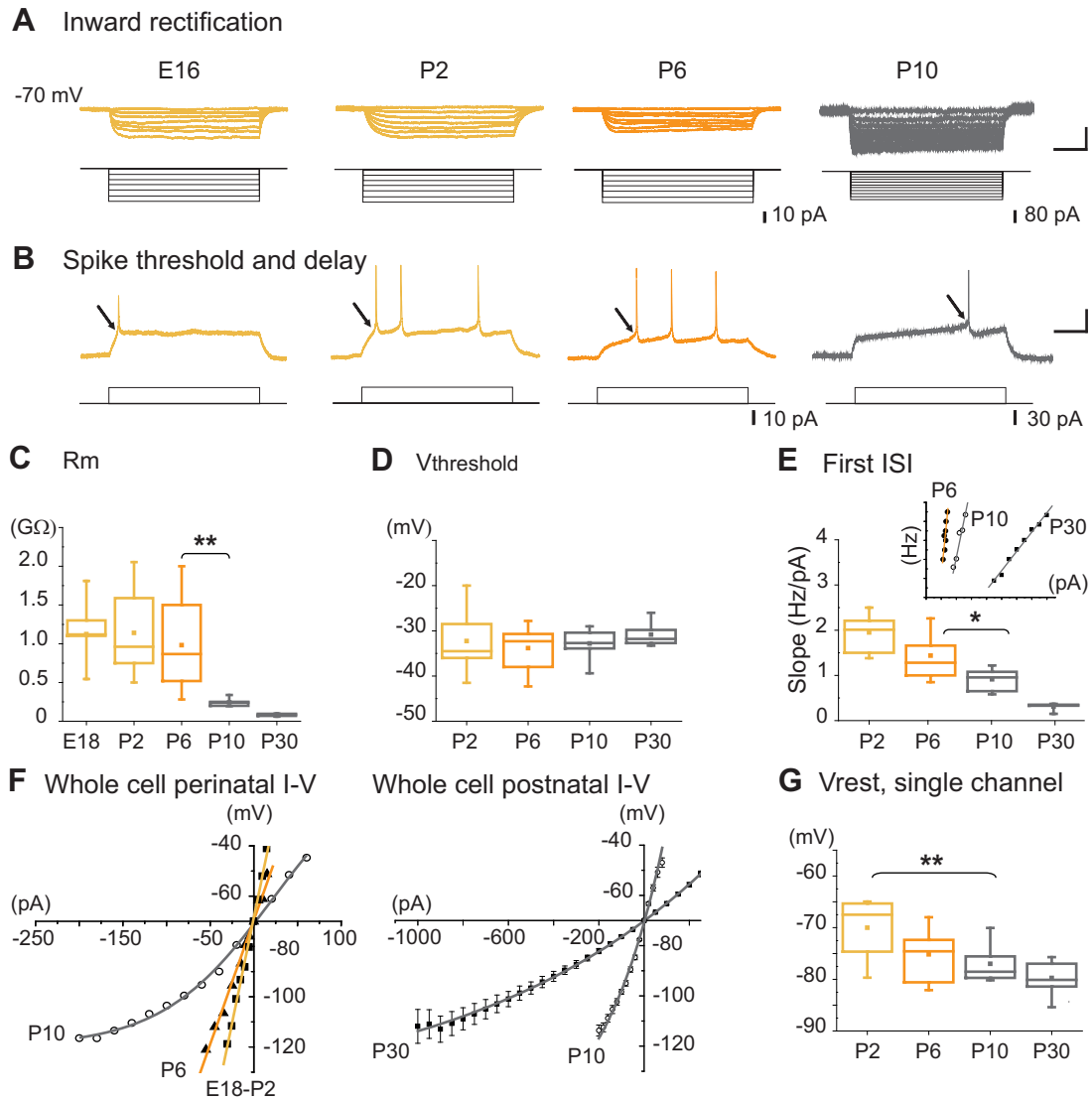


**Figure 4:** Intrinsic membrane properties of MSNs abruptly change between P6 and P10

(A) Representative whole cell current clamp responses of embryonic and postnatal MSNs to intracellular hyperpolarizing steps to determine the presence of inward rectification ( $V_m = -70$  mV). Scale bars: 25 mV; 200 ms.

(B) Representative whole cell current clamp responses to intracellular depolarizing steps ( $V_m = -70$  mV). At E16-E18 few MSNs generated overshooting  $\text{Na}^+$  spikes (14%,  $n = 1/8$ ), half of them (3/6) at P0, 64% (16/25) at P2, 87% (21/24) at P5 and 100% (12/12) at P7. Scale bars: 25 mV; 200 ms.

(C) Input membrane resistance ( $R_m$ ) obtained from responses to hyperpolarizing steps in A, was 4 times higher at perinatal stages compared to adult ( $1180 \pm 197$  M $\Omega$  at P8,  $n = 16$  vs  $273 \pm 91$  M $\Omega$  at P30,  $n = 14$ ) (D) Threshold potential ( $V_{\text{threshold}}$ ) calculated from experiments in A did not change between P0-P2 ( $32.2 \pm 1.7$  mV,  $n = 14$ ) and P3-P6 ( $33.8 \pm 0.8$  mV,  $n = 32$ ) or P30 ( $-31.0 \pm 0.8$  mV,  $n = 10$ ) ( $p = 0.65$  for all). (E) The first interspike interval (ISI) frequency is plotted as a function of injected current (insert, Belleau and Warren, 2000, scale: 20 Hz, 100 pA). Slope values given by each linear regression lines (correlation coefficient were all  $> 0.9$ ) are plotted as a function of postnatal age. Slopes at P10 ( $1.27 \pm 0.12$ ,  $n = 5$ ) were significantly different from that at P30 ( $0.31 \pm 0.04$ ,  $n = 5$ ). The linearity of the I-V relationships at E18, P2 and P6 shows that most of the MSNs do not express  $K_{\text{IR}}$  current at these ages (left) compared to adult MSNs (right).

(F) Whole cell I-V relationships at the indicated ages, obtained from experiments in A.

(G) MSNs resting membrane potential ( $V_{\text{rest}}$ ) determined from the reversal potential of unitary NMDA currents significantly hyperpolarized from P2 to P10 by around 10 mV (from  $-70.0 \pm 1.7$  mV,  $n = 11$  to  $-77.0 \pm 1.3$  mV,  $n = 11$ ). \* $P < 0.05$ ; \*\* $P < 0.01$ : one-way ANOVA for C-G).

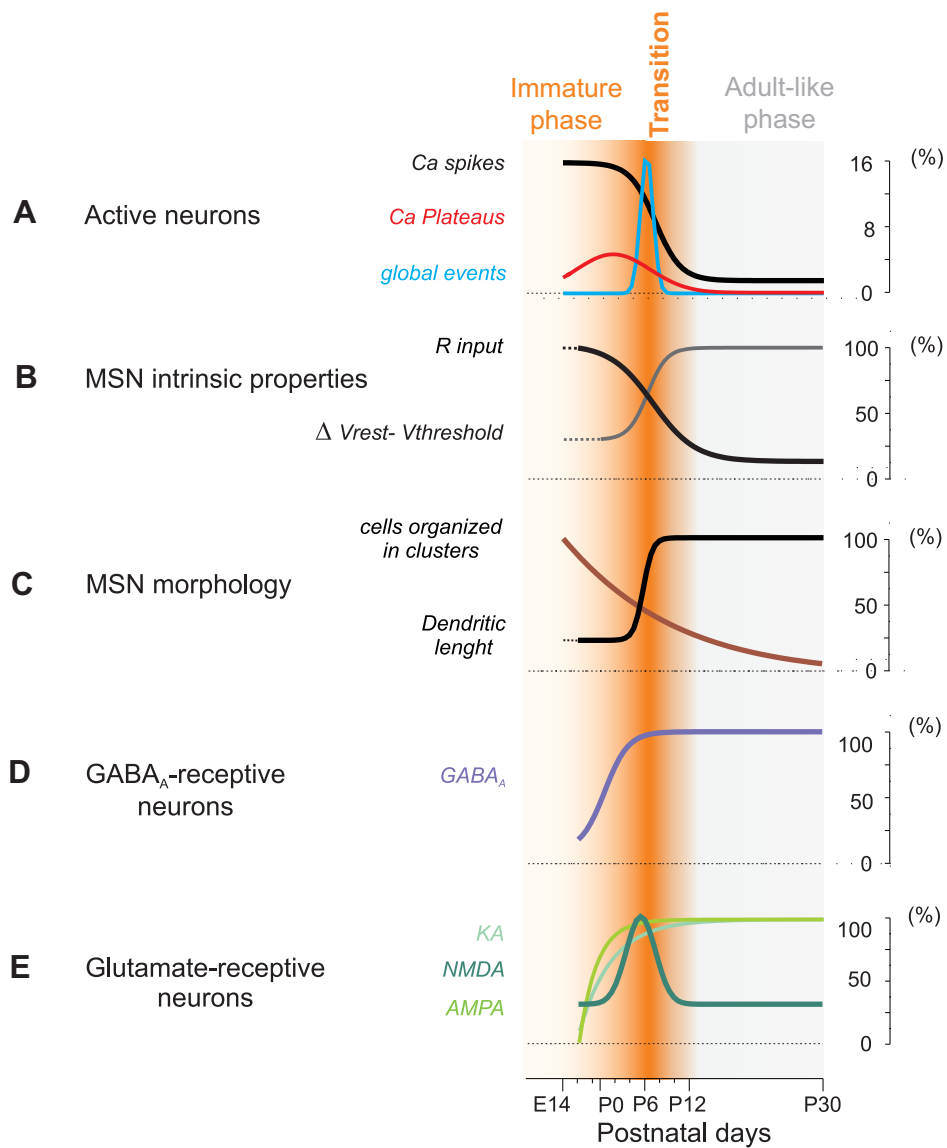


**Figure 5:** Summary of MSNs properties and activities from E14 to P12

Light orange period when MSNs generate immature activities; grey: period when MSNs are mostly silent in vitro; bright orange: period of transition between the immature phase and the adult-like phase.  $V_{\text{threshold}}$  measured with whole cell recordings did not significantly change between P7 ( $-37.3 \pm 1.9$  mV,  $n = 9$ ) compared to P30 ( $-38.3 \pm 0.6$  mV,  $n = 7$ ;  $P = 0.65$ : one way ANOVA).

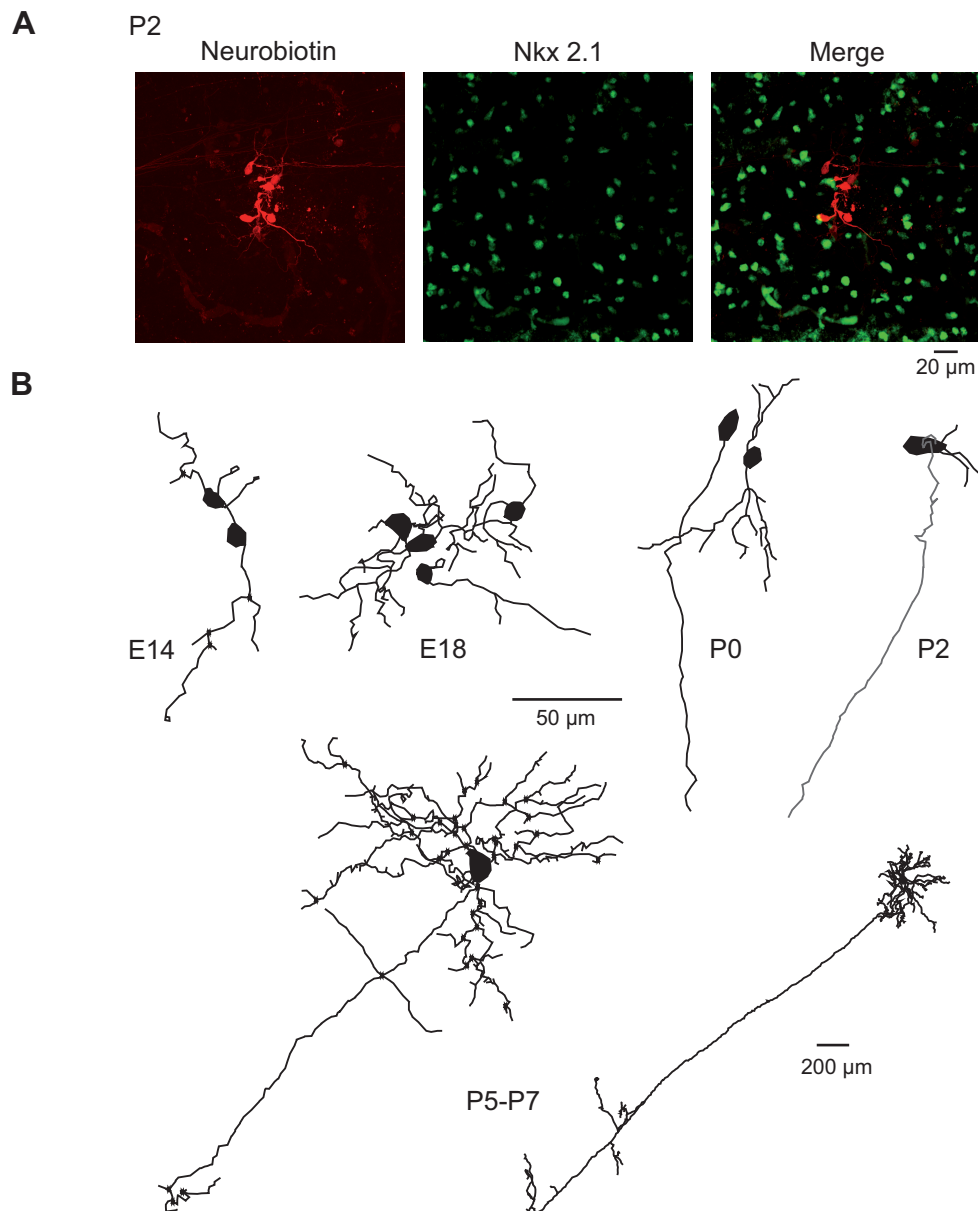


### Figure S3: MSNs are organized in clusters at perinatal ages

**(A)** The double immunocytochemistry for neurobiotin (left) and Nkx2.1 (middle) performed on a P2 striatal slice after whole cell recording of a single MSN revealed a cluster of 7 neurobiotin-filled cells (red) that are all Nkx-negative MSNs (not green, right). Scale bar 20  $\mu$ m.

**(B)** Neurolucida reconstruction of neurobiotin-filled Nkx-negative neurons (MSNs) at E14, E18 and P7. When single MSNs were labeled with neurobiotin, clusters of 2-7 cells were observed in 75 % ( $n = 13/17$ ) of the recordings before birth (E14-E18) (scale bar 50  $\mu$ m). In 97 % of the cases, clusters exclusively consisted of MSNs ( $n = 36$  out of 37) (see supplementary figure 3). Clusters of  $6 \pm 1$  neurobiotin-labeled neurons were observed in 75 % ( $n = 13/17$ ) of the recordings before birth (E14-E18) compared to 8% of clusters composed of 2 MSNs ( $n = 3/38$ ) in the adult (P30-P40). MSNs had  $2.8 \pm 0.3$  primary dendrites at E16-E18 ( $n = 23$ ),  $3.9 \pm 0.4$  at P0 ( $n = 19$ ),  $5.1 \pm 1.1$  at P2 ( $n = 9$ ) and  $5.8 \pm 0.3$  at P7 ( $n = 11$ ). They gave rise to around 6 - 25 dendritic ends (6 at E16-18, 13 at P0, 17 at P2, 18 at P5 and 25 at P7).

The total dendritic length was multiplied by 5 between E16-18 and P7 ( $339 \pm 64$   $\mu$ m at E16-18,  $646 \pm 148$   $\mu$ m at P0,  $574 \pm 123$   $\mu$ m at P2,  $818 \pm 161$   $\mu$ m at P5 and  $1751 \pm 219$   $\mu$ m at P7). Dendritic spines were virtually absent at all ages. Average cell capacitance progressively increased from E16 to P7 ( $14.3 \pm 0.9$  pF at P2,  $n=47$  vs  $51.7 \pm 5.3$  pF at P30,  $n = 74$ ; \*\*\* $P < 0.001$ : one way ANOVA). Axons coursing down to the globus pallidus were identified in few E18 MSNs but were consistently observed for P5-P7 MSNs.

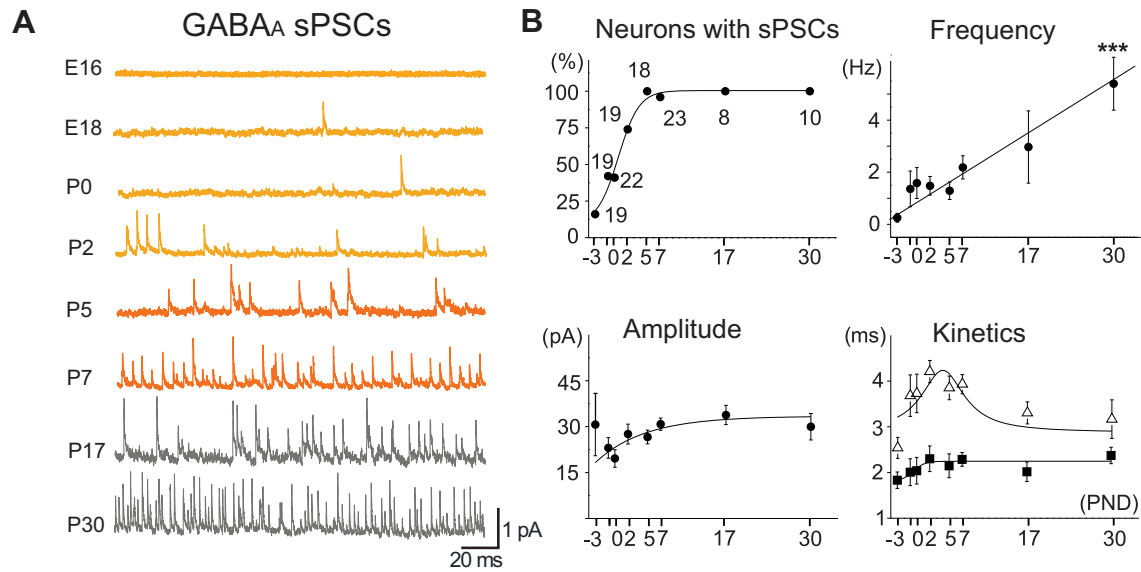


**Figure S4:** Spontaneous GABA<sub>A</sub> postsynaptic currents (GABA<sub>A</sub>-PSCs) recorded from E16 to P30 MSNs

**(A)** Voltage clamp recordings of spontaneous GABA<sub>A</sub>-PSCs with CsGlu intrapipette solution during development ( $V_H = +10$  mV). Scale: 50 pA, 500 ms. At the youngest ages tested (E16-P2), a fraction of the recorded MSNs did not generate any GABA<sub>A</sub> sPSCs or only few of them with a frequency lower than 0.05 Hz (85% at E16, 60% at E18-P0 and 25% at P2). These were not included in the analysis of GABA<sub>A</sub> sPSCs frequency and amplitude.

**(B)** Fraction of the recorded MSNs which displayed spontaneous GABA<sub>A</sub>-PSCs as a function of time. From P5-P7, all MSNs display spontaneous GABA<sub>A</sub> currents. GABA<sub>A</sub>-PSCs Frequency gradually increased during development ( $R > 0.9$ ) whereas amplitude of the PSCs remained stable ( $P > 0.05$ : one way ANOVA). GABA<sub>A</sub> sPSCs frequency at P30 ( $5.4 \pm 1.0$  Hz;  $n = 10$ ,  $***P < 0.001$ : one way ANOVA) was significantly different from the frequency at P7 ( $2.1 \pm 0.4$  Hz;  $n = 22$ ). GABA<sub>A</sub> sPSCs amplitude was not statistically different between E16 ( $30.3 \pm 2.0$  pA,  $n = 19$ ) and P30 ( $30.0 \pm 4.3$  pA;  $n = 10$ ,  $P = 0.93$ : one way ANOVA). Rise time around 2 ms ( $2.3 \pm 0.1$  ms at P7 and  $2.4 \pm 0.2$  ms at P30) and decay time around 35 ms ( $39.3 \pm 2.1$  ms at P7 vs  $32.0 \pm 4.2$  ms at P30) of GABA<sub>A</sub>-PSCs remained stable during development ( $n = 22$ ,  $P = 0.7$  and  $n = 10$ ,  $P = 0.12$ : one way ANOVA).

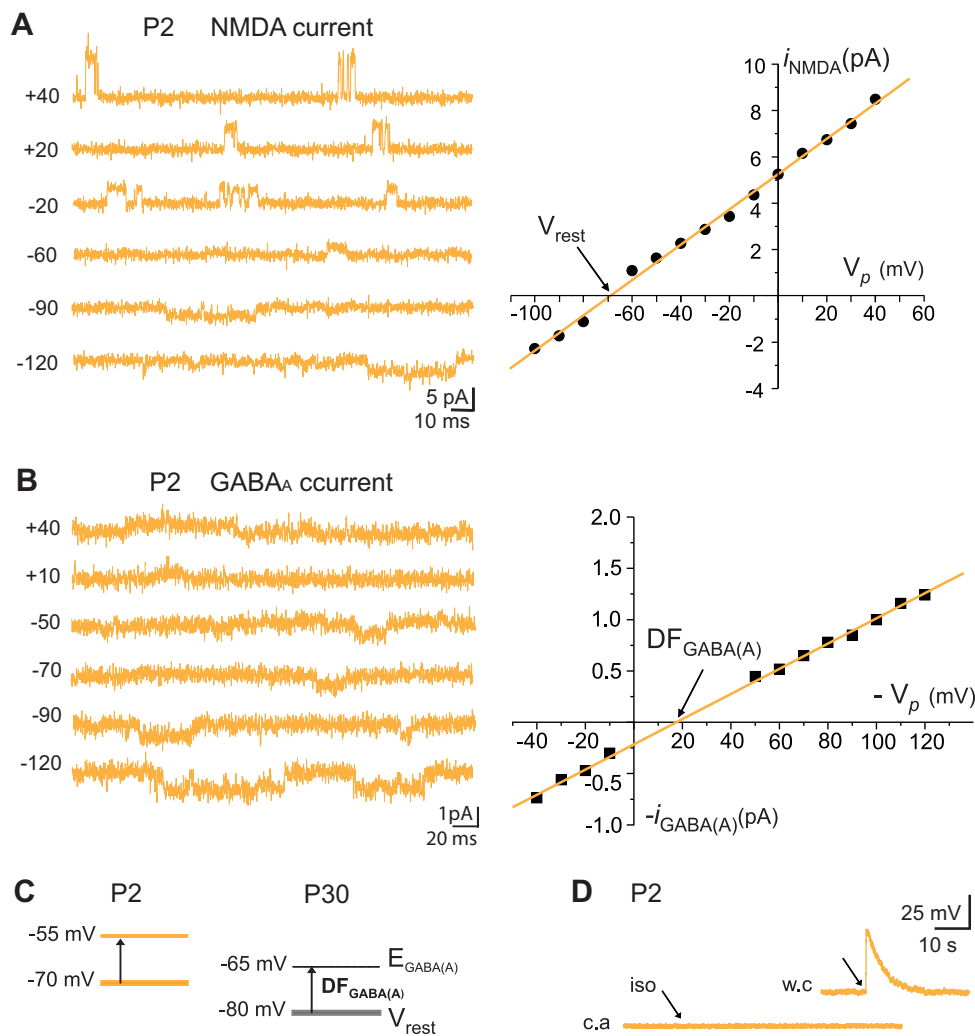


**Figure S5:** Resting membrane potential ( $V_{rest}$ ) and reversal potential for  $GABA_A$  – mediated currents ( $E_{GABA_A}$ ) of P2 MSNs.

**(A)** Representative cell-attached recordings of unitary NMDA currents at the indicated  $V_H$  (in mV) from a P2 MSN (Scale bars: 5 pA; 10 ms) and corresponding I-V relationship of the recorded currents to determine  $V_{rest}$  (-67 mV).

**(B)** Representative cell-attached recordings of unitary  $GABA_A$  currents at the indicated  $V_H$  (in mV) from a P2 MSN (scale bars: 1 pA, 20 ms) and corresponding I-V relationship of the recorded  $GABA_A$  currents to determine  $DF_{GABA_A}$ .

**(C)** The driving force for GABA was similar at P2 and P30 ( $DF_{GABA} = 15.3 \pm 3.4$  mV;  $n = 8$  vs  $16.1 \pm 1.9$  mV,  $n = 11$ ;  $P = 0.8$ : Student t test) (Dehorter et al, 2009).

**(D)** Pressure application of isoguvacine (iso, 100  $\mu$ M) during cell-attached recordings did not elicit any action potential at P2 (Scale bars: 100 pA, 125 ms). Inset shows the depolarization evoked by the same pressure application of isoguvacine during whole cell recording of the same P2 MSN (Scale bars: 25 mV, 5 s).

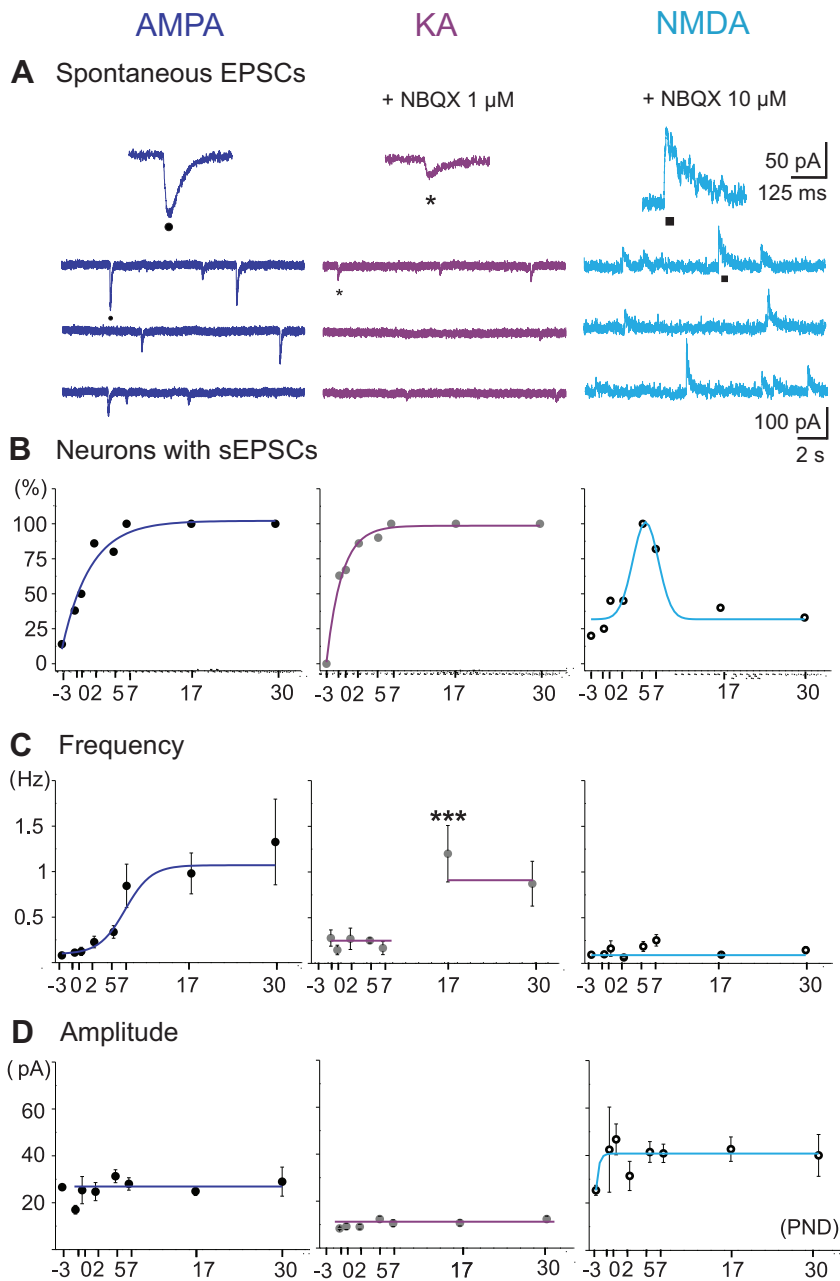


**Figure S6:** Spontaneous AMPA, KA and NMDA receptor-mediated postsynaptic currents (EPSCs) recorded from E16-P30 MSNs.

**(A)** Representative voltage-clamp recordings of spontaneous AMPA ( $V_H = -80$  mV), kainate (KA,  $V_H = -80$  mV in NBQX 1  $\mu$ M) and NMDA ( $V_H = +40$  mV in NBQX 10  $\mu$ M) receptor-mediated EPSCs (CsGlu intrapipette solution) at P6. Scale: 100 pA, 200 ms (AMPA and KA) and 2 s (NMDA). Insets show each spontaneous current at an expanded time scale (50 pA, 125 ms). Between E16 and P2, around half of the recorded MSNs did not generate glutamatergic sEPSCs (non-NMDA component,  $n = 32/67$ ) and NMDA component ( $n = 27/41$ ) or displayed currents with a frequency lower than 0.05 Hz. These neurons were not included in the quantification.

**(B)** The fraction of the recorded MSNs which displayed spontaneous glutamatergic currents as a function of time increases with age and is close to 100% at P5-P7 for AMPA, KA and NMDA sEPSCs ( $n = 16, 22$  and  $16$ ). This increase is transient for NMDA sEPSCs.

**(C)** The frequency of AMPA and KA receptor-mediated sEPSCs significantly increased by a factor 10 from E18 (-1) ( $0.11 \pm 0.04$  Hz and  $0.3 \pm 0.1$  Hz;  $n = 5$  and  $5$  MSNs, respectively) to P30 ( $1.3 \pm 0.7$  Hz and  $0.9 \pm 0.2$  Hz;  $n = 5$  and  $6$  MSNs), respectively (\* $P < 0.05$  and \*\* $P < 0.01$ : one way ANOVA). In contrast the frequency of NMDA receptor-mediated sEPSCs remained stable around 0.1 Hz from E16 to P30 ( $P > 0.05$ : one way ANOVA).

**(D)** The amplitude of the three glutamatergic PSCs remained stable along development ( $P > 0.05$ : one way ANOVA).

# Article 2

*Journal of Neuroscience, 2009 June*

## **Dopamine-Deprived Striatal GABAergic Interneurons Burst and Generate Repetitive Gigantic IPSCs in Medium Spiny Neurons**

Nathalie Dehorter, Céline Guigoni, Catherine Lopez, June Hirsch, Alexandre Eusebio,  
Yehezkel Ben-Ari and Constance Hammond

## Article 2

Le striatum étant la structure d'entrée des ganglions de la base, cette structure représente un point clé dans l'intégration des afférences corticales. Comprendre quelle est l'activité des micro-circuits GABAergiques au stade adulte est crucial pour mieux appréhender le rôle du striatum dans l'intégration et le traitement de l'information corticale au sein des ganglions de la base. L'étude réalisée s'est portée sur l'impact de l'absence chronique d'innervation dopaminergique dans le striatum, à savoir si cette déplétion perturbait l'activité des micro-réseaux GABAergiques du striatum? Plus particulièrement au sein de ces microcircuits GABAergiques, quelles sont les cellules affectées?

En utilisant les techniques électrophysiologiques de patch clamp sur des tranches sagittales inclinées de cerveau de souris, nous avons enregistré les courants post-synaptiques GABAergiques spontanés (IPSCs) générés par les MSNs. Dans le striatum adulte contrôle, les IPSCs GABA afférents aux MSNs ont une fréquence régulière (4 Hz) et sont de faible amplitude (30 pA). Les interneurons GABA sont en effet peu actifs dans cette préparation in vitro et les collatérales récurrentes GABA des MSNs sans doute silencieuses car les MSNs le sont.

Par contre, en l'absence chronique de dopamine (modèle 6-hydroxydopamine), les courants GABA afférents à environ 50% des MSNs deviennent géants, soit sous forme d'évènements isolés soit organisés en bouffées (autour de 60 Hz). Ce changement de patron de décharge qui est très frappant, ne s'accompagne pas de changements post-synaptiques comme le potentiel d'inversion des courants GABA, ni de changements du contrôle pré-synaptique de la libération de GABA par l'acétylcholine. Les interneurons GABA de type FS et les interneurons cholinergiques (TANs) ne changent pas d'activité en fonction de la présence ou de l'absence chronique de dopamine.

Par contre des interneurons GABA de type LTS déchargent de façon répétitive en bouffées de potentiels d'action à haute fréquence (60-120 Hz) en l'absence chronique de dopamine alors qu'ils ont une activité en potentiels d'action isolés dans le striatum contrôle. Ils seraient donc les seuls responsables du changement de patron de décharge des courants synaptiques GABA afférents aux MSNs.

# Dopamine-Deprived Striatal GABAergic Interneurons Burst and Generate Repetitive Gigantic IPSCs in Medium Spiny Neurons

Nathalie Dehorter,<sup>1</sup> Celine Guigoni,<sup>2</sup> Catherine Lopez,<sup>1</sup> June Hirsch,<sup>1</sup> Alexandre Eusebio,<sup>1</sup> Yehezkel Ben-Ari,<sup>1</sup> and Constance Hammond<sup>1</sup>

<sup>1</sup>Institut de Neurobiologie de la Méditerranée Unité Mixte de Recherche (UMR) 901, Inserm and Aix Marseille II University, 13009 Marseille, France, and

<sup>2</sup>Centre National de la Recherche Scientifique UMR 5227, Université Bordeaux 2, 33076 Bordeaux, France

Striatal GABAergic microcircuits modulate cortical responses and movement execution in part by controlling the activity of medium spiny neurons (MSNs). How this is altered by chronic dopamine depletion, such as in Parkinson's disease, is not presently understood. We now report that, in dopamine-depleted slices of the striatum, MSNs generate giant spontaneous postsynaptic GABAergic currents (single or in bursts at 60 Hz) interspersed with silent episodes, rather than the continuous, low-frequency GABAergic drive (5 Hz) observed in control MSNs. This shift was observed in one-half of the MSN population, including both "D<sub>1</sub>-negative" and "D<sub>1</sub>-positive" MSNs. Single GABA and NMDA channel recordings revealed that the resting membrane potential and reversal potential of GABA were similar in control and dopamine-depleted MSNs, and depolarizing, but not excitatory, actions of GABA were observed. Glutamatergic and cholinergic antagonists did not block the GABAergic oscillations, suggesting that they were generated by GABAergic neurons. In support of this, cell-attached recordings revealed that a subpopulation of intrastriatal GABAergic interneurons generated bursts of spikes in dopamine-deprived conditions. This subpopulation included low-threshold spike interneurons but not fast-spiking interneurons, cholinergic interneurons, or MSNs. Therefore, a population of local GABAergic interneurons shifts from tonic to oscillatory mode when dopamine is deprived and gives rise to spontaneous repetitive giant GABAergic currents in one-half the MSNs. We suggest that this may in turn alter integration of cortical signals by MSNs.

## Introduction

The striatum plays a central role in movement elaboration, most notably by integrating the converging glutamatergic inputs from the neocortex. The GABAergic medium spiny projection neurons (MSNs) that constitute 95% of all striatal neurons provide the only output of the striatum and are the final step of this integration process. Local GABAergic and cholinergic interneurons represent the remaining 5%. The striatal network is controlled by dopaminergic synapses, whose loss in Parkinson's disease leads to major motor deficits. The manner by which dopamine controls the operation of the striatal network is not yet understood. In contrast to the extensive investigations performed on the fate of spontaneous or evoked glutamatergic currents (PSCs) in dopamine (DA)-depleted MSNs (Calabresi et al., 2007) and despite

the overwhelming role of GABA microcircuits in the striatum (Wilson, 2007), little is known on the alterations of GABAergic currents under these conditions.

Two types of intrastriatal GABAergic interneurons control the activity of MSNs: fast-spiking (FS) interneurons and low-threshold spike (LTS) interneurons (Kawaguchi, 1993; Tepper and Bolam, 2004) that innervate the soma and proximal dendrites of MSNs (Kita et al., 1990; Bennett and Bolam, 1994; Kubota and Kawaguchi, 2000). They exert feedforward inhibition that prevents or delays the generation of action potentials (Plenz and Kitai, 1998; Koós and Tepper, 1999; Mallet et al., 2005; Gustafson et al., 2006). There is also a dense network of recurrent GABAergic synapses between MSNs, located on dendritic spines and shafts (Wilson and Groves, 1980). These provide lateral inhibition as a result of summation of the small amplitude IPSCs (Czubayko and Plenz, 2002; Tunstall et al., 2002; Venance et al., 2004; Tepper et al., 2008). Dopaminergic input from the substantia nigra modulates the activity of GABAergic interneurons via several presynaptic and postsynaptic dopamine receptor subtypes (Bracci et al., 2002; Momiyama, 2002; Centonze et al., 2002, 2003), as do cholinergic interneurons [the tonically active neurons (TANs)] (Zhou et al., 2002; Sullivan et al., 2008) via muscarinic and nicotinic receptors (Koós and Tepper, 2002).

Using the basal ganglia slice (BGS) (Beurrier et al., 2006) and slices of isolated striatum in which the striatum is deprived of its cortical and thalamic inputs, we now report that, in chronically

Received March 31, 2009; revised May 6, 2009; accepted May 6, 2009.

This work was supported by Inserm, Fondation de France, and Association France Parkinson. N.D. is supported by a PhD grant from the region Provence-Alpes-Côte d'Azur and the company Neuroservice. We thank Alfonso Represa, François Michel, Christophe Porcher, and Igor Medina for their help with immunocytochemical data.

Correspondence should be addressed to Constance Hammond, Institut de Neurobiologie de la Méditerranée Unité 901, Inserm, 163 route de Luminy, BP 13, 13273 Marseille Cedex 9, France. E-mail: hammond@inmed.univ-mrs.fr.

A. Eusebio's present addresses: Department of Neurology and Movement Disorders, Centre Hospitalier Universitaire Timone, 13385 Marseille, France; and Sobell Department of Motor Neuroscience and Movement Disorders, Institute of Neurology, Queen Square, London WC1N 3BG, UK.

DOI:10.1523/JNEUROSCI.1527-09.2009

Copyright © 2009 Society for Neuroscience 0270-6474/09/297776-12\$15.00/0

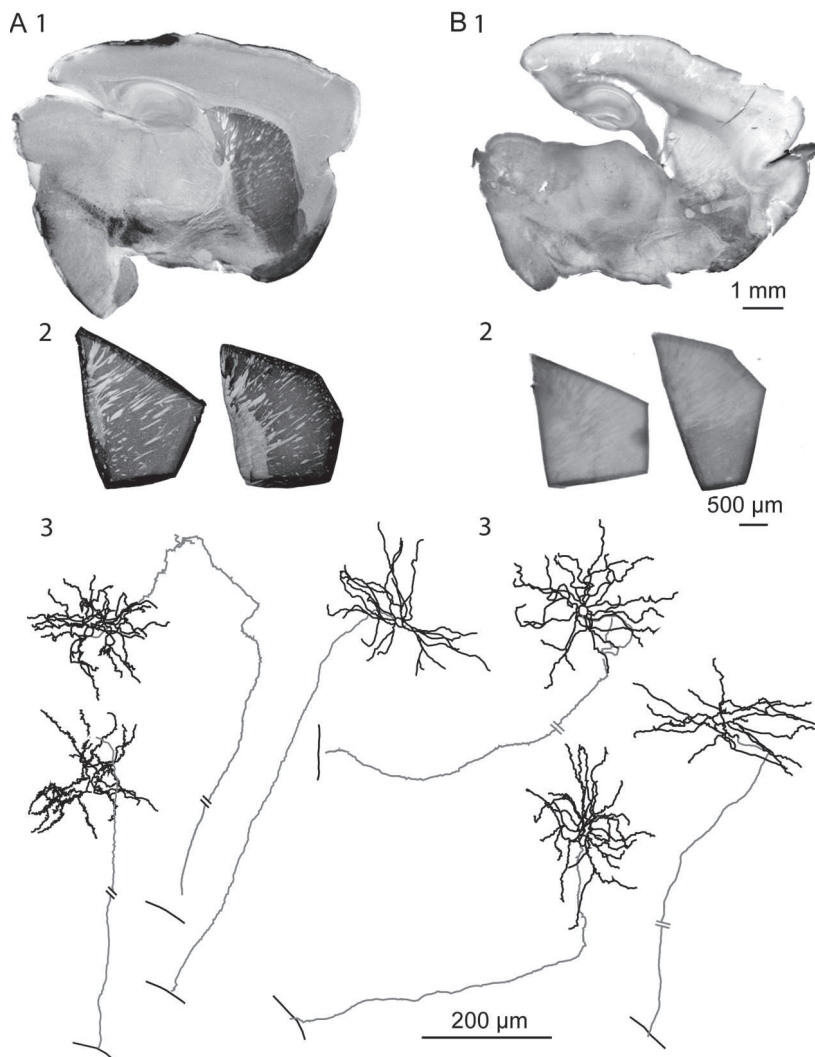


**Figure 1.** Extent of DA depletion in the striatum and identification of the recorded MSNs. TH immunohistochemistry of adult BGS (**1**) and isolated striatum (**2**) from control (**A**) and DA-depleted (**B**) mice. The striatum was isolated from the corresponding BGS before the recording session. Note the absence of dark TH labeling in the BGS (**B1**) and in the two isolated striatum (**B2**) from 6-OHDA-treated mice compared with the corresponding control ones (**A1, A2**). Neurolucida reconstruction of biocytin-filled MSNs recorded in control (**A3**) and DA-depleted (**B3**) isolated striatum is shown. Somas and dendritic trees are in black and axons are in gray. The single bars crossing the axons indicate GP boundary; the double bars indicate interruption in the drawing because of the length of the axon.

DA-depleted MSNs, the continuous activity of small amplitude GABAergic sPSCs is replaced in one-half of the MSN population by giant GABAergic events separated by silent episodes. These were not affected by nicotinic or muscarinic receptor antagonists. Cell-attached recordings of single GABA<sub>A</sub> and NMDA channels from MSNs showed that this shift is not attributable to modifications of resting membrane potential ( $V_{rest}$ ) or of the reversal potential for GABA ( $E_{GABA}$ ). Nor did we find alterations of the spike threshold. Giant GABAergic currents are depolarizing but do not generate spikes in either control or DA-depleted MSNs. Chronic DA depletion did not affect the activity of MSNs (silent) or cholinergic interneurons (TANs, tonically active) or GABAergic FS interneurons (tonically active or silent) recorded in the cell-attached configuration *in vitro*. Rather, it led to remarkable intrinsic oscillations in a subpopulation of GABAergic LTS interneurons. We propose that the ensuing powerful GABAergic barrage of giant GABA sPSCs profoundly alters the integrative functions of the striatum by interacting with cortical information traveling throughout the striatum.

## Materials and Methods

**Chronic lesion of the dopaminergic innervation of the striatum.** We lesioned the dopaminergic innervation in one striatum of C57BL/6 mice (15–25 g) aged postnatal day 15 (P15) to P50 by local stereotaxic injection of 6-hydroxydopamine (6-OHDA) under 5% ketamine (Imalgène 1000)/2.5% xylazine (Rompun 2%) anesthesia (10  $\mu$ l/g, i.p.). Two microinjections of 6-OHDA were performed through a NanoFIL syringe (outside diameter, 135  $\mu$ m; WPI) placed into the left dorsal striatum at the following coordinates using a David Kopf stereotaxic apparatus: 1.0 and 1.2 mm rostral to bregma, 1.8 and 2.2 mm lateral to the midline, 2.7 and 2.8 mm, respectively, below the surface of the skull. 6-OHDA was dissolved in saline containing 0.05% ascorbic acid, and injected at a dose of 6  $\mu$ g in a volume of 0.5  $\mu$ l over a 5 min period. The syringe was left in place for 5 min after the end of injection. We performed *in vitro* recordings 15–30 d after the lesion. The efficacy of the 6-OHDA-induced lesion of dopaminergic terminals in the striatum was determined 2–3 d before the recording session by apomorphine-induced rotation (0.5 mg/kg in 0.1% ascorbic acid, i.p.; Sigma-Aldrich) (Iancu et al., 2005). Lesioned mice performed  $7.0 \pm 0.3$  right turns per minute and no left turn ( $n = 47$ ). In contrast, control mice performed  $0.18 \pm 0.07$  right turns per minute and  $0.23 \pm 0.06$  left turns per minute ( $n = 11$ ). We checked the extent of the lesion after the recording session by immunohistochemical visualization of tyrosine hydroxylase (TH) in the striatum (see below, Immunocytochemistry).

**Slice preparation.** C57BL/6 mice (P25–P60), either control or bearing a chronic lesion of the dopaminergic fibers in the striatum, were killed by decapitation under halothane anesthesia. Oblique parasagittal slices (380  $\mu$ m thick) were cut with an angle of  $10 \pm 2^\circ$  to obtain the BGS as previously described (Beurrier et al., 2006) (Fig. 1A1, B1). For the slicing procedure, the ice-cold oxygenated solution contained the following (in mM): 110 choline, 2.5 KCl, 1.25  $\text{NaH}_2\text{PO}_4$ , 7  $\text{MgCl}_2$ , 0.5  $\text{CaCl}_2$ , 25  $\text{NaHCO}_3$ , 7 glucose. To test for a possible role of choline, slices were also cut in a sucrose solution containing the following (in mM): 85 NaCl, 2.5 KCl, 1  $\text{NaH}_2\text{PO}_4$ , 4  $\text{MgCl}_2$ , 1  $\text{CaCl}_2$ , 25  $\text{NaHCO}_3$ , 25 glucose, 75 sucrose ( $n = 4$ ). During the recovery period, BGSs were placed at room temperature (RT) with standard artificial CSF (ACSF) saturated with 95%  $\text{O}_2$ /5%  $\text{CO}_2$  and containing the following (in mM): 126 NaCl, 3.5 KCl, 1.2  $\text{NaH}_2\text{PO}_4$ , 1.3  $\text{MgCl}_2$ , 2  $\text{CaCl}_2$ , 25  $\text{NaHCO}_3$ , 11 glucose. To isolate the striatum from its surrounding structures (cortex, thalamus, pallidum), we performed a knife cut along its borders under a dissecting microscope before the recording session (Fig. 1A2, B2). These slices were prepared to study the direct effect of bath-applied drugs on the striatal network.

**Electrophysiology: solutions, data acquisition, and analysis.** All recordings were made at 32°C. Cells were visualized with infrared–differential interference optics (Axioskop2; Zeiss). For whole-cell voltage-clamp recordings of postsynaptic GABA<sub>A</sub> currents, the pipette (6–10 M $\Omega$ ) contained the following (in mM): 120 Cs-gluconate, 13 CsCl, 1  $\text{CaCl}_2$ , 10 HEPES, 10 EGTA, pH 7.2–7.4 (275–285 mOsm), or 110 CsCl, 30 K-gluconate, 0.1  $\text{CaCl}_2$ , 10 HEPES, 1.1 EGTA, 4 MgATP, and 0.3 NaGTP. We used the CsGlu solution to measure spontaneous GABA<sub>A</sub> currents at the reversal potential for glutamatergic (+10 mV) events (Cossart et al.,

2000) and the CsCl solution to measure the miniature GABA<sub>A</sub> currents at  $V_H = -60$  mV (in the continuous presence of  $1 \mu\text{M}$  TTX plus  $10 \mu\text{M}$  CNQX plus  $40 \mu\text{M}$  APV). For current-clamp recordings, patch electrodes contained the following (in mM): 128.5 K-gluconate, 11.5 KCl, 1 CaCl<sub>2</sub>, 10 EGTA, 10 HEPES, 2.5 MgATP, and 0.3 NaGTP, pH 7.32, 280 mOsm or the following (in mM): 125 KMeSO<sub>4</sub>, 15 KCl, 5 NaCl, 10 HEPES, 2.5 Mg-ATP, 0.3 Na-GTP. The CsGlu, CsCl, and KGlu pipette solutions gave a reversal potential for chloride close to  $-58$ ,  $-5$ , and  $-63$  mV at  $35^\circ\text{C}$ , respectively. Biocytin (Sigma-Aldrich; 5 mg/ml) was added in all pipette solutions and osmolarity corrected when necessary. We performed patch-clamp recordings in whole-cell or cell-attached configuration using the Digidata 1344A interface, the Multiclamp 700A amplifier, and pClamp8 software (Molecular Devices). Spontaneous and miniature GABA<sub>A</sub> receptor-mediated PSCs (sPSCs and mPSCs) were recorded at a holding potential of  $+10$  and  $-60$  mV, respectively. Currents were stored on pClamp8 (Molecular Devices) and analyzed off-line with Mini Analysis program (Synaptosoft 6.0), Clampfit 9.2, Origin 5.0, and Autosignal 1.7 to determine the frequency and amplitude of GABAergic synaptic events. All detected currents were then visually inspected to reject artifactual events. To generate the averaged GABA<sub>A</sub> mPSCs, multiple overlapping events were first discarded, and the remaining events were aligned on their rising phase. Only MSNs that exhibited a stable pattern of GABA<sub>A</sub> mPSCs during 20–30 min were taken into account. The histogram and cumulative distributions were constructed using GABA<sub>A</sub> mPSCs recorded over 3 min. In the sPSC recordings, we defined as “giant” any sPSC with an amplitude  $>200$  pA and as “burst” a minimum of five sPSCs associated with a baseline elevation. More than five giant events and three bursts were required during the 3 min analysis for the pattern to be deemed “oscillatory.”

For cell-attached recordings of single GABA<sub>A</sub> channels, the pipette (4–5 M $\Omega$ ) contained the following (in mM): 120 NaCl, 20 TEA-Cl (tetraethylammonium chloride), 5 KCl, 5 4-aminopyridine, 0.1 CaCl<sub>2</sub>, 10 MgCl<sub>2</sub>, 10 glucose, 10 HEPES-NaOH buffered to pH 7.2–7.3, osmolality of 300–320 mosmol. GABA ( $5 \mu\text{M}$ ) was included in the above pipette saline together with isoguvacine ( $5 \mu\text{M}$ ) and CsCl ( $3 \mu\text{M}$ ) to optimize channel openings (because of the negative charge of GABA, positive currents may repulse GABA far from the membrane; under these conditions, isoguvacine may thus replace it). For single NMDA channels, pipettes were filled with nominally magnesium-free ACSF containing the following (in mM): 140 NaCl, 3.5 KCl, 1.8 CaCl<sub>2</sub>, 10 HEPES, buffered to pH 7.43, osmolality of 300–320 mosmol. NMDA ( $10 \mu\text{M}$ ) and glycine ( $10 \mu\text{M}$ ) were included in the above saline to optimize channel openings and strychnine ( $1 \mu\text{M}$ ) to block glycinergic receptors. For cell-attached recordings of neuronal activity, pipettes (4–5 M $\Omega$ ) contained 150 mM NaCl. To identify the morphology of neurons recorded in cell-attached configuration, we repatched them with a conventional whole-cell electrode containing biocytin (see above). The single-channel currents were filtered at 1 kHz (GABA<sub>A</sub> channels) or 3 kHz (NMDA channels) and digitized at 10 kHz. Multilevel and short ( $<2$  ms) openings were discarded during analysis.  $I$ - $V$  relationships were performed by measuring amplitude of unitary GABA and NMDA currents evoked by steps from  $-120$  to  $+40$  mV. Histograms of cursor-measured amplitudes allowed determination of the mean unitary current amplitude at each voltage tested. Series resistance ( $R_s$ ), membrane capacitance ( $C_m$ ), and input resistance ( $R_{\text{input}}$ ) were determined by on-line fitting analysis of the transient currents in response to a  $-5/10$  mV pulse. Criteria for considering a recording included  $R_{\text{input}} > 100$  M $\Omega$ ,  $R_s < 25$  M $\Omega$ , with  $\Delta R_s < 30\%$  change. Average values are presented as means  $\pm$  SEM and statistical comparisons were performed with the Student's  $t$  test (SigmaStat 3.1, Origin 5.0) or Mann-Whitney rank sum test (SigmaStat 3.1). The level of significance was set as  $p < 0.05$ .

We performed extracellular unit recording of striatal neurons with either conventional extracellular tungsten electrodes or with the multi-electrode array (MEA) technology (Heuschkel et al., 2002; Steidl et al., 2006). The MEA setup (Multi Channel Systems) is composed of a 60 channel amplifier head stage connected to a 60 channel A/D card. The slice is gently positioned on the array of 60 platinum electrodes (spaced by  $100 \mu\text{m}$ ) used as recording electrodes (Ayanda Biosystems). Record-

ings were acquired and analyzed with the MC Rack software commercially available from Multi Channel Systems.

**Measurements of  $V_{\text{rest}}$ ,  $E_{\text{GABA}_A}$ ,  $V_{\text{threshold}}$ .** To determine the action of GABA in a given neuron (depolarizing or hyperpolarizing), one must measure the reversal potential of the GABA<sub>A</sub>-mediated current ( $E_{\text{GABA}_A}$ ) and the resting membrane potential ( $V_{\text{rest}}$ ). However, conventional whole-cell recordings introduce a number of errors in these measures. We therefore estimated the value of  $V_{\text{rest}}$  from cell-attached recordings of the single-channel NMDA current ( $i_{\text{NMDA}}$ ), which is known to reverse at a membrane potential ( $V_m$ ) close to 0 mV (Nowak et al., 1984) (see Discussion). We plotted the relationship between  $i_{\text{NMDA}}$  and the extracellular potential applied to the patch of membrane ( $V_p$ ) from experimental data (see Fig. 5A). This curve [ $i_{\text{NMDA}} = f(V_p)$ ] gives the value of  $V_p$  when  $i_{\text{NMDA}} = 0$  pA. At this value of  $V_p$ , single-channel NMDA current is null because  $V_m = V_p - V_{\text{rest}} = 0$  mV. This allows estimation of  $V_{\text{rest}}$  ( $V_{\text{rest}} = V_p$ ). To estimate ( $E_{\text{GABA}_A}$ ), we plotted the relationship between the single-channel GABA<sub>A</sub> current ( $i_{\text{GABA}_A}$ ) and  $V_p$ . This curve [ $i_{\text{GABA}_A} = f(V_p)$ ] gives the value of  $V_p$  when  $i_{\text{GABA}_A} = 0$  pA (see Fig. 5B), because by definition when  $i_{\text{GABA}_A}$  is null,  $V_m = E_{\text{GABA}_A}$ . Therefore, when  $i_{\text{GABA}_A} = 0$  pA,  $V_m = V_p - V_{\text{rest}} = E_{\text{GABA}_A}$  (i.e.,  $E_{\text{GABA}_A} - V_{\text{rest}} = -V_p$ ). By definition,  $E_{\text{GABA}_A} - V_{\text{rest}} = DF_{\text{GABA}_A}$ , the driving force of chloride ions through the GABA<sub>A</sub> channel (Tyzio et al., 2003). Therefore, when  $i_{\text{GABA}_A} = 0$  pA,  $DF_{\text{GABA}_A} = -V_p$ . Knowing  $V_{\text{rest}}$  and  $DF_{\text{GABA}_A}$ , it is easy to calculate  $E_{\text{GABA}_A} = DF_{\text{GABA}_A} + V_{\text{rest}}$ . In addition, the slopes of the  $i_{\text{NMDA}} - V_p$  and  $i_{\text{GABA}_A} - V_p$  relationships provide an estimate of the conductance of NMDA and GABA<sub>A</sub> channels, respectively. The threshold potential for Na<sup>+</sup> spikes ( $V_{\text{threshold}}$ ) was estimated in whole-cell current-clamp recordings by applying successive depolarizing steps [duration, 250 or 950 ms (Centonze et al., 2003)] or by evoking spikes by cortical stimulation, both from the value of  $V_{\text{rest}}$  calculated above.

**Identification of recorded striatal neurons.** We identified MSNs during recording based on their typical rectification during hyperpolarizing steps and their firing delay in response to depolarizing steps (see Fig. 5C). They had a round dendritic field with extremely spiny dendrites and axons that extended outside the striatum toward the globus pallidus (Fig. 1A3,B3). Cholinergic interneurons were readily identified in the slice by their large somata and thick primary dendrites. Negative-current pulses produced an initial hyperpolarization followed by a depolarizing sag in the membrane potential. Depolarizing pulses resulted in nonadapting, regular spiking. Examination of biocytin-filled neurons confirmed the above morphological criteria (see Fig. 6B). FS interneurons discharged in trains of narrow action potentials. Epochs of firing were interspersed with periods of silence during depolarizing steps just above threshold. Their aspiny dendrites branched modestly (see Fig. 7A). In addition to fast spikes, LTS interneurons also displayed low-threshold spikes when depolarized from potentials near  $-70$  mV or after cessation of hyperpolarized pulses (see Fig. 7B). They had a high input resistance compared with the other neuronal types ( $\sim 600$  M $\Omega$ ). Their dendrites radiated a long distance and were infrequently branched (Kawaguchi, 1993; Tepper and Bolam, 2004).

**Drugs.** Drugs were prepared as concentrated stock solutions and diluted in ACSF for bath application: bicuculline, a GABA<sub>A</sub> receptor antagonist; carbachol, a cholinergic agonist; muscarine, a muscarinic cholinergic agonist; nicotine, a nicotinic cholinergic agonist; mecamylamine, a nicotinic antagonist; scopolamine, a muscarinic antagonist; D-APV, a NMDA receptor antagonist; 6-cyano-7-nitroquinoxaline 2,3-dione (CNQX), an AMPA/kainate receptor antagonist; tetrodotoxin (TTX), a Na<sup>+</sup> channel blocker; R(+)-7-chloro-8-hydroxy-3-methyl-1-phenyl-2,3,4,5-tetrahydro-1H-3-benzazepine hydrochloride (SCH23390), a D<sub>1</sub>-like receptor antagonist; and sulpiride, a D<sub>2</sub> receptor antagonist. All drugs were purchased from Sigma-Aldrich.

**Immunocytochemistry.** To visualize the lesion of dopaminergic axons in the striatum, we performed immunocytochemistry of TH in the recorded slices, or those just medial or lateral to those recorded. After 12 h in paraformaldehyde (3%) at  $4^\circ\text{C}$ , the sections were rinsed in PBS and pretreated with 30% H<sub>2</sub>O<sub>2</sub> (30 min) and blocked by 2% normal goat serum (NGS) in PBS containing 0.3% Triton X-100 for 30 min, and then incubated for 12 h with anti-TH polyclonal antibody (Pel-Freez) at a dilution of 1:1000. After rinsing with PBS, they were incubated for 1.5 h

with anti-mouse IgG secondary antibody (Tebu) at a dilution of 1:300 in PBS plus 2% normal goat serum. Sections were washed with PBS and incubated for 1.5 h in ABC complex at a dilution of 1:500 (Euromedex). They were rinsed and incubated for ~10 min in 3,3'-diaminobenzidine (DAB) (0.7 mg/ml) with peroxide (0.2 mg/ml) (SigmaFast), rinsed, mounted in Crystal/Mount (Electron Microscopy Sciences), coverslipped, and examined with a conventional microscope. Electrophysiological data were taken into account only when a severe loss (>90%) of tyrosine hydroxylase immunoreactivity was present in the dorsomedial striatum in which recordings were performed (Fig. 1B1,B2). To visualize the recorded cells in the striatum and identify them, we revealed the biocytin injected during whole-cell recordings. After 12 h in paraformaldehyde (3%) at 4°C, the sections were rinsed in PBS, left 12 h in 20% sucrose in phosphate buffer (PB), and left at -80°C for at least 2 h. They were thawed at room temperature, rinsed in PB, and incubated 30 min in 1% H<sub>2</sub>O<sub>2</sub> in PB. Sections were washed with PB and KPBS and incubated for 12 h in ABC complex at a dilution of 1:100 in KPBS plus 0.3% Triton (Abcys). They were rinsed in KPBS and incubated for ~10 min in DAB (0.7 mg/ml) with peroxide (0.2 mg/ml) (SigmaFast), rinsed, mounted in Crystal/Mount (Electron Microscopy Sciences), coverslipped, and examined. Dendritic and axonal arbors were reconstructed for morphological analysis using the Neurolucida system (MicroBrightField).

To identify the D<sub>1</sub> phenotype of the MSNs recorded, D<sub>1</sub>R was detected by immunohistochemistry using a monoclonal antibody raised in rat against a 97 aa sequence corresponding to the C terminus of the human D<sub>1</sub>R (Sigma-Aldrich) (Levey et al., 1993; Guigoni et al., 2007). Slices were cryoprotected in PBS with 25% saccharose, freeze-thawed in isopentane, and rinsed in PBS. Slices were then incubated in 4% NGS for 30 min and then in D<sub>1</sub>R antibody (1:1000) supplemented with 1% NGS overnight at RT. After thorough rinsing, slices were incubated for 90 min at RT in Alexa 568 goat anti-rat (1:200 in PBS; Invitrogen) with streptavidin coupled with DTAF (dichlorotriazinylamino-fluorescein) (1:200; Fluor-Probes; Interchim) to detect biocytin injected in the recorded neurons. After thorough rinsing, slices were again incubated in D<sub>1</sub>R antibody for 60 min, rinsed again, and incubated with secondary antibody for 60 min. This step was repeated once more. After thorough rinsing, slices were mounted in Vectashield (Vector Laboratories/Biovalley), coverslipped, and examined with a confocal microscope (Zeiss LSM 510).

## Results

### Spontaneous GABA<sub>A</sub> currents increase in amplitude and shift to oscillatory mode in DA-depleted MSNs

We have recorded the activity of 97 control and 98 DA-depleted MSNs in slices of isolated striatum that have been disconnected from their glutamatergic afferent neurons (cortical and thalamic) and of 10 control and 18 DA-depleted MSNs in BGS. In whole-cell or cell-attached configuration (current-clamp mode), all the recorded MSNs were silent at resting membrane potential in both the control and DA-depleted states. The pattern of GABA<sub>A</sub> sPSCs in identified MSNs ( $n = 40$ ) was mainly tonic, with low-frequency ( $4.5 \pm 0.4$  Hz) and low-amplitude ( $34.1 \pm 1.8$  pA) events in isolated striatum (Fig. 2A). The overall mean current density of this tonic pattern was  $459 \pm 40$  nA · ms (Fig. 2C, top). In 10 of the 40 MSNs, we also observed rare giant (>200 pA) currents (mean amplitude,  $306 \pm 8$  pA; range, 200–650 pA; mean frequency,  $0.14 \pm 0.03$  Hz) or rare bursts (mean intraburst frequency,  $29.3 \pm 1.1$  Hz; mean intraburst amplitude,  $51.3 \pm 1.0$  pA;  $n = 3$  of 40) (Figs. 2A, middle and bottom traces; C, top; 3A, control). The results obtained in BGS were totally similar as those from isolated striatum ( $5.6 \pm 1.0$  Hz,  $p = 0.31$ ;  $30.0 \pm 4.3$  pA,  $p = 0.44$ ).

After chronic DA depletion, a new pattern emerged, characterized by a higher current density ( $1311 \pm 142$  nA · ms) and the higher occurrence of giant GABA<sub>A</sub> sPSCs such as (1) single sPSCs of higher amplitude ( $340 \pm 6$  pA; range, 240–1900 pA;  $p < 0.01$ ) and frequency ( $0.29 \pm 0.07$  Hz;  $p < 0.05$ ) compared with control

and (2) bursts of sPSCs, which recurred at regular intervals of  $6.0 \pm 0.8$  s during periods varying from 6 to 1650 s (Fig. 2B1,C). The mean intraburst frequency of sPSCs ( $58.7 \pm 1.3$  Hz) and amplitude ( $95.9 \pm 2.6$  pA) both doubled compared with control ( $p < 0.001$  for both) (Fig. 3A, DA-depleted). This new giant and oscillatory pattern was observed in 45% of the recorded MSNs ( $n = 20$  of 45). In the remaining 55% MSNs ( $n = 25$  of 45), the pattern of afferent GABA<sub>A</sub> sPSCs was relatively unchanged by the DA lesion. The mean current density, frequency, and amplitude of sPSCs was not statistically different from control ( $496 \pm 59$  nA · ms,  $p = 0.35$ ;  $5.6 \pm 0.6$  Hz,  $p = 0.11$ ;  $35.3 \pm 2.0$  pA,  $p = 0.67$ ;  $n = 25$ ) (Fig. 2B2,C, top). The results obtained in DA-depleted BGS were similar as those recorded in isolated DA-depleted striatum with the presence of the oscillatory pattern of PSCs in 45% of MSNs (intraburst frequency,  $73.3 \pm 3.1$  Hz, and intraburst amplitude,  $111.4 \pm 4.2$  pA; giants amplitude,  $270 \pm 39$  pA;  $n = 8$  of 18) and of the regular pattern in the remaining 55%. In conclusion, spontaneous GABA<sub>A</sub> sPSCs became strikingly oscillatory in ~50% of the MSNs in chronically DA-depleted striatum independently of the presence of corticostriatal neurons. We never observed such a pattern in control conditions.

The oscillatory pattern of GABA<sub>A</sub> sPSCs did not depend on the internal pipette solution, holding membrane potential, or spontaneous glutamate synaptic activity. This pattern was observed with a recording solution with low internal chloride (CsGlu-filled electrodes) from  $V_H = -75$  to  $+10$  mV (Fig. 3B) or with high internal chloride (CsCl-filled electrode) (data not shown) and in the absence or presence of CNQX ( $10$ – $30$  μM) and APV ( $40$  μM) (Fig. 3C). As expected, bicuculline ( $10$  μM), an antagonist of GABA<sub>A</sub> receptors, suppressed all sPSCs (Fig. 3C). To test whether the oscillatory pattern resulted from chronic or acute dopamine depletion, we acutely blocked dopaminergic transmission in control slices by simultaneously applying D<sub>1</sub>R and D<sub>2</sub>R antagonists (SCH23390,  $10$  μM; sulpiride,  $10$  μM). Acute blockade did not mimic chronic DA depletion. This treatment did not cause sPSCs to become oscillatory, nor did it significantly affect their frequency (from  $6.6 \pm 1.0$  to  $5.5 \pm 1.5$  Hz;  $p = 0.91$ ) or amplitude (from  $29.6 \pm 1.6$  to  $24.8 \pm 3.5$ ;  $p = 0.45$ ) (data not shown) ( $n = 7$ ). This strongly suggested that the oscillatory pattern of GABA<sub>A</sub> sPSCs resulted from the chronic, rather than acute, absence of dopaminergic terminals.

To understand whether giant currents had a postsynaptic or a presynaptic origin, we recorded miniature GABA<sub>A</sub> currents. Their mean frequency and mean amplitude were not significantly different between control and DA-depleted MSNs that displayed the oscillatory pattern (frequency:  $1.5 \pm 0.2$  Hz,  $n = 15$ , vs  $1.8 \pm 0.5$  Hz,  $n = 7$ ,  $p = 0.5$ ; amplitude:  $31.9 \pm 1.5$  pA,  $n = 15$ , vs  $32.7 \pm 2.8$ ,  $n = 7$ ,  $p = 0.8$ ), suggesting that the oscillatory pattern has a presynaptic origin (supplemental Fig. 1, available at [www.jneurosci.org](http://www.jneurosci.org) as supplemental material).

### D<sub>1</sub>-positive and D<sub>1</sub>-negative MSNs generate the oscillatory pattern

Since MSNs are composed of D<sub>2</sub> striatopallidal and D<sub>1</sub> striatonigral subtypes, with a relatively selective distribution of D<sub>1</sub> and D<sub>2</sub> dopamine receptors that are not altered by chronic dopamine depletion (Nadjar et al., 2006), we reasoned that the two types of GABA<sub>A</sub> sPSCs patterns recorded could correspond to these two types of MSNs. To test this hypothesis, we performed immunocytochemical labeling of intracellularly injected biocytin with D<sub>1</sub> dopamine receptor antibodies (see Materials and Methods). Of the 30 double-labeled MSNs recorded in DA-depleted striatum, 13 generated the oscillatory

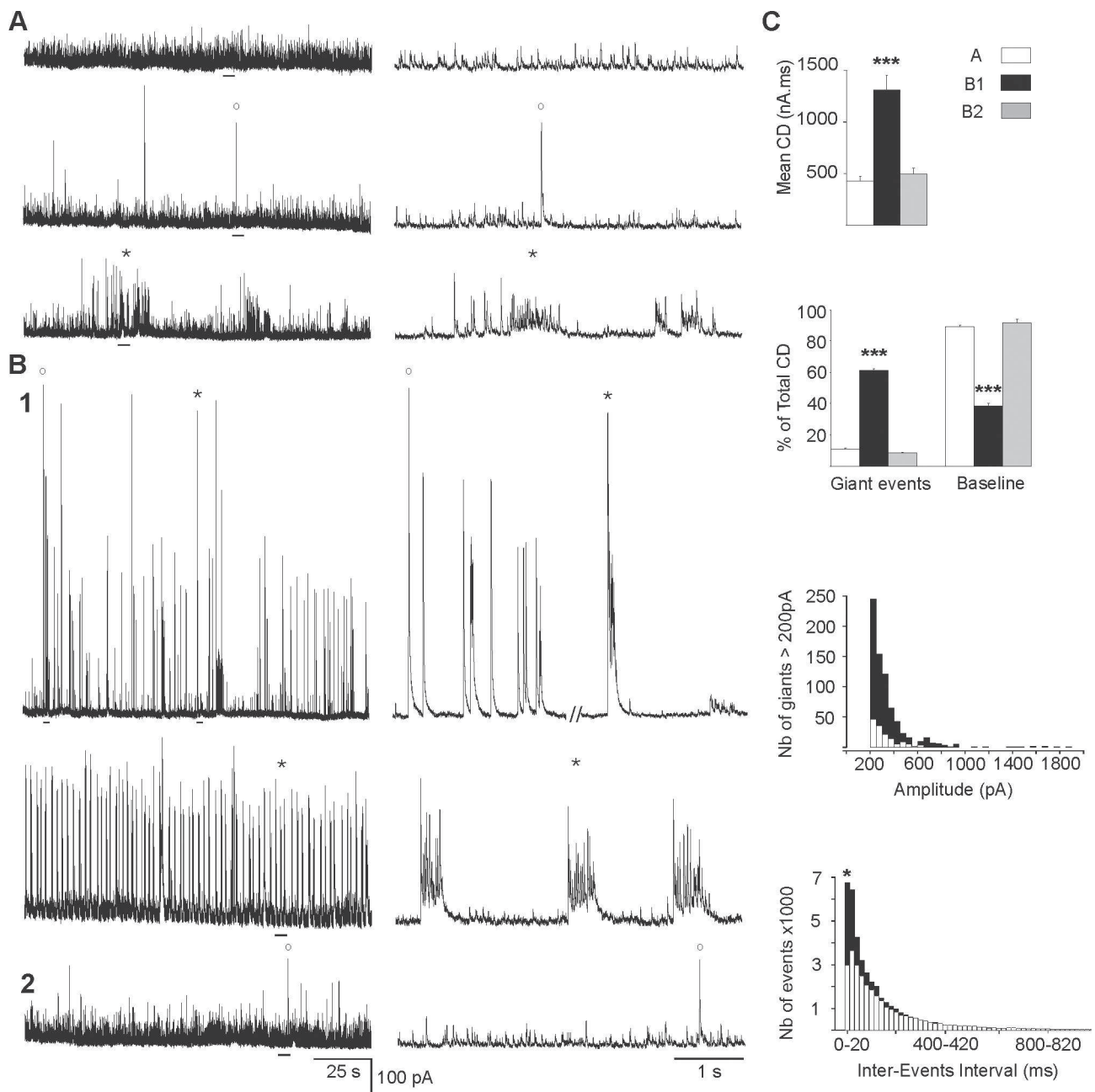


**Figure 2.** Spontaneous GABA<sub>A</sub> currents recorded in MSNs before and after chronic DA depletion. Voltage-clamp recordings of GABA<sub>A</sub> sPSCs with CsGlu-filled electrodes ( $V_H = +10$  mV). **A**, Tonic pattern of GABA<sub>A</sub> sPSCs in control isolated striatum (68% of MSNs; top traces) with the rare presence of single sPSCs  $>200$  pA ( $^{\circ}$ ) (23% of MSNs; middle traces) and bursts of sPSCs ( $^*$ ) (9% of MSNs; bottom traces). **B**, The two patterns of GABA<sub>A</sub> sPSCs recorded from DA-depleted isolated striatum. **B1**, Oscillatory pattern observed in 45% of the MSNs and characterized by the frequent presence of giant events: single sPSCs ( $^{\circ}$ ) and bursts of sPSCs ( $^*$ ). **B2**, Tonic pattern in the remaining MSNs (55%). The calibration bars are the same for all recordings in **A** and **B**. **C** (from top to bottom), Quantification of the data from control MSNs as shown in **A** (white) and from DA-depleted MSNs as shown in **B1** (black) or **B2** (gray). The mean current density (CD) of GABA<sub>A</sub> sPSCs increased threefold between **A** and **B1** or **B2** and **B1**. Giant events represented 11 and 8% of the total CD in **A** and **B2**, respectively, but 61% in **B1**. The baseline events ( $<200$  pA) represented 89 and 92% of the total CD in **A** and **B2**, respectively, but 38% in **B1**. The distribution of single giant sPSCs  $>200$  pA shows the increased number of these events and the presence of very large amplitude events (1000–1800 pA) in **B1** compared with **A**. Intervent intervals were shorter in **B1** than in **A** as most of the events were present in the interval 0–20 ms. Error bars indicate SEM.  $^*p < 0.05$ ;  $***p < 0.001$ .

GABA<sub>A</sub> pattern and 17 the tonic one. Among the 13 MSNs with the oscillatory pattern, 6 MSNs expressed D<sub>1</sub> dopamine receptors and 7 MSNs did not (Fig. 4). Among the 17 MSNs with a tonic GABA<sub>A</sub> pattern, 4 MSNs expressed D<sub>1</sub> receptors and 13 MSNs did not. Therefore, both “D<sub>1</sub> positive” and “D<sub>1</sub> negative” MSNs can generate the oscillatory GABA<sub>A</sub> pattern when dopamine deprived.

#### $V_{rest}$ , $E_{GABA_A}$ , and $V_{threshold}$ of MSNs are identical in control and DA-depleted striatum

Alterations of intrinsic parameters or the polarity of GABAergic synapses could also underlie the shift in the firing pattern of MSNs. Indeed, GABA signals in neuronal disorders have been reported to shift from inhibition to excitation (Cohen et al., 2002). To determine whether dopamine depletion leads to simi-

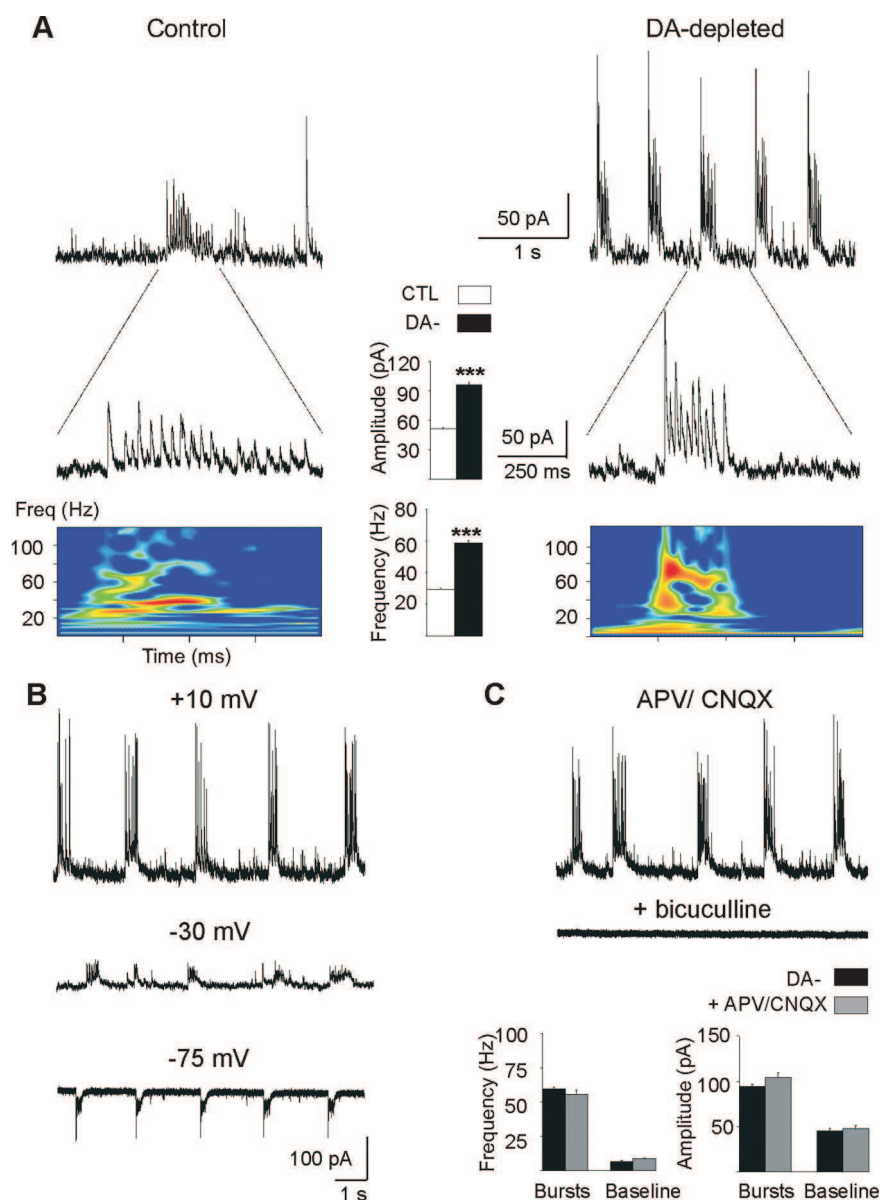


**Figure 3.** Burst characteristics. **A**, Whole-cell recordings ( $V_H = +10$  mV) of rare bursts (**A**) and recurrent bursts (**B**) of GABA<sub>A</sub> sPSCs in control (left) and DA-depleted (right) MSNs and corresponding power spectrum analysis of a single burst. Intraburst frequency of GABA<sub>A</sub> sPSCs are visualized by time–frequency representations (bottom colored diagrams) that enables determining the implication of different frequency ranges within the burst. The field power is here coded in colors so that red corresponds to higher amplitudes. The calibrations are identical for the left and right traces. Histograms in the center, Mean intraburst amplitude and frequency of GABA<sub>A</sub> sPSCs in control MSNs (□) and in DA-depleted MSNs with an oscillatory pattern (■). **B**, Recordings of recurrent bursts in a DA-depleted MSN at the indicated holding potentials (whole-cell configuration, internal CsGlu). **C**, Application of APV (40  $\mu$ M) plus CNQX (10  $\mu$ M) at  $V_H = +10$  mV did not significantly affect the frequency and amplitude of bursts or baseline events (bottom histograms), whereas bicuculline at 20  $\mu$ M totally abolished them. Error bars indicate SEM. \*\*\* $p < 0.001$ .

lar alterations, we performed single NMDA and GABA channel recordings to determine  $V_{rest}$  and  $E_{GABA}$ , respectively. We also measured the threshold for spike generation ( $V_{threshold}$ ) (see Materials and Methods). Each tested neuron was successively patched in cell-attached configuration to record NMDA or GABA<sub>A</sub> single-channel currents and then in whole-cell configuration to test the  $I$ – $V$  relationship and label them with biocytin to confirm their identity as MSNs.

Current–voltage relationships of single NMDA channel currents from identified MSNs in control striatum yielded a mean resting membrane potential of  $V_{rest} = -79.7 \pm 1.0$  mV ( $n = 9$ )

(mean NMDA conductance,  $79 \pm 3$  pS;  $n = 9$ ) (Fig. 5A). The extracellular  $Ca^{2+}$  concentration (1.8 mM) and the recording temperature (32°C) may explain this large conductance compared with the typical value obtained from cell-attached recordings in central neurons (50–60 pS) (Clark et al., 1997). Current–voltage relationships of single GABA<sub>A</sub> channel currents recorded in identified MSNs yielded a mean driving force of  $DF_{GABA} = 16.1 \pm 1.9$  mV ( $n = 11$ ) (Fig. 5B), suggesting a mean reversal potential of GABA<sub>A</sub> currents of  $E_{GABA} = -63.6 \pm 2.9$  mV (conductance,  $14.9 \pm 1.1$  pS;  $n = 11$ ). The threshold potential for Na<sup>+</sup> spikes in response to 250 ms depolarizing steps (Fig. 5C, control) was  $V_{threshold} = -35.7 \pm 1.4$  mV ( $n = 22$ ). The threshold of spikes evoked in response to cortical stimulation in control MSNs was  $V_{threshold} = -38.3 \pm 0.6$  mV ( $n = 7$ ) (Fig. 5C, control).  $V_{threshold}$  obtained with these two methods were not statistically different ( $p = 0.18$ ).

In DA-depleted striatum, the results obtained with the same methods were not statistically different from control:  $V_{rest} = -80.1 \pm 1.0$  mV ( $n = 7$ ;  $p = 0.8$ ) (Fig. 5A, right),  $DF_{GABA} = 17.1 \pm 1.6$  mV ( $n = 10$ ;  $p = 0.7$ ) (Fig. 5B, right),  $E_{GABA} = -63.0 \pm 2.9$  mV ( $n = 10$ ), and  $V_{threshold} = -35.0 \pm 0.9$  mV ( $n = 36$ ;  $p = 0.6$ ) or  $-40.8 \pm 1.0$  mV for cortical stimulation evoked spikes ( $n = 8$ ;  $p = 0.06$ ) (Fig. 5C, right). Pressure-applied isoguvacine (100  $\mu$ M; 100 ms), a GABA<sub>A</sub> receptor agonist, never excited control or DA-depleted MSNs recorded in cell-attached configuration ( $n = 8$ ) (Fig. 5D). Therefore, in DA-depleted striatum GABA<sub>A</sub> PSCs have the same effect on membrane potential of MSNs as in control striatum. Specifically, GABA depolarizes MSNs by 16–17 mV from  $V_{rest}$  (Fig. 5E), without evoking Na<sup>+</sup> spikes, as the threshold potential for spikes was  $\sim 25$  mV more depolarized than  $E_{GABA}$ .

### GABA oscillations of DA-depleted MSNs are not mediated by cholinergic signaling

Several mechanisms could lead to the novel pattern of GABAergic oscillations observed, including changes in (1) activity of cholinergic interneurons, (2) presynaptic inhibition of GABA release by muscarinic receptors, (3) MSN–MSN recurrent collateral activity, or (4) activity of GABAergic interneurons, which would in turn generate GABA oscillations in MSNs. Interestingly, acetylcholine released by TANs excites GABA interneurons via nicotinic receptors (nAChRs) (Koós and Tepper, 2002), and in a primate Parkinson's disease model, TANs were said to shift to a bursting and oscillatory mode of activity (Raz et al., 1996). We performed the following pharmacological experiments in isolated striatum to avoid activation of structures afferent to striatum. Although nic-

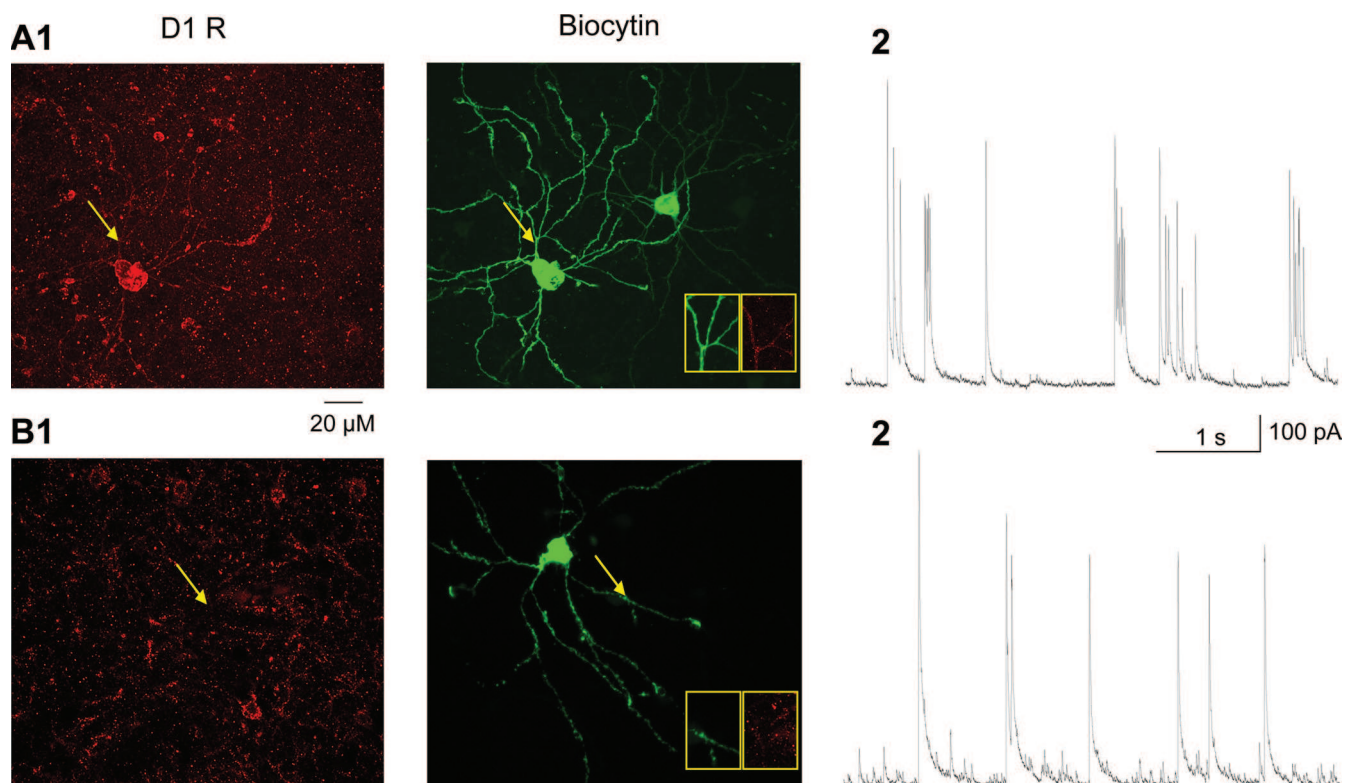


**Figure 4.** Oscillatory pattern recorded from MSNs positive (**A**) or negative (**B**) for  $D_1$  dopamine receptor expression. Confocal microphotographs (z-projections) of DA-depleted slices, double labeled for  $D_1$  receptor (red) and biocytin (green) (**A1**, **B1**). The boxes contain enlarged portions of dendritic arbors to show the presence (**A**) or the absence (**B**) of colabeling. In **A1**, the recorded MSN is on the left. The MSN on the right was indirectly filled with biocytin, likely because of gap junction connections with the recorded MSN. Both recorded neurons in **A** and **B** generated the oscillatory pattern of GABA<sub>A</sub> sPSCs (**A2**, **B2**).

otine (10–30  $\mu$ M) increased the mean current density of GABA<sub>A</sub> sPSCs 13-fold (from  $1655 \pm 44$  to  $20,941 \pm 1052$  nA  $\cdot$  ms;  $n = 7$ ;  $p < 0.005$ ) (data not shown) in DA-depleted oscillating MSNs, the specific nicotinic antagonist mecamylamine (3–10  $\mu$ M) altered neither their mean current density (from  $2508 \pm 862$  to  $1975 \pm 985$  nA  $\cdot$  ms;  $n = 6$ ;  $p = 0.13$ ) nor their oscillatory pattern (Fig. 6A). Alternately, acetylcholine released by TANs could affect GABA interneurons via muscarinic receptors (mAChRs). Muscarine (10  $\mu$ M) did not significantly affect the current density of oscillatory GABA<sub>A</sub> sPSCs ( $n = 6$ ) (data not shown), and scopolamine (10  $\mu$ M), a broad spectrum muscarinic antagonist, also did not affect their mean current density (from  $1894 \pm 300$  to  $1497 \pm 400$  nA  $\cdot$  ms;  $n = 5$ ;  $p = 0.21$ ) or their oscillatory pattern (Fig. 6A).

To further investigate a presynaptic modulation by muscarinic receptors of GABA release (Koós and Tepper, 2002), we determined the effects of carbachol on miniature GABA<sub>A</sub> PSCs. Carbachol (30  $\mu$ M) significantly decreased this frequency by 33% in control striatum (from  $1.5 \pm 0.2$  to  $1.0 \pm 0.1$  Hz;  $p < 0.01$ ;  $n = 9$  cells), an effect that was totally reversed by scopolamine (10  $\mu$ M) (from  $1.0 \pm 0.1$  to  $1.9 \pm 0.2$  Hz;  $n = 9$  cells) (supplemental Fig. 1A, available at [www.jneurosci.org](http://www.jneurosci.org) as supplemental material). In DA-depleted striatum, carbachol decreased the frequency of miniature GABA<sub>A</sub> events by 18% (from  $2.2 \pm 0.5$  to  $1.8 \pm 0.5$  Hz;  $p < 0.05$ ;  $n = 9$  cells), an effect that was completely reversed by scopolamine (from  $1.8 \pm 0.5$  to  $2.2 \pm 0.6$  Hz;  $n = 9$  cells). The effects of carbachol on miniature GABA<sub>A</sub> currents was not statistically different between control and DA-depleted striatum ( $p = 0.12$ ) (supplemental Fig. 1B, available at [www.jneurosci.org](http://www.jneurosci.org) as supplemental material).

Finally, cell-attached recordings of identified TANs confirmed that DA-depletion did not affect their tonic pattern of activity recorded *in vitro* (mean control frequency,  $2.7 \pm 1.1$  Hz;  $n = 9$ ; mean DA-depleted frequency,  $4.0 \pm 1.4$  Hz;  $n = 8$ ;  $p = 0.4$ ) nor their basic characteristics (Fig. 6B). All of the above results strongly suggest that the oscillatory pattern of GABA<sub>A</sub> sPSCs is independent of TAN activity.

#### LTS GABA interneurons show bursting activity in DA-depleted slices

Because all MSNs recorded in cell-attached or whole-cell configuration were silent in both control and DA-depleted striatum (Fig. 5D) and the strength of MSN–MSN connections dramatically reduced in DA-depleted conditions (Taverna et al., 2008), the synchronization of GABA<sub>A</sub> currents observed here likely resulted from a direct effect of chronic dopamine depletion on the activity of GABAergic interneurons. As these interneurons are rare and difficult to target with single-cell electrophysiological techniques, particularly in lesioned tissue, we first performed extracellular recordings with conventional extracellular electrodes or multiarray electrodes (see Materials and Methods) to test for the presence of oscillatory activities under control or lesioned conditions. In control BGS ( $n = 3$  slices) and control isolated striatum ( $n = 12$  slices), we never recorded oscillatory activities. Neurons were either silent or showed single-spike activity. In contrast, in DA-depleted BGS ( $n = 2$ ) and isolated striatum ( $n = 11$ ), oscillatory activity was observed together with single-spike activity (data not shown).

Cell-attached recordings combined with subsequent whole-cell recording of spike responses to intracellular current steps and

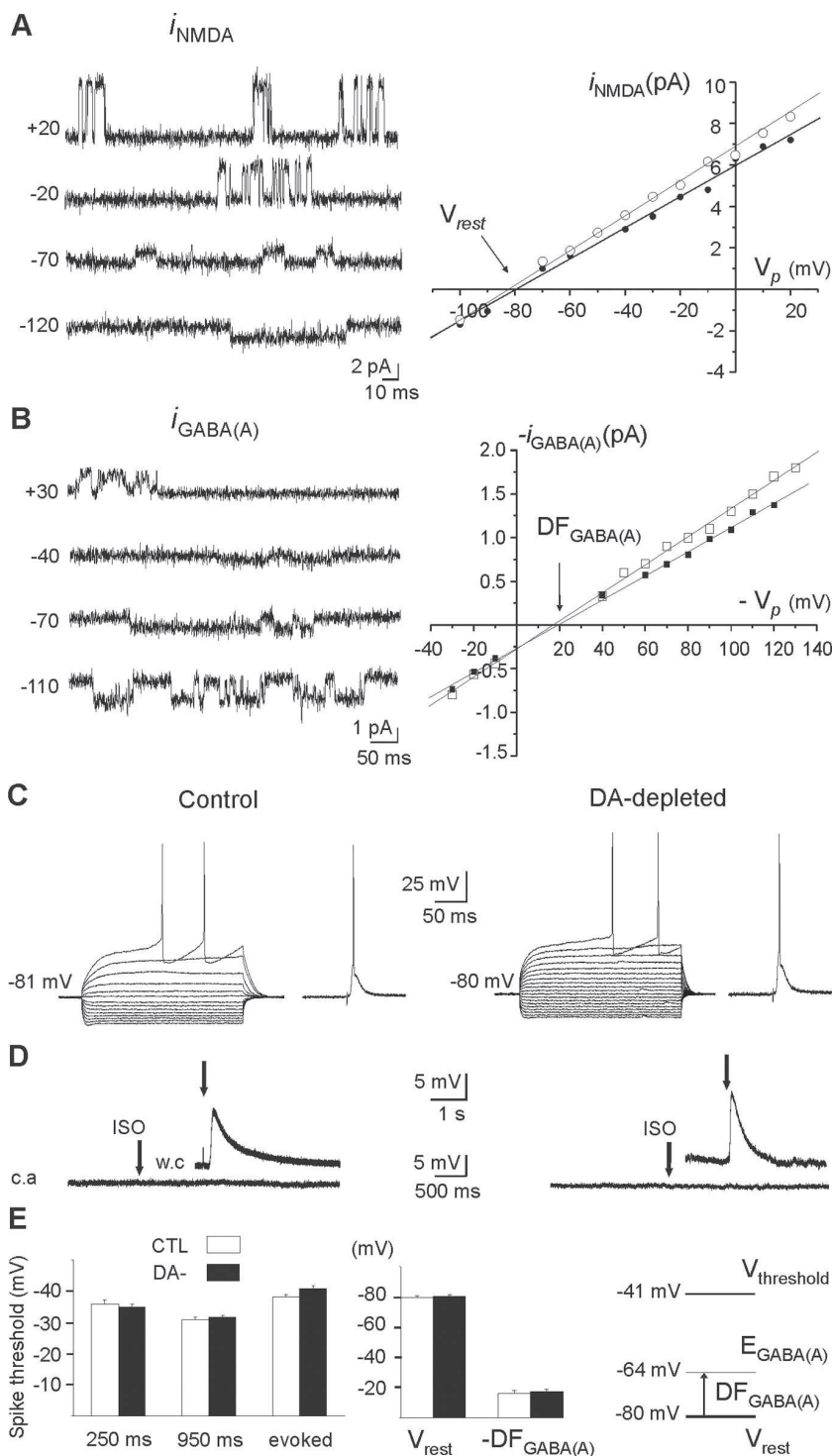


**Figure 5.**  $V_{\text{rest}}$ ,  $E_{\text{GABA(A)}}$ , and  $V_{\text{threshold}}$  in MSNs of control and DA-depleted striatum. **A**, Cell-attached recordings of unitary NMDA currents at the indicated holding potentials (in millivolts) from a DA-depleted MSN (left) and  $i_{\text{NMDA}}-V$  relationship in control (○) and DA-depleted (●) MSNs (right). **B**, Cell-attached recordings of unitary GABA<sub>A</sub> currents at the indicated holding potentials (in millivolts) from a DA-depleted MSN (left) and  $i_{\text{GABA(A)}}-V$  relationship in control (○) and DA-depleted (●) MSNs (right). The illustrated traces and corresponding  $I-V$  curves for NMDA and GABA currents are from the same cells. **C**, Whole-cell current-clamp recordings of the responses of control (left) and DA-depleted (right) MSNs to intracellular hyperpolarizing and depolarizing steps and to cortical stimulation. **D**, Absence of excitatory responses of cell-attached (c.a.) recorded MSNs to local pressure application of isoguvacine (100  $\mu\text{M}$ ), a GABA<sub>A</sub> receptor agonist, in control (left) and DA-depleted (right) state. The insets show the depolarizing effect of isoguvacine (100  $\mu\text{M}$ ) after rupture of the membrane [whole-cell recording (w.c.)] to check the efficacy of pressure application. **E**, Spike threshold was not significantly different in control and DA-depleted MSNs when tested in response to 250 or 950 ms intracellular currents pulses or evoked by cortical stimulation. Resting membrane potential ( $V_{\text{rest}}$ ), driving force for chloride ions ( $DF_{\text{GABA(A)}}$ ) or reversal potential for GABA<sub>A</sub> current, and threshold potential for spikes ( $V_{\text{threshold}}$ ) were not significantly different in control and DA-depleted MSNs. Error bars indicate SEM. See Results for additional explanations.

*post hoc* morphological examination of the recorded neurons showed that FS (Fig. 7A, left) and LTS (Fig. 7B, left) interneurons were silent or tonically active in control striatum. FS mean frequency of activity was  $10.1 \pm 0.2$  Hz ( $n = 2$  of 5) and LTS mean frequency was  $8.8 \pm 1.1$  Hz with rare trains at  $\sim 20$  Hz ( $n = 3$  of 5). In lesioned conditions, FS interneurons still discharged in single-spike mode ( $7.4 \pm 2.5$  Hz;  $n = 6$  of 18) or stayed silent (Fig. 7, compare B3, B4, with A3, A4). In contrast, some LTS interneurons shifted to an oscillatory activity consisting of long bursts of spikes at a mean frequency of  $71 \pm 30$  Hz separated by silent periods of  $3.9 \pm 1.6$  s ( $n = 3$  of 5). This LTS bursting activity was insensitive to the presence of blockers of glutamatergic transmission (Fig. 7B4), suggesting that it is not generated by corticostriatal activity. The remaining LTS displayed a tonic activity at  $9.7 \pm 1.7$  Hz ( $n = 2$  of 5). Interestingly, the intraburst frequency of spikes generated by LTS interneurons in DA-depleted condition was close to the intraburst frequency of GABA<sub>A</sub> currents recorded in DA-depleted MSNs (see results above).

## Discussion

Our results show that chronic dopamine depletion profoundly alters the pattern of GABA<sub>A</sub> activity, shifting the currents in one-half of the MSN population from a continuous tonic pattern of sPSCs to an oscillatory pattern consisting of giant single sPSCs, and/or bursts of sPSCs at a gamma frequency ( $\sim 60$  Hz). Using, for the first time, single-channel recordings of NMDA and GABA receptors in the striatum, we show that these alterations are not associated with shifts of the reversal potential for GABA or the resting membrane potential, suggesting that they are not attributable to excitatory actions of GABA. The threshold for spike generation is also unaltered by chronic dopamine depletion and cholinergic signals are not involved. We propose that the fundamental effect of the chronic removal of dopaminergic control on GABAergic circuits of the striatum is the shift of activity of GABAergic LTS interneurons from single-spike to bursting pattern and the increase in efficacy of GABAergic synaptic transmission. This leads in turn to the generation of repetitive giant bursts of GABA currents by one-half of the MSN population.

In both sagittal striatal slices from control mice (the present experiment) and coronal slices from control rats (Centonze et al., 2004; Cummings et al., 2008), MSNs generate a tonic pattern of low amplitude

GABA<sub>A</sub> currents (5–30 pA) at low frequency (~2.5–4 Hz). DA depletion shifted this pattern to an oscillatory one in D<sub>1</sub>-positive as well as D<sub>1</sub>-negative MSNs, suggesting that the effect of DA depletion on the pattern of GABA<sub>A</sub> currents did not target a particular subpopulation of MSNs. The 55% of the MSNs that generated the tonic GABA<sub>A</sub> pattern rather than the oscillatory one may be explained by their low degree of connectivity to GABA interneurons in the slice, or to a true difference in GABAergic innervation between the two MSNs groups.

What is the origin of the shift to the oscillatory pattern? Cholinergic interneurons, the TANs, were good candidates, as they are supposed to oscillate in the chronic absence of dopamine (Raz et al., 1996). However, in our experimental conditions, nicotinic and muscarinic blockers did not affect the oscillatory pattern, and identified TANs displayed the same tonic pattern of activity in the presence or absence of dopaminergic innervation. In simultaneous whole-cell recording of pairs of FS interneurons and MSNs, acetylcholine attenuates GABAergic inhibition of MSNs through activation of presynaptic muscarinic receptors located on GABA axon terminals (Marchi et al., 1990; Koós and Tepper, 2002). We showed that dopamine depletion of the striatum does not affect this process, suggesting that chronic alterations of presynaptic inhibition of GABA release by muscarinic receptors is also unlikely to be responsible for the generation of oscillatory GABA sPSCs. Concerning presynaptic control of GABA release by dopamine receptors, recordings of spontaneous GABA<sub>A</sub> currents from D<sub>2</sub> receptor knock-out mice revealed a loss of the inhibitory effect of the D<sub>2</sub> agonist quinpirole (Centonze et al., 2004).

Therefore, dopamine deprivation may produce a dual action: alteration of the basic activity pattern of a subpopulation of GABA interneurons, and decrease of presynaptic inhibition of GABA release leading to repetitive giant GABA<sub>A</sub> currents. Approximately 4–27 FS interneurons project to each MSN (Koós and Tepper, 1999), and each FS cell establishes a mean of six release sites per MSN (up to 18) that are often organized in clusters of synaptic contacts on the soma or proximal dendrites (Kita et al., 1990). This distribution and the proximity to the cell body enable an efficient inhibitory control of MSNs. In contrast, MSN–MSN recurrent synapses are on distal dendrites with only a small number of release sites (average of three) (Wilson and Groves, 1980). These may thus be less prone to generation of giant sPSCs. Despite the relatively high degree of convergence (each MSN receives ~500 synapses from other MSNs) (Czubayko and Pleniz, 2002; Guzmán et al., 2003; Koós et al., 2004), this recurrent system is unlikely to mediate the generation of giant GABAergic currents, because MSNs were silent in BGS and isolated striatum and their strength mostly de-

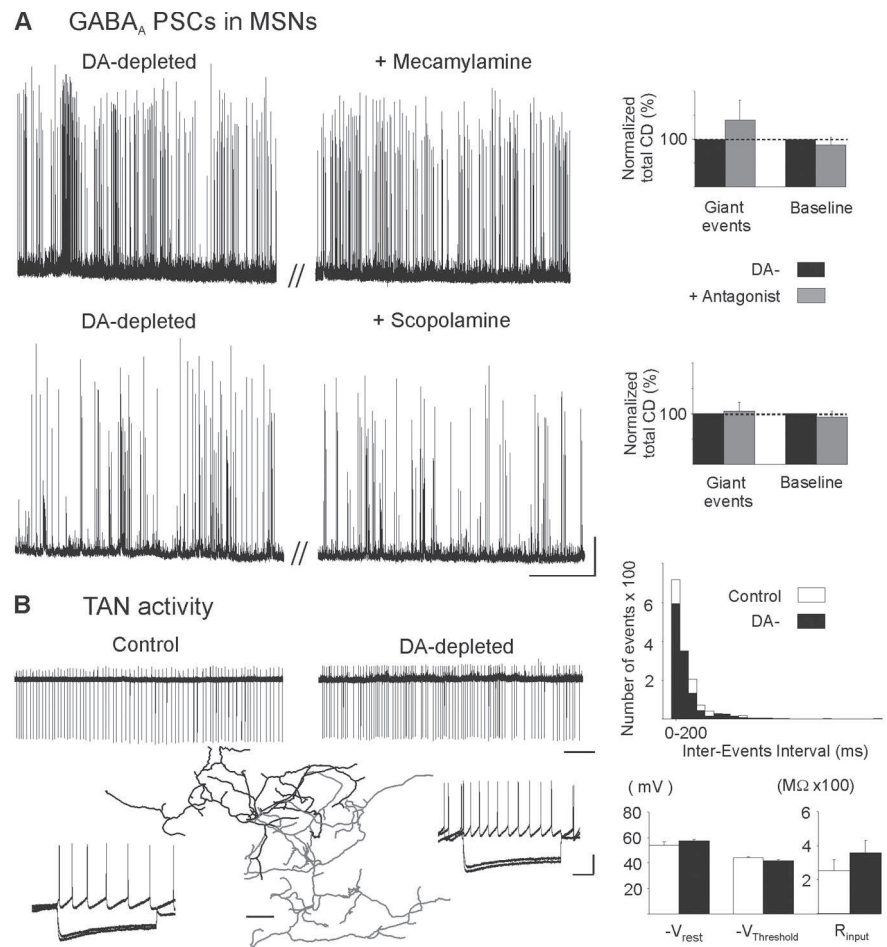


**Figure 6.** Effect of cholinergic antagonists on the oscillatory pattern of GABA<sub>A</sub> sPSCs and TAN activity in DA-depleted state. **A**, Lack of effect of bath application of mecamylamine (5  $\mu$ M) (top traces) or scopolamine (10  $\mu$ M) (bottom traces) on the oscillatory pattern of GABA<sub>A</sub> PSCs recorded in MSNs from DA-depleted isolated striatum. These nicotinic and muscarinic receptor antagonists did not affect current density (CD) of giant or baseline events of the oscillatory pattern (right diagrams). **B**, Current-clamp, cell-attached (top), and subsequent whole-cell (bottom) recordings from the same TANs in control (left) or in DA-depleted BGS (right). Current steps were applied from  $V_{rest} = -57$  mV in control and  $-59$  mV in DA-depleted TANs to  $V_m = -90$ ,  $-85$ , and  $-40$  mV. Notice the characteristic sag in response to hyperpolarizing current steps. NeuroLucida reconstruction of a biocytin-filled TAN with its dendritic tree in black and its collateralized axon in gray. Scale bar, 50  $\mu$ m. DA depletion did not affect TANs spontaneous pattern of activity (see the distribution of interevents intervals) nor their mean values of  $V_{rest}$  ( $-54.0 \pm 2.7$  vs  $-57.2 \pm 1.2$  mV;  $n = 7$  and  $11$ ;  $p = 0.4$ ),  $V_{threshold}$  ( $-44.2 \pm 0.3$  vs  $-41.7 \pm 0.9$  mV;  $n = 7$  and  $11$ ;  $p = 0.1$ ) and input resistance ( $R_{input}$ ) ( $255 \pm 63$  vs  $357 \pm 74$  M $\Omega$ ;  $p = 0.4$ ) (right diagrams). Calibration: **A**, 25 s, 100 pA; **B**, 5 s (top) and 200 ms, 25 mV (bottom steps). Error bars indicate SEM.

creased in the chronic absence of dopamine (Taverna et al., 2008). FS interneurons are also unlikely to mediate bursts of GABAergic currents because DA depletion did not affect their single-spike firing pattern. In contrast, we showed for the first time that identified LTS interneurons spontaneously discharge with a striking bursting pattern in the absence of dopamine, a type of activity not recorded under control conditions. Moreover, the intraburst frequency of LTS spikes was close to that of GABAergic currents recorded in MSNs.

Our single GABA and NMDA channel recordings (Tyzio et al., 2003) indicate for the first time a value for the reversal potential of GABA current ( $E_{GABA} = -63.0 \pm 2.9$  mV) of DA-depleted MSNs. We also showed that the resting membrane potential ( $V_{rest} = -80$  mV) and  $E_{GABA}$  of MSNs are not affected by dopamine depletion. All these values are based on the assumption that the NMDA current reverses at 0 mV in MSNs. Although an error of ~5 mV may exist (Tyzio et al., 2003), the comparison of  $V_{rest}$

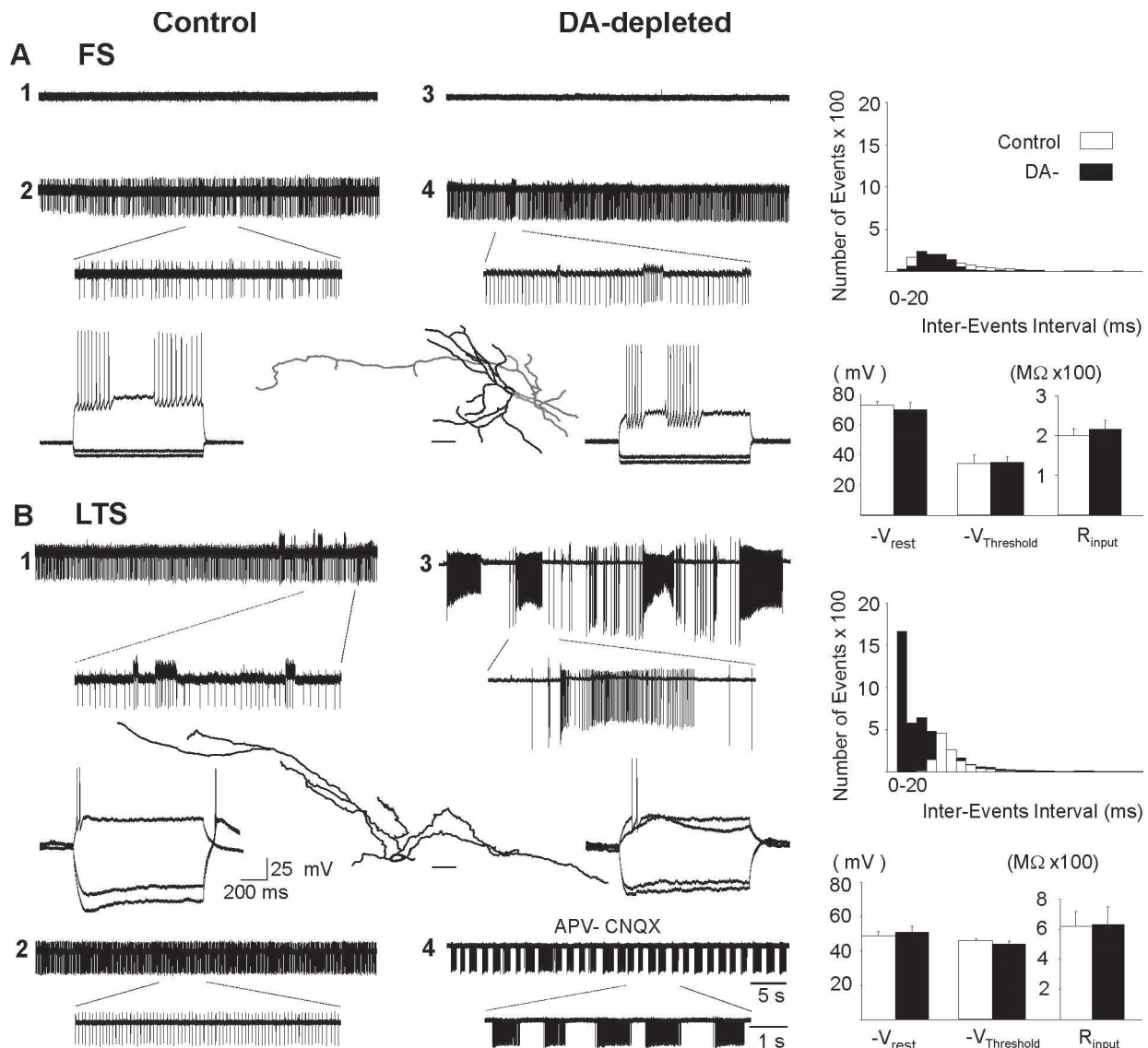


**Figure 7.** Spontaneous activity of GABAergic FS and LTS interneurons in control and DA-depleted striatum. **A**, Activity of FS interneurons recorded in cell-attached configuration in control (**1, 2**) and DA-depleted (**3, 4**) striatum. Sixty percent of FS were silent in control striatum (**1**) and 67% in DA-depleted one (**3**). The remaining FS displayed single-spike regular activity with rare trains of spikes (**4**). The bottom traces in **2** and **4** are expanded traces of the top ones as indicated. Note the typical FS firing in response to depolarizing steps (bottom traces) recorded in control from neuron **2** and in DA-depleted striatum from neuron **4**. Current steps were applied from  $V_{rest} = -74.8$  mV to  $V_m = -82, -78,$  and  $-29$  mV in control and from  $V_{rest} = -78$  mV to  $-90, -85,$  and  $-37$  mV in DA-depleted FS neurons. NeuroLucida reconstruction of the biocytin-filled FS interneuron **2** show the aspiny dendrites (black) and the collateralized axon (gray). The right diagrams show that the interevent intervals distribution and the mean value of  $V_{rest}$  ( $-73.0 \pm 2.3$  vs  $-69.6 \pm 5.0$  mV;  $n = 5$  and  $6$ ;  $p = 0.6$ ),  $V_{threshold}$  ( $-34.0 \pm 5.8$  vs  $-34.8 \pm 3.7$  mV;  $n = 5$  and  $7$ ;  $p = 0.9$ ), and input resistance ( $R_{input}$ ) ( $199 \pm 18$  vs  $217 \pm 21$  M $\Omega$ ;  $n = 5$  and  $7$ ;  $p = 0.6$ ) were unchanged by DA depletion. **B**, LTS interneurons switch from a tonic control activity to a bursting one in DA-depleted condition. Two examples of control (**1, 2**) and DA-depleted (**3, 4**) LTS activities are shown. LTS in **4** was recorded in the continuous presence of the glutamatergic antagonists APV ( $10 \mu\text{M}$ ) and CNQX ( $40 \mu\text{M}$ ). Note the typical rebound after hyperpolarizing steps giving rise to spikes and the low-threshold  $\text{Ca}^{2+}$  spike in response to depolarizing steps (bottom traces) recorded in control from neuron **1** and in DA-depleted striatum from neuron **3**. Current steps were applied from  $V_m = -70$  mV to  $V_m = -130, -115,$  and  $-43$  mV in control and from  $V_m = -71$  mV to  $-120, -115, -55,$  and  $-47$  mV in DA-depleted LTS neurons. NeuroLucida reconstruction of the biocytin-filled LTS interneuron **3** show the extended dendritic field and the aspiny dendrites (the axon was not visible). The right diagrams show that the interevent intervals distribution was shifted to the left. The mean values of  $V_{rest}$  ( $-48.7 \pm 2.5$  vs  $-51.0 \pm 3.1$  mV;  $n = 5$  and  $6$ ;  $p = 0.6$ ),  $V_{threshold}$  ( $-46.5 \pm 0.7$  vs  $-42.4 \pm 1.4$  mV;  $n = 5$  and  $5$ ;  $p = 0.06$ ), and input resistance ( $R_{input}$ ) ( $622 \pm 97$  vs  $630 \pm 118$  M $\Omega$ ;  $n = 5$  and  $6$ ;  $p = 0.9$ ) were unchanged by DA depletion. Calibrations are identical for all cell-attached recordings (5 s for main traces and 1 s for enlarged ones) and for all whole-cell recordings (25 mV, 200 ms). Scale bar for neurons, 50  $\mu\text{m}$ . Error bars indicate SEM.

and  $E_{\text{GABA}}$  obtained with the same methods in control and DA-depleted MSNs confirms the validity of our conclusions. Another noninvasive method to determine  $V_{rest}$  consists in estimating the reversal potential for  $\text{K}^+$  ions using cell-attached recordings with pipettes containing 145–155 mM  $\text{K}^+$  ions. With the symmetric  $\text{K}^+$  gradient, the  $\text{K}^+$  current through the membrane patch reverses when the potential of the pipette is equal to the membrane potential ( $V_{rest}$ ) (Verheugen et al., 1999). This measure is based on the approximation of the internal  $\text{K}^+$  concentration. Interest-

ingly, both protocols (single NMDA current or equimolar  $\text{K}^+$ ) gave similar results ( $-80/-81$  mV) in control MSNs (Ade et al., 2008). These values are also close to those obtained with gramicidin perforated patch that leaves the internal chloride concentration intact ( $-81$  and  $-64 \pm 4$  mV, respectively) (Bracci and Panzeri, 2006) [for more depolarized values in organotypic cultures, see also Gustafson et al. (2006)]. Our determination of spike threshold in control and DA-depleted MSNs in whole-cell recordings and KGlu electrodes is close to that previously identi-

fied under the same conditions [−36 mV (Taverna et al., 2007); −38 mV (Fino et al., 2007)]. Therefore, GABAergic synapses depolarize MSNs from  $V_{rest}$  (Misgeld et al., 1982; Koós and Tepper, 1999) but do not trigger action potentials and hence can exert inhibitory actions (Plenz and Aertsen, 1996). The membrane potential of MSNs *in vivo*, under urethane or sodium pentobarbital anesthesia, oscillates between down and up states, the latter being generated by glutamatergic afferents (Wilson and Kawaguchi, 1996; Mahon et al., 2001; Tseng et al., 2001). Spontaneous or evoked activation of GABA<sub>A</sub> receptors depolarize the MSN membrane *in vivo* during the down state (Mercuri et al., 1991) and hyperpolarize it during the up state (Plenz and Kitai, 1998), suggesting that GABA exerts an inhibitory action on MSN activity.

We propose that the fundamental feature of the dopamine-depleted striatum is a shift from a continuous tonic GABA pattern to one that oscillates between repetitive giant sPSCs and silent episodes. This results from alterations of the firing properties of a subpopulation of GABA interneurons that shifts from low-frequency tonic to high-frequency oscillatory activity. The shift in the GABA<sub>A</sub> pattern may profoundly alter the response of one-half the MSNs to cortical inputs *in vivo*, thus destabilizing striatal function. During down states, GABA-induced depolarization decreases the impact of the hyperpolarization-activated inward rectifier K<sup>+</sup> current that prevents MSNs from excitation-induced rapid firing (Surmeier and Kitai, 1993; Nicola et al., 2000). It will also drive the MSN membrane to a potential (−65 mV) at which its input resistance and time constant are close to maximal (Wilson, 2007), which may facilitate glutamatergic inputs and lead to the generation of action potentials (Bracci and Panzeri, 2006). Along the same lines, blockade of spontaneous and tonic GABA<sub>A</sub> synaptic transmission decreased the cortically evoked excitation recorded from MSNs in the cell-attached configuration (Ade et al., 2008). In contrast, during up states that are more frequent in DA-depleted striatum [MSNs spend a longer time in up states in chronically 6-hydroxydopamine-lesioned rats (Murer et al., 2002)], giant GABAergic currents should efficiently and transiently inhibit cortical inputs, preventing information transfer and integration.

## References

- Ade KK, Janssen MJ, Ortinski PI, Vicini S (2008) Differential tonic GABA conductances in striatal medium spiny neurons. *J Neurosci* 28:1185–1197.
- Bennett BD, Bolam JP (1994) Localisation of parvalbumin-immunoreactive structures in primate caudate-putamen. *J Comp Neurol* 347:340–356.
- Beurrier C, Ben-Ari Y, Hammond C (2006) Preservation of the direct and indirect pathways in an *in vitro* preparation of the mouse basal ganglia. *Neuroscience* 140:77–86.
- Bracci E, Panzeri S (2006) Excitatory GABAergic effects in striatal projection neurons. *J Neurophysiol* 95:1285–1290.
- Bracci E, Centonze D, Bernardi G, Calabresi P (2002) Dopamine excites fast-spiking interneurons in the striatum. *J Neurophysiol* 87:2190–2194.
- Calabresi P, Picconi B, Tozzi A, Di Filippo M (2007) Dopamine-mediated regulation of corticostriatal synaptic plasticity. *Trends Neurosci* 30:211–219.
- Centonze D, Bracci E, Pisani A, Gubellini P, Bernardi G, Calabresi P (2002) Activation of dopamine D1-like receptors excites LTS interneurons of the striatum. *Eur J Neurosci* 15:2049–2052.
- Centonze D, Grande C, Usiello A, Gubellini P, Erbs E, Martin AB, Pisani A, Tognazzi N, Bernardi G, Moratalla R, Borrelli E, Calabresi P (2003) Receptor subtypes involved in the presynaptic and postsynaptic actions of dopamine on striatal interneurons. *J Neurosci* 23:6245–6254.
- Centonze D, Gubellini P, Usiello A, Rossi S, Tschertner A, Bracci E, Erbs E, Tognazzi N, Bernardi G, Pisani A, Calabresi P, Borrelli E (2004) Differential contribution of dopamine D2S and D2L receptors in the modulation of glutamate and GABA transmission in the striatum. *Neuroscience* 129:157–166.
- Clark BA, Farrant M, Cull-Candy SG (1997) A direct comparison of the single-channel properties of synaptic and extrasynaptic NMDA receptors. *J Neurosci* 17:107–116.
- Cohen I, Navarro V, Clemenceau S, Baulac M, Miles R (2002) On the origin of interictal activity in human temporal lobe epilepsy *in vitro*. *Science* 298:1418–1421.
- Cossart R, Hirsch JC, Cannon RC, Dinocourt C, Wheal HV, Ben-Ari Y, Esclapez M, Bernard C (2000) Distribution of spontaneous currents along the somato-dendritic axis of rat hippocampal CA1 pyramidal neurons. *Neuroscience* 99:593–603.
- Cummings DM, Yamazaki I, Cepeda C, Paul DL, Levine MS (2008) Neuronal coupling via connexin36 contributes to spontaneous synaptic currents of striatal medium-sized spiny neurons. *J Neurosci Res* 86:2147–2158.
- Czubayko U, Plenz D (2002) Fast synaptic transmission between striatal spiny projection neurons. *Proc Natl Acad Sci U S A* 99:15764–15769.
- Fino E, Glowinski J, Venance L (2007) Effects of acute dopamine depletion on the electrophysiological properties of striatal neurons. *Neurosci Res* 58:305–316.
- Guigoni C, Doudnikoff E, Li Q, Bloch B, Bezard E (2007) Altered D(1) dopamine receptor trafficking in parkinsonian and dyskinetic non-human primates. *Neurobiol Dis* 26:452–463.
- Gustafson N, Gireesh-Dharmaraj E, Czubayko U, Blackwell KT, Plenz D (2006) A comparative voltage and current-clamp analysis of feedback and feedforward synaptic transmission in the striatal microcircuit *in vitro*. *J Neurophysiol* 95:737–752.
- Guzmán JN, Hernández A, Galarraga E, Tapia D, Laville A, Vergara R, Aceves J, Vargas J (2003) Dopaminergic modulation of axon collaterals interconnecting spiny neurons of the rat striatum. *J Neurosci* 23:8931–8940.
- Heuschkel MO, Fejtl M, Raggenbass M, Bertrand D, Renaud P (2002) A three-dimensional multi-electrode array for multi-site stimulation and recording in acute brain slices. *J Neurosci Methods* 114:135–148.
- Iancu R, Mohapel P, Brundin P, Paul G (2005) Behavioral characterization of a unilateral 6-OHDA-lesion model of Parkinson's disease in mice. *Behav Brain Res* 162:1–10.
- Kawaguchi Y (1993) Physiological, morphological, and histochemical characterization of three classes of interneurons in rat neostriatum. *J Neurosci* 13:4908–4923.
- Kita H, Kosaka T, Heizmann CW (1990) Parvalbumin-immunoreactive neurons in the rat neostriatum: a light and electron microscopic study. *Brain Res* 536:1–15.
- Koós T, Tepper JM (1999) Inhibitory control of neostriatal projection neurons by GABAergic interneurons. *Nat Neurosci* 2:467–472.
- Koós T, Tepper JM (2002) Dual cholinergic control of fast-spiking interneurons in the neostriatum. *J Neurosci* 22:529–535.
- Koós T, Tepper JM, Wilson CJ (2004) Comparison of IPSCs evoked by spiny and fast-spiking neurons in the neostriatum. *J Neurosci* 24:7916–7922.
- Kubota Y, Kawaguchi Y (2000) Dependence of GABAergic synaptic areas on the interneuron type and target size. *J Neurosci* 20:375–386.
- Levey AI, Hersch SM, Rye DB, Sunahara RK, Niznik HB, Kitt CA, Price DL, Maggio R, Brann MR, Ciliax BJ (1993) Localization of D1 and D2 dopamine receptors in brain with subtype-specific antibodies. *Proc Natl Acad Sci U S A* 90:8861–8865.
- Mahon S, Deniau JM, Charpier S (2001) Relationship between EEG potentials and intracellular activity of striatal and cortico-striatal neurons: an *in vivo* study under different anesthetics. *Cereb Cortex* 11:360–373.
- Mallet N, Le Moine C, Charpier S, Gonon F (2005) Feedforward inhibition of projection neurons by fast-spiking GABA interneurons in the rat striatum *in vivo*. *J Neurosci* 25:3857–3869.
- Marchi M, Sanguineti P, Raiteri M (1990) Muscarinic receptors mediate direct inhibition of GABA release from rat striatal nerve terminals. *Neurosci Lett* 116:347–351.
- Mercuri NB, Calabresi P, Stefani A, Stratta F, Bernardi G (1991) GABA depolarizes neurons in the rat striatum: an *in vivo* study. *Synapse* 8:38–40.
- Misgeld U, Wagner A, Ohno T (1982) Depolarizing IPSPs and depolarization by GABA of rat neostriatum cells *in vitro*. *Exp Brain Res* 45:108–114.
- Momiyama T (2002) Dopamine receptors and calcium channels regulating

- striatal inhibitory synaptic transmission (in Japanese). *Nippon Yakurigaku Zasshi* 120:61P–63P.
- Murer MG, Tseng KY, Kasanetz F, Belluscio M, Riquelme LA (2002) Brain oscillations, medium spiny neurons, and dopamine. *Cell Mol Neurobiol* 22:611–632.
- Nadjar A, Brotchie JM, Guigoni C, Li Q, Zhou SB, Wang GJ, Ravenscroft P, Georges F, Crossman AR, Bezard E (2006) Phenotype of striatofugal medium spiny neurons in parkinsonian and dyskinetic nonhuman primates: a call for a reappraisal of the functional organization of the basal ganglia. *J Neurosci* 26:8653–8661.
- Nicola SM, Surmeier J, Malenka RC (2000) Dopaminergic modulation of neuronal excitability in the striatum and nucleus accumbens. *Annu Rev Neurosci* 23:185–215.
- Nowak L, Bregestovski P, Ascher P, Herbet A, Prochiantz A (1984) Magnesium gates glutamate-activated channels in mouse central neurones. *Nature* 307:462–465.
- Plenz D, Aertsen A (1996) Neural dynamics in cortex-striatum co-cultures—II. Spatiotemporal characteristics of neuronal activity. *Neuroscience* 70:893–924.
- Plenz D, Kitai ST (1998) Up and down states in striatal medium spiny neurons simultaneously recorded with spontaneous activity in fast-spiking interneurons studied in cortex–striatum–substantia nigra organotypic cultures. *J Neurosci* 18:266–283.
- Raz A, Feingold A, Zelanskaya V, Vaadia E, Bergman H (1996) Neuronal synchronization of tonically active neurons in the striatum of normal and parkinsonian primates. *J Neurophysiol* 76:2083–2088.
- Steidl EM, Neveu E, Bertrand D, Buisson B (2006) The adult rat hippocampal slice revisited with multi-electrode arrays. *Brain Res* 1096:70–84.
- Sullivan MA, Chen H, Morikawa H (2008) Recurrent inhibitory network among striatal cholinergic interneurons. *J Neurosci* 28:8682–8690.
- Surmeier DJ, Kitai ST (1993) D1 and D2 dopamine receptor modulation of sodium and potassium currents in rat neostriatal neurons. *Prog Brain Res* 99:309–324.
- Taverna S, Canciani B, Pennartz CM (2007) Membrane properties and synaptic connectivity of fast-spiking interneurons in rat ventral striatum. *Brain Res* 1152:49–56.
- Taverna S, Ilijic E, Surmeier DJ (2008) Recurrent collateral connections of striatal medium spiny neurons are disrupted in models of Parkinson's disease. *J Neurosci* 28:5504–5512.
- Tepper JM, Bolam JP (2004) Functional diversity and specificity of neostriatal interneurons. *Curr Opin Neurobiol* 14:685–692.
- Tepper JM, Wilson CJ, Koós T (2008) Feedforward and feedback inhibition in neostriatal GABAergic spiny neurons. *Brain Res Rev* 58:272–281.
- Tseng KY, Kasanetz F, Kargieman L, Riquelme LA, Murer MG (2001) Cortical slow oscillatory activity is reflected in the membrane potential and spike trains of striatal neurons in rats with chronic nigrostriatal lesions. *J Neurosci* 21:6430–6439.
- Tunstall MJ, Oorschot DE, Kean A, Wickens JR (2002) Inhibitory interactions between spiny projection neurons in the rat striatum. *J Neurophysiol* 88:1263–1269.
- Tyzio R, Ivanov A, Bernard C, Holmes GL, Ben-Ari Y, Khazipov R (2003) Membrane potential of CA3 hippocampal pyramidal cells during postnatal development. *J Neurophysiol* 90:2964–2972.
- Venance L, Glowinski J, Giaume C (2004) Electrical and chemical transmission between striatal GABAergic output neurones in rat brain slices. *J Physiol* 559:215–230.
- Verheugen JA, Fricker D, Miles R (1999) Noninvasive measurements of the membrane potential and GABAergic action in hippocampal interneurons. *J Neurosci* 19:2546–2555.
- Wilson CJ (2007) GABAergic inhibition in the neostriatum. *Prog Brain Res* 160:91–110.
- Wilson CJ, Groves PM (1980) Fine structure and synaptic connections of the common spiny neuron of the rat neostriatum: a study employing intracellular inject of horseradish peroxidase. *J Comp Neurol* 194:599–615.
- Wilson CJ, Kawaguchi Y (1996) The origins of two-state spontaneous membrane potential fluctuations of neostriatal spiny neurons. *J Neurosci* 16:2397–2410.
- Zhou FM, Wilson CJ, Dani JA (2002) Cholinergic interneuron characteristics and nicotinic properties in the striatum. *J Neurobiol* 53:590–605.

# DISCUSSION

## DISCUSSION

I have focused my research during my thesis on the activity of the GABAergic microcircuits of the striatum in embryonic and perinatal developmental states and in adult pathological state. We have identified that:

(1) The spontaneous developmental activities of the striatal network consist of first, intrinsic voltage-gated calcium signals, followed by synapse driven activities. They disappear around P8-P10 in vitro;

(2) The frequency of the spontaneous GABAergic and glutamatergic currents afferent to the MSNs increases from E16 to P30 and from P8 all MSNs already receive both types of synapses. Interestingly there is a transient increase of the NR2DC-mediated component of the glutamatergic EPSP which peaks around P6;

(3) The silencing of all the immature activities generated by MSNs is due to an increase in the number of MSN expressing the inward rectifier  $K^+$  conductance and the parallel decrease of the NMDA conductances. This occurs just before the onset of locomotor behaviour (P10-P12);

(4) GABAergic interneurons (P/LTS) are overactive in adult parkinsonian state. They generate long bursts of spikes that evoke bursts of GABAergic currents in MSNs. Interestingly, the bursting activity is found in both toxin-based and genetic models of PD, suggesting a common patho-physiological signature of the disease in the striatum. This again stresses the importance of GABAergic neurons and derived patterns in the generation of pathological activities as they are engaged in the modulation and maturation of physiological patterns.

In the present chapter, we discuss the functional role and the origin of the striatal activities, the mechanisms underlying the silencing of the MSNs at the beginning of the second postnatal week, and the role of GABAergic interneurons during development and in adult-depleted striatum.

## **1. What is the origin and functional significance of the immature activities in the striatum?**

Neuronal synchronization in the basal ganglia plays a key role in encoding movement, procedural memory storage and habit formation (For review, Obeso et al., 2008). The functional significance of synchronized activities in the immature striatum remains unknown at the end of our study. Nevertheless we propose here some hypotheses concerning the GAP-junction and synaptic-driven activities.

### **1.1. Functional role of the intrinsic and synaptic immature activities in the developing striatum.**

Synchronized voltage-gated calcium plateaus in small cell assemblies connected by gap junctions (SPAs) may represent a key step in the initiation of calcium waves that notably coordinate cell cycle and enable diffusion of morphogenetic cues (For review, Bruzzone and Dermietzel, 2006), regulate modulating signals involved in programmed cell death or survival (For review, Krysko et al., 2005). They could also provide a mechanism to reinforce the initial connectivity between neurons and may represent an early form of functional units preceding the network organization by synaptic activity (Crépel et al., 2006).

Synaptic activity gradually mature during development and by the end of the first postnatal week, all MSNs receive GABAergic and glutamatergic innervation. At that moment spontaneous synchronous synapse-driven events occur in the mouse striatum. They are generated by depolarizing GABA and glutamate, notably via the activation of the NMDA receptor subunits NR2C/D. Synchronous synapse-driven events may represent a crucial developmental stage for the cortico-striatal entity and more precisely for the establishment of functional connections between the two structures.

Indeed, in parallel to these activities, an intense cell death period occurs in the striatum by the beginning of the second postnatal week (P8) (Fishell and Van der Kooy 1991; Fentress et al., 1981). Such a cell death period occurs in roughly one third of the neuronal population and affects both the patch and matrix compartments. This massive neuronal death may select neurons none misconnected during development. This hypothesis can be easily tested by studying for instance the effect of the absence of gap-junction expression during development, notably by using KO mice for the different connexins (Cummings et al., 2008; Venance et al., 2004).

## **1.2. What is the origin of the synchronous synapse-driven events of the striatum?**

Glutamatergic innervation arising mainly from the cortex is crucial for the generation of the highly synchronized events observed between P5 and P7 in the striatum (Article 1 Dehorter). Besides, cortical GDPs have been described between P4 and P9 in rats (Allène et al., 2008). We are logically tempted to ask whether the GDPs recorded in the striatum are driven by the cortical ones. Before P5 in the striatum, synaptic connectivity is poor and thus the probability of a connection between a cortical GDP-cell (representing 50% of the cells in the deep cortical layers) and a striatal cell is small. At P5-P7 this probability increases since all MSNs receive few glutamatergic inputs and thus could receive synchronized glutamatergic inputs.

The spontaneous GABAergic synaptic currents afferent to the MSN are in 11 and 13% of the recorded MSNs organized in recurrent bursts at P5 and P7, respectively. These bursts are absent at P10 and P17 (unpublished data from Dehorter). Bursts are probably the consequence of synchronized burst firing in neighboring GABAergic neurons, either MSNs or interneurons. Together with the GABA depolarizing effect, glutamate should trigger the synchronization observed in the striatum. Simultaneous calcium imaging recording of the cortex and striatum should test this possibility.

Low observation occurrence of the striatal GDPs in slices (only 10% of our slices), suggests that emergence of synchronization demands the requirement of a minimum of connected microcircuits. We expect that using a more appropriate *in vitro* preparation preserving the inter-neuronal connections, one might expect an increase in the percentage of observed “GDP-expressing” slices.

## 2. What are the mechanisms underlying the silencing of the striatal network?

“Silencing” of the MSNs is observed in our *in vitro* and *in vivo* conditions after P8 concomitantly with the disappearance of the synchronized events recorded between P5 and P7. The underlying signal triggering the silencing remains to be explored. This issue is of particular interest since silencing of MSNs occurs just before the onset of coordinated locomotion. Indeed, the descending cortico-spinal tract reaches the lumbar level only at P9 (Gianino et al., 1999). Two days later the lumbar cortico-spinal synapses are functional. It seems therefore logical that the immature activities of the striatum have disappeared to avoid involuntary movements.

We propose that the expression of  $K^+$  conductances develop in the MSNs with a highly appropriate time dependent sequence. This leads to the decrease of membrane resistance, hyperpolarisation of the resting membrane potential and of the reversal potential for GABA. In parallel, we observed that the functional expression of the NMDA-mediated receptors drops at the beginning of the second postnatal week leading to shorter and reduced NMDA components to ongoing activity notably as NR2D subunits have a lesser voltage dependent blockade by  $Mg^{2+}$ . Consequently, the concomitant expression of  $K_{IR}$  and decrease in the NMDA receptors expression leads to the decreased probability of MSNs excitation. At this point, it would be interesting to investigate whether the blockade of expression of  $IK_{IR}$  in MSNs delays the silencing of the network. Or conversely, does the over-expression of  $IK_{IR}$  in MSNs suppress their spontaneous immature activities?

Interestingly, several studies report potassium channel dysfunction in Huntington’s disease transgenic mice (Ariano et al., 2005) that leads to a depolarization of the membrane potential and an increase in the input resistance of the MSNs. The corticostriatal pathway is also altered in these mice (Cepeda et al., 2003) since response to NMDA receptor activation are largely increased (Cepeda et al., 2001).

Kitai and Surmeier (1993) emphasized the crucial role of both acetylcholine and dopamine in the modulation of  $I_{K_{IR}}$  (Kitai and Surmeier, 1993). It should be of a particular interest to determine the developmental profile of the activity in the striatum in the absence of cholinergic or dopaminergic ongoing signals. For instance the “aphakia” transgenic mice, deficient for the transcription factor Pitx3, could be a useful model to address this issue. Indeed, these mice show a complete cell loss already at birth, specifically in the SNc, and locomotor deficits in the adult (Van der Munckhof et al., 2006).

### **3. What are the functional roles of the GABAergic interneurons during development and in adult parkinsonian state?**

We described the developmental sequence of the immature activities in the striatum. Our imaging recordings in Nkx2.1-GFP mice enabled us to distinguish the MSNs (Nkx2.1 negative) from the interneurons (Nkx2.1 positive, GABAergic and cholinergic interneurons). From embryonic and perinatal stages, we observed that activity of the interneurons is not different from the MSNs one. Indeed interneurons also display calcium plateaus and individual calcium spikes. However, in contrast with the MSNs, they do not silence after P8. Interneurons represent 40% of the total active cells at P10, compared to 12% at P2 (Article 1 Dehorter). An accurate study of the maturation of striatal interneurons should provide insights into their functional role during development.

The main physiological hallmark of PD is over-activity of the STN neurons consisting of recurrent bursts of spikes instead of a tonic single spike activity (For review, Hamani et al., 2003). Based on this observation, STN lesion (Bergman et al., 1990) or STN high-frequency stimulation (Benazzouz et al., 1993) has been proposed for the surgical treatment of PD since 15 years (For review, Benabid et al., 2009).

Our study in the adult 6-OHDA, PINK1 KO and SNCA-surexpressing mouse models reveals a new patho-physiological signature in the striatum: recurrent bursts of postsynaptic GABAergic currents in the MSNs (Fig. 20).

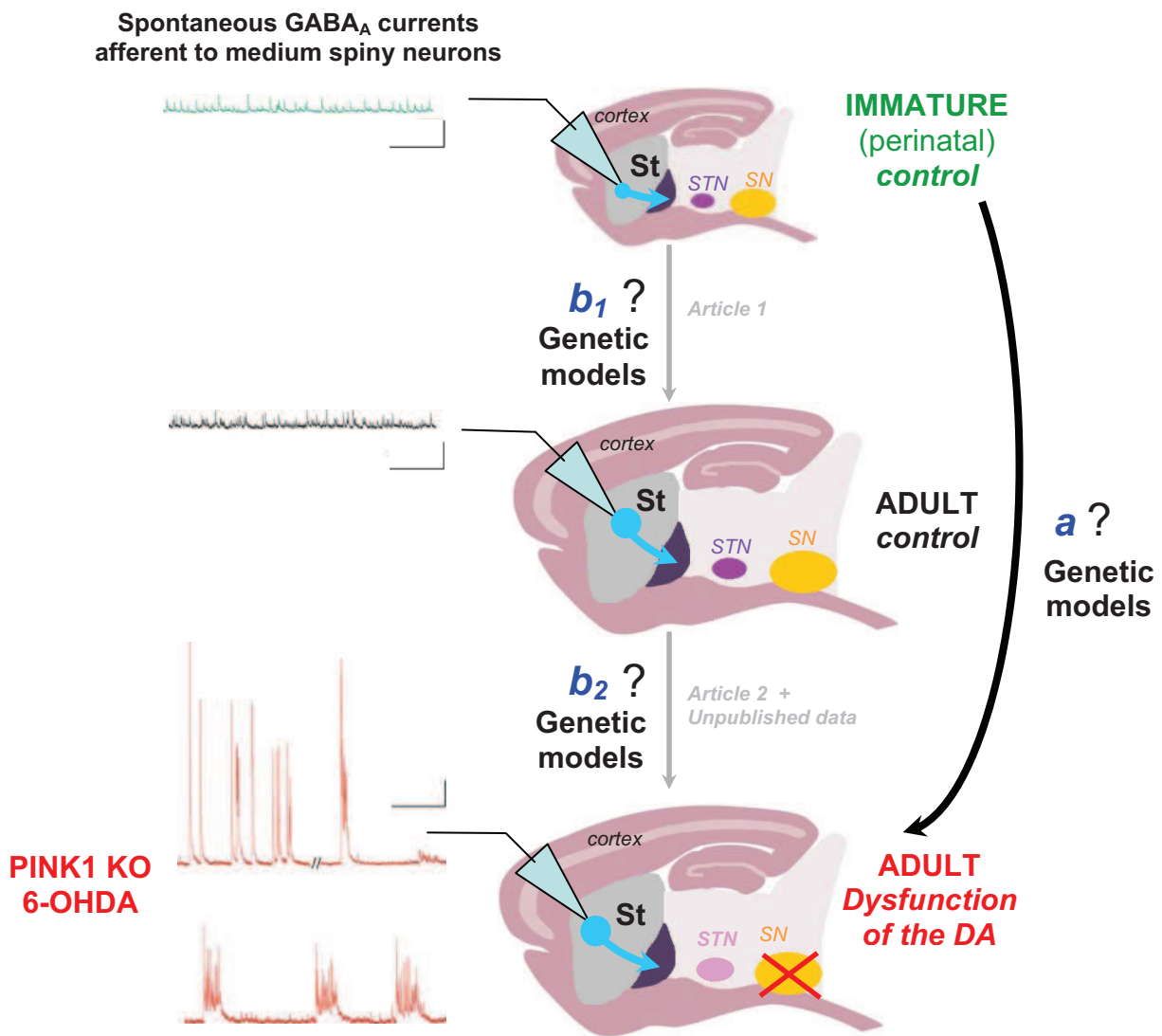


**Figure 20:** Spontaneous postsynaptic GABAergic currents represent a new electrophysiological signature of Parkinson state in the striatum.

The spontaneous GABAergic activity (IPSCs) afferent to MSNs (blue neurons) recorded in voltage clamp at +10 mV have a low frequency, a small amplitude and a tonic pattern at perinatal ages (green trace, P7) (article 1). Their frequency gradually increases until adulthood following the same tonic pattern (black trace, P30; article 1). Alteration of dopaminergic signalling (Red Cross; SN in orange) in both genetic models (PINK1 KO and  $\alpha$ -synuclein surexpressing 19-month old mice) and 6-OHDA-treated mice, leads to single or bursts of gigantic IPSCs in MSNs (red traces, article 2 and unpublished data). This change of pattern of GABA<sub>A</sub> currents is due to a change of spontaneous discharge pattern of a subtype of striatal interneurons, the LTS interneurons. It would contribute to alter striatal output activity (blue arrow). Together with the abnormal firing of the STN in parkinsonian state (pink), bursting GABA currents in the striatum are the electrophysiological signatures of the disease.

It will be of interest to birth date the electrophysiological signature in the striatum of genetic mice models of PD. Do GABAergic microcircuits of the striatum are 'pathological' from early ages(a)? Or do they appear in the old adult after a correct maturation and functioning of the circuit (*b<sub>1</sub>*) (*b<sub>2</sub>*) ?

Scale: 100 pA, 1s. SN: Substantia Nigra; STN: Subthalamic Nucleus; St: Striatum.  
 Modified from Kreitzer and Malenka, 2008, Dehorter et al., 2009 and Dehorter et al., in prep.

We have identified the generators, the GABAergic interneurons of P/LTS-type that switch their firing pattern in the chronic absence of dopamine (Dehorter et al., 2009). Along the same line, study from Carrillo-Reid and collaborators suggested that GABAergic interneurons are involved in NMDA-induced network oscillatory dynamics in striatal slices (Carrillo-Reid et al., 2008).

We still have to identify the precise mechanisms underlying the switch of pattern of activity of LTS GABAergic interneurons following dopaminergic depletion. Double patch recording in DA-depleted condition of Nkx2.1 or Lhx6 GFP-neurons in the striatum of transgenic mice where striatal interneurons are specifically labelled (see Chapter 1, 1.2.2) will allow recording the cells displaying a bursting pattern and studying its underlying mechanisms. To identify a possible synchronization among interneurons we should use calcium imaging in slices from animal models of PD.

#### **4. Are the adult pathological oscillations similar as the immature synchronous activities of the developing striatum?**

Recordings of the adult striatal network activity with calcium imaging in slices from P14-P24 6-OHDA-treated rats revealed an increase in the overall network activity and synchrony compared to the control (Jaidar et al., 2010). NMDA receptors may contribute to the overall excitability of MSNs by regulating the transition to up-states *in vitro* in the adult rat (Vergara et al 2003; Carrillo-reid et al., 2008). Indeed NMDA receptor channels regulate different signalling mechanisms via intracellular calcium increase that influence notably synapse formation, gene transcriptional profiles, glutamate receptor expression or neuronal excitability (For review, Sheng and Kim, 2002; Butler et al., 1999; Adesnik et al., 2008).

Many studies reveal a complex interplay between DA and NMDA receptors (Cepeda et al. 1998) and specially in motor syndromes like PD (For review, Chase, 2004; see also Bagetta et al., 2010) or Huntington's disease (For review, Levine et al., 2010).

These data suggest that a set of unitary central pattern generators capable of generating oscillations reside in both the immature and adult striatal network (Grillner 2006). Indeed, it is interesting to emphasize that the immature synchronized activities occur in the developing striatum at P5-P7, at the time when the expression of NMDA receptors is maximal and when all the MSNs generate spontaneous NMDA currents (see chapter 1, 2.4 and article 1 Dehorter). Conversely, disappearance of such oscillatory immature activities is associated with a large drop in NMDA receptors subunits expression and functional NMDA receptor-mediated currents in the MSNs (see chapter 1, 2.4 and article 1 Dehorter).

Since NMDA receptors activation is directly correlated to the immature and pathological oscillatory patterns generation, we wonder whether the NMDA-induced pathological synchrony in the adult is reminiscent of the synchronized activity observed in the developmental period (For review, Ben-Ari, 2008) and thus based on the same mechanisms of initiation? In such case, differential experience of plasticity at early and late stages of the development would lead to deleterious effects of the oscillatory pattern in the adult but not in the more plastic immature striatum (see chapter 1, 2.4).

## Conclusion

This original study on the functional development of the striatum opens the path for further investigations. It will be of a great interest to determine:

1. The role of dopamine on the maturation of striatal activities? More particularly, does dopamine act on the signalling pathway inducing the onset of synaptically-driven immature activities (GDPs)?
2. The mechanisms underlying the electrophysiological signature of PD in the adult striatum observed in both toxin-based and genetic models of the disease?
3. The origin, birth date and role during development of the GABAergic interneurons whose activity is strongly altered by dopaminergic depletion in the adult?
4. whether and how does an early insult during maturation leads to the late expression and manifestation of the clinical symptoms of Parkinson and other disorders ?

# REFERENCES

## REFERENCES

- Abeliovich A, Schmitz Y, Fariñas I, Choi-Lundberg D, Ho WH, Castillo PE, Shinsky N, Verdugo JM, Armanini M, Ryan A, Hynes M, Phillips H, Sulzer D, Rosenthal A. Mice lacking alpha-synuclein display functional deficits in the nigrostriatal dopamine system. *Neuron*. 2000 Jan; 25(1):239-52.
- Adesnik H, Li G, During MJ, Pleasure SJ, Nicoll RA. NMDA receptors inhibit synapse unsilencing during brain development. *Proc Natl Acad Sci U S A*. 2008 Apr 8; 105(14):5597-602.
- Allène C, Cattani A, Ackman JB, Bonifazi P, Aniksztejn L, Ben-Ari Y, Cossart R. Sequential generation of two distinct synapse-driven network patterns in developing neocortex. *J Neurosci*. 2008 Nov 26; 28(48):12851-63.
- Anderson KD, Reiner A. Immunohistochemical localization of DARPP-32 in striatal projection neurons and striatal interneurons: implications for the localization of D1-like dopamine receptors on different types of striatal neurons. *Brain Res*. 1991 Dec 24; 568(1-2):235-43.
- Anderson SA, Qiu M, Bulfone A, Eisenstat DD, Meneses J, Pedersen R, Rubenstein JL. Mutations of the homeobox genes *Dlx-1* and *Dlx-2* disrupt the striatal subventricular zone and differentiation of late born striatal neurons. *Neuron*. 1997 Jul; 19(1):27-37.
- Andrews WD, Barber M, Parnavelas JG. Slit-Robo interactions during cortical development. *J Anat*. 2007 Aug; 211(2):188-98.
- Araki KY, Sims JR, Bhide PG. Dopamine receptor mRNA and protein expression in the mouse corpus striatum and cerebral cortex during pre- and postnatal development. *Brain Res*. 2007 Jul 2; 1156:31-45. Epub 2007 Apr 22.
- Ariano MA, Cepeda C, Calvert CR, Flores-Hernández J, Hernández-Echeagaray E, Klapstein GJ, Chandler SH, Aronin N, DiFiglia M, Levine MS. Striatal potassium channel dysfunction in Huntington's disease transgenic mice. *J Neurophysiol*. 2005 May; 93(5):2565-74.
- Aubert I, Cécyre D, Gauthier S, Quirion R. Comparative ontogenic profile of cholinergic markers, including nicotinic and muscarinic receptors, in the rat brain. *J Comp Neurol*. 1996 May 20; 369(1):31-55.
- Aymerich MS, Barroso-Chinea P, Pérez-Manso M, Muñoz-Patiño AM, Moreno-Igoa M, González-Hernández T, Lanciego JL. Consequences of unilateral nigrostriatal denervation on the thalamostriatal pathway in rats. *Eur J Neurosci*. 2006 Apr; 23(8):2099-108.
- Azdad K, Chávez M, Don Bishop P, Wetzelaer P, Marescau B, De Deyn PP, Gall D, Schiffmann SN. Homeostatic plasticity of striatal neurons intrinsic excitability following dopamine depletion. *PLoS One*. 2009 Sep 4; 4(9):e6908.
- Aznavour N, Mechawar N, Watkins KC, Descarries L. Fine structural features of the acetylcholine innervation in the developing neostriatum of rat. *J Comp Neurol*. 2003 May 26; 460(2):280-91.
- Bachy I, Rétaux S. GABAergic specification in the basal forebrain is controlled by the LIM-hd factor *Lhx7*. *Dev Biol*. 2006 Mar 15; 291(2):218-26.
- Ballion B, Mallet N, Bézard E, Lanciego JL, Gonon F. Intratelencephalic corticostriatal neurons equally excite striatonigral and striatopallidal neurons and their discharge activity is selectively reduced in experimental parkinsonism. *Eur J Neurosci*. 2008 May; 27(9):2313-21.
- Belleau ML, Warren RA. Postnatal development of electrophysiological properties of nucleus accumbens neurons. *J Neurophysiol*. 2000 Nov; 84(5):2204-16.

- Benabid AL, Chabardes S, Mitrofanis J, Pollak P. Deep brain stimulation of the subthalamic nucleus for the treatment of Parkinson's disease. *Lancet Neurol*. 2009 Jan; 8(1):67-81.
- Ben-Ari Y. Neuro-archaeology: pre-symptomatic architecture and signature of neurological disorders. *Trends Neurosci*. 2008 Dec; 31(12):626-36.
- Ben-Ari Y, Gaiarsa JL, Tyzio R, Khazipov R. GABA: a pioneer transmitter that excites immature neurons and generates primitive oscillations. *Physiol Rev*. 2007 Oct; 87(4):1215-84.
- Benazzouz A, Gross C, Féger J, Boraud T, Bioulac B. Reversal of rigidity and improvement in motor performance by subthalamic high-frequency stimulation in MPTP-treated monkeys. *Eur J Neurosci*. 1993 Apr 1; 5(4):382-9.
- Bennett BD, Bolam JP. Synaptic input and output of parvalbumin-immunoreactive neurons in the neostriatum of the rat. *Neuroscience*. 1994 Oct; 62(3):707-19.
- Bennett BD, Wilson CJ. Spontaneous activity of neostriatal cholinergic interneurons in vitro. *J Neurosci*. 1999 Jul 1; 19(13):5586-96.
- Bennett BD, Callaway JC, Wilson CJ. Intrinsic membrane properties underlying spontaneous tonic firing in neostriatal cholinergic interneurons. *J Neurosci*. 2000 Nov 15; 20(22):8493-503.
- Bennett MV, Zukin RS. Electrical coupling and neuronal synchronization in the Mammalian brain. *Neuron*. 2004 Feb 19; 41(4):495-511.
- Bergman H, Wichmann T, DeLong MR. Reversal of experimental parkinsonism by lesions of the subthalamic nucleus. *Science*. 1990 Sep 21; 249(4975):1436-8.
- Bernard V, Somogyi P, Bolam JP. Cellular, subcellular, and subsynaptic distribution of AMPA-type glutamate receptor subunits in the neostriatum of the rat. *J Neurosci*. 1997 Jan 15; 17(2):819-33.
- Betarbet R, Sherer TB, Greenamyre JT. Animal models of Parkinson's disease. *Bioessays*. 2002 Apr; 24(4):308-18.
- Bezard E, Gross CE, Brotchie JM. Presymptomatic compensation in Parkinson's disease is not dopamine-mediated. *Trends Neurosci*. 2003 Apr; 26(4):215-21.
- Bhide PG. Cell cycle kinetics in the embryonic mouse corpus striatum. *J Comp Neurol*. 1996 Oct 28; 374(4):506-22.
- Blandini F, Armentero MT, Martignoni E. The 6-hydroxydopamine model: news from the past. *Parkinsonism Relat Disord*. 2008; 14 Suppl 2:S124-9.
- Blum D, Torch S, Lambeng N, Nissou M, Benabid AL, Sadoul R, Verna JM. Molecular pathways involved in the neurotoxicity of 6-OHDA, dopamine and MPTP: contribution to the apoptotic theory in Parkinson's disease. *Prog Neurobiol*. 2001 Oct; 65(2):135-72.
- Bolam JP, Hanley JJ, Booth PA, Bevan MD. Synaptic organisation of the basal ganglia. *J Anat*. 2000 May; 196 (Pt 4):527-42.
- Bracci E, Panzeri S. Excitatory GABAergic effects in striatal projection neurons. *J Neurophysiol*. 2006 Feb; 95(2):1285-90.
- Bradbury AJ, Costall B, Domeney AM, Jenner P, Kelly ME, Marsden CD, Naylor RJ. 1-methyl-4-phenylpyridine is neurotoxic to the nigrostriatal dopamine pathway. *Nature*. 1986 Jan 2-8; 319(6048):56-7.
- Brose K, Tessier-Lavigne M. Slit proteins: key regulators of axon guidance, axonal branching, and cell migration. *Curr Opin Neurobiol*. 2000 Feb; 10(1):95-102. Review.

- Bruzzone R, Dermietzel R. Structure and function of gap junctions in the developing brain. *Cell Tissue Res.* 2006 Nov; 326(2):239-48.
- Burré J, Sharma M, Tsetsenis T, Buchman V, Etherton M, Südhof TC.  $\alpha$ -Synuclein Promotes SNARE-Complex Assembly in Vivo and in Vitro. *Science.* 2010 Aug 26.
- Butt SJ, Sousa VH, Fuccillo MV, Hjerling-Leffler J, Miyoshi G, Kimura S, Fishell G. The requirement of Nkx2-1 in the temporal specification of cortical interneuron subtypes. *Neuron.* 2008 Sep 11; 59(5):722-32.
- Calabresi P, Mercuri NB, Sancesario G, Bernardi G. Electrophysiology of dopamine-denervated striatal neurons. Implications for Parkinson's disease. *Brain.* 1993 Apr; 116 (Pt 2):433-52.
- Campbell K, Olsson M, Björklund A. Regional incorporation and site-specific differentiation of striatal precursors transplanted to the embryonic forebrain ventricle. *Neuron.* 1995 Dec;15(6):1259-73.
- Carrillo-Reid L, Tecuapetla F, Tapia D, Hernández-Cruz A, Galarraga E, Drucker-Colin R, Bargas J. Encoding network states by striatal cell assemblies. *J Neurophysiol.* 2008 Mar; 99(3):1435-50.
- Carter AG, Sabatini BL. State-dependent calcium signaling in dendritic spines of striatal medium spiny neurons. *Neuron.* 2004 Oct 28; 44(3):483-93.
- Centonze D, Gubellini P, Usiello A, Rossi S, Tschertter A, Bracci E, Erbs E, Tognazzi N, Bernardi G, Pisani A, Calabresi P, Borrelli E. Differential contribution of dopamine D2S and D2L receptors in the modulation of glutamate and GABA transmission in the striatum. *Neuroscience.* 2004; 129(1):157-66.
- Centonze D, Gubellini P, Rossi S, Picconi B, Pisani A, Bernardi G, Calabresi P, Baunez C. Subthalamic nucleus lesion reverses motor abnormalities and striatal glutamatergic overactivity in experimental parkinsonism. *Neuroscience.* 2005; 133(3):831-40.
- Cepeda C, Ariano MA, Calvert CR, Flores-Hernández J, Chandler SH, Leavitt BR, Hayden MR, Levine MS. NMDA receptor function in mouse models of Huntington disease. *J Neurosci Res.* 2001 Nov 15; 66(4):525-39.
- Cepeda C, Hurst RS, Calvert CR, Hernández-Echeagaray E, Nguyen OK, Jocoy E, Christian LJ, Ariano MA, Levine MS. Transient and progressive electrophysiological alterations in the corticostriatal pathway in a mouse model of Huntington's disease. *J Neurosci.* 2003 Feb 1; 23(3):961-9.
- Cepeda C, Walsh JP, Buchwald NA, Levine MS. Neurophysiological maturation of cat caudate neurons: evidence from in vitro studies. *Synapse.* 1991 Apr; 7(4):278-90.
- Chandra S, Gallardo G, Fernández-Chacón R, Schlüter OM, Südhof TC. Alpha-synuclein cooperates with CSP alpha in preventing neurodegeneration. *Cell.* 2005 Nov 4; 123(3):383-96.
- Chang HT, Kita H. Interneurons in the rat striatum: relationships between parvalbumin neurons and cholinergic neurons. *Brain Res.* 1992 Mar 6; 574(1-2):307-11.
- Chapman DE, Keefe KA, Wilcox KS. Evidence for functionally distinct synaptic NMDA receptors in ventromedial versus dorsolateral striatum. *J Neurophysiol.* 2003 Jan; 89(1):69-80.
- Chesselet MF. In vivo alpha-synuclein overexpression in rodents: a useful model of Parkinson's disease? *Exp Neurol.* 2008 Jan; 209(1):22-7.
- Chesselet MF, Plotkin JL, Wu N, Levine MS. Development of striatal fast-spiking GABAergic interneurons. *Prog Brain Res.* 2007; 160:261-72.
- Christensen J, Sørensen JC, Ostergaard K, Zimmer J. Early postnatal development of the rat corticostriatal pathway: an anterograde axonal tracing study using biocytin pellets. *Anat Embryol (Berl).* 1999 Jul; 200(1):73-80.
- Clarke KA, Still J. Development and consistency of gait in the mouse. *Physiol Behav.* 2001 May; 73(1-2):159-64.

Cobos I, Long JE, Thwin MT, Rubenstein JL. Cellular patterns of transcription factor expression in developing cortical interneurons. *Cereb Cortex*. 2006 Jul; 16 Suppl 1:i82-8.

Colin-Le Brun I, Ferrand N, Caillard O, Tosetti P, Ben-Ari Y, Gaiarsa JL. Spontaneous synaptic activity is required for the formation of functional GABAergic synapses in the developing rat hippocampus. *J Physiol*. 2004 Aug 15; 559(Pt 1):129-39.

Cossette M, Lecomte F, Parent A. Morphology and distribution of dopaminergic neurons intrinsic to the human striatum. *J Chem Neuroanat*. 2005 Jan; 29(1):1-11.

Crandall JE, McCarthy DM, Araki KY, Sims JR, Ren JQ, Bhide PG. Dopamine receptor activation modulates GABA neuron migration from the basal forebrain to the cerebral cortex. *J Neurosci*. 2007 Apr 4; 27(14):3813-22.

Crépel V, Aronov D, Jorquera I, Represa A, Ben-Ari Y, Cossart R. A parturition-associated nonsynaptic coherent activity pattern in the developing hippocampus. *Neuron*. 2007 Apr 5; 54(1):105-20.

Crossman AR. Functional anatomy of movement disorders. *J Anat*. 2000 May; 196 (Pt 4):519-25.

Cummings DM, Yamazaki I, Cepeda C, Paul DL, Levine MS. Neuronal coupling via connexin36 contributes to spontaneous synaptic currents of striatal medium-sized spiny neurons. *J Neurosci Res*. 2008 Aug 1; 86(10):2147-58.

Dawson TM. New animal models for Parkinson's disease. *Cell*. 2000 Apr 14; 101(2):115-8.

Dawson T, Mandir A, Lee M. Animal models of PD: pieces of the same puzzle? *Neuron*. 2002 Jul 18; 35(2):219-22.

Dawson TM, Dawson VL. Molecular pathways of neurodegeneration in Parkinson's disease. *Science*. 2003 Oct 31; 302(5646):819-22.

Dawson TM, Ko HS, Dawson VL. Genetic animal models of Parkinson's disease. *Neuron*. 2010 Jun 10; 66(5):646-61.

Deacon TW, Pakzaban P, Isacson O. The lateral ganglionic eminence is the origin of cells committed to striatal phenotypes: neural transplantation and developmental evidence. *Brain Res*. 1994 Dec 30; 668(1-2):211-9.

Dehorter N, Guigoni C, Lopez C, Hirsch J, Eusebio A, Ben-Ari Y, Hammond C. Dopamine-deprived striatal GABAergic interneurons burst and generate repetitive gigantic IPSCs in medium spiny neurons. *J Neurosci*. 2009 Jun 17; 29(24):7776-87.

Delgado A, Sierra A, Querejeta E, Valdiosera RF, Aceves J. Inhibitory control of the GABAergic transmission in the rat neostriatum by D2 dopamine receptors. *Neuroscience*. 2000; 95(4):1043-8.

Deniau JM, Mailly P, Maurice N, Charpier S. The pars reticulata of the substantia nigra: a window to basal ganglia output. *Prog Brain Res*. 2007; 160:151-72.

De Vries TJ, Mulder AH, Schoffelmeer AN. Differential ontogeny of functional dopamine and muscarinic receptors mediating presynaptic inhibition of neurotransmitter release and postsynaptic regulation of adenylate cyclase activity in rat striatum. *Brain Res Dev Brain Res*. 1992 Mar 20; 66(1):91-6.

Dunah AW, Yasuda RP, Wang YH, Luo J, Dávila-García M, Gbadegesin M, Vicini S, Wolfe BB. Regional and ontogenic expression of the NMDA receptor subunit NR2D protein in rat brain using a subunit-specific antibody. *J Neurochem*. 1996 Dec; 67(6):2335-45.

Du T, Xu Q, Ocbina PJ, Anderson SA. NKX2.1 specifies cortical interneuron fate by activating Lhx6. *Development*. 2008 Apr; 135(8):1559-67.

Eisenstat DD, Liu JK, Mione M, Zhong W, Yu G, Anderson SA, Ghattas I, Puelles L, Rubenstein JL. DLX-1, DLX-2, and DLX-5 expression define distinct stages of basal forebrain differentiation. *J Comp Neurol*. 1999 Nov 15; 414(2):217-37.

Elias LA, Potter GB, Kriegstein AR. A time and a place for *nkx2-1* in interneuron specification and migration. *Neuron*. 2008 Sep 11; 59(5):679-82.

Ericson J, Muhr J, Placzek M, Lints T, Jessell TM, Edlund T. Sonic hedgehog induces the differentiation of ventral forebrain neurons: a common signal for ventral patterning within the neural tube. *Cell*. 1995 Jun 2; 81(5):747-56.

Eriksen JL, Dawson TM, Dickson DW, Petrucelli L. Caught in the act: alpha-synuclein is the culprit in Parkinson's disease. *Neuron*. 2003 Oct 30; 40(3):453-6.

Fentress JC, Stanfield BB, Cowan WM. Observation on the development of the striatum in mice and rats. *Anat Embryol (Berl)*. 1981; 163(3):275-98.

Fernagut PO, Hutson CB, Fleming SM, Tetreault NA, Salcedo J, Masliah E, Chesselet MF. Behavioral and histopathological consequences of paraquat intoxication in mice: effects of alpha-synuclein over-expression. *Synapse*. 2007 Dec; 61(12):991-1001.

Fernández-Ruiz J, Huber L, Rohrer H, Barrera M, Reichert AS, Rüb U, Chen A, Nussbaum RL, Auburger G. Parkinson phenotype in aged PINK1-deficient mice is accompanied by progressive mitochondrial dysfunction in absence of neurodegeneration. *PLoS One*. 2009 Jun 3; 4(6):e5777.

Fino E, Glowinski J, Venance L. Effects of acute dopamine depletion on the electrophysiological properties of striatal neurons. *Neurosci Res*. 2007 Jul; 58(3):305-16.

Fishell G, van der Kooy D. Pattern formation in the striatum: developmental changes in the distribution of striatonigral neurons. *J Neurosci*. 1987 Jul; 7(7):1969-78.

Fishell G, van der Kooy D. Pattern formation in the striatum: developmental changes in the distribution of striatonigral projections. *Brain Res Dev Brain Res*. 1989 Feb 1; 45(2):239-55.

Fishell G, van der Kooy D. Pattern formation in the striatum: neurons with early projections to the substantia nigra survive the cell death period. *J Comp Neurol*. 1991 Oct 1; 312(1):33-42.

Flames N, Pla R, Gelman DM, Rubenstein JL, Puelles L, Marín O. Delineation of multiple subpallial progenitor domains by the combinatorial expression of transcriptional codes. *J Neurosci*. 2007 Sep 5; 27(36):9682-95.

Fleming SM, Fernagut PO, Chesselet MF. Genetic mouse models of parkinsonism: strengths and limitations. *NeuroRx*. 2005 Jul; 2(3):495-503.

Flores-Barrera E, Vizcarra-Chacón BJ, Tapia D, Bargas J, Galarraga E. Different corticostriatal integration in spiny projection neurons from direct and indirect pathways. *S Front Syst Neurosci*. 2010. Jun 10; 4:15.

Foster GA, Schultzberg M, Hökfelt T, Goldstein M, Hemmings HC Jr, Ouimet CC, Walaas SI, Greengard P. Development of a dopamine- and cyclic adenosine 3':5'-monophosphate-regulated phosphoprotein (DARPP-32) in the prenatal rat central nervous system, and its relationship to the arrival of presumptive dopaminergic innervation. *J Neurosci*. 1987 Jul; 7(7):1994-2018.

Fragkouli A, van Wijk NV, Lopes R, Kessar N, Pachnis V. LIM homeodomain transcription factor-dependent specification of bipotential MGE progenitors into cholinergic and GABAergic striatal interneurons. *Development*. 2009 Nov; 136(22):3841-51.

Galarreta M, Hestrin S. Electrical synapses between GABA-releasing interneurons. *Nat Rev Neurosci*. 2001 Jun; 2(6):425-33.

Garaschuk O, Linn J, Eilers J, Konnerth A. Large-scale oscillatory calcium waves in the immature cortex. *Nat Neurosci*. 2000 May; 3(5):452-9.

Gates MA, Coupe VM, Torres EM, Fricker-Gates RA, Dunnett SB. Spatially and temporally restricted chemoattractive and chemorepulsive cues direct the formation of the nigro-striatal circuit. *Eur J Neurosci*. 2004 Feb; 19(4):831-44.

Gates MA, Torres EM, White A, Fricker-Gates RA, Dunnett SB. Re-examining the ontogeny of substantia nigra dopamine neurons. *Eur J Neurosci*. 2006 Mar; 23(5):1384-90.

Gerfen CR. The neostriatal mosaic: compartmentalization of corticostriatal input and striatonigral output systems. *Nature*. 1984 Oct 4-10; 311(5985):461-4.

Gerfen CR. The neostriatal mosaic. I. Compartmental organization of projections from the striatum to the substantia nigra in the rat. *J Comp Neurol*. 1985 Jun 22; 236(4):454-76.

Gerfen CR, Baimbridge KG, Thibault J. The neostriatal mosaic: III. Biochemical and developmental dissociation of patch-matrix mesostriatal systems. *J Neurosci*. 1987 Dec; 7(12):3935-44.

Gerfen CR, Herkenham M, Thibault J. The neostriatal mosaic: II. Patch- and matrix-directed mesostriatal dopaminergic and non-dopaminergic systems. *J Neurosci*. 1987 Dec; 7(12):3915-34.

Gerfen CR. The neostriatal mosaic: striatal patch-matrix organization is related to cortical lamination. *Science*. 1989 Oct 20; 246(4928):385-8.

Gerfen CR, Engber TM, Mahan LC, Susel Z, Chase TN, Monsma FJ Jr, Sibley DR. D1 and D2 dopamine receptor-regulated gene expression of striatonigral and striatopallidal neurons. *Science*. 1990 Dec 7; 250(4986):1429-32.

Gerfen CR, Engber TM. Molecular neuroanatomic mechanisms of Parkinson's disease: a proposed therapeutic approach. *Neurol Clin*. 1992 May; 10(2):435-49.

Gerfen CR. D1 dopamine receptor supersensitivity in the dopamine-depleted striatum animal model of Parkinson's disease. *Neuroscientist*. 2003 Dec; 9(6):455-62.

Gianino S, Stein SA, Li H, Lu X, Biesiada E, Ulas J, Xu XM. Postnatal growth of corticospinal axons in the spinal cord of developing mice. *Brain Res Dev Brain Res*. 1999 Feb 5; 112(2):189-204.

Giasson BI, Duda JE, Quinn SM, Zhang B, Trojanowski JQ, Lee VM. Neuronal alpha-synucleinopathy with severe movement disorder in mice expressing A53T human alpha-synuclein. *Neuron*. 2002 May 16; 34(4):521-33.

Gibson JR, Beierlein M, Connors BW. Functional properties of electrical synapses between inhibitory interneurons of neocortical layer 4. *J Neurophysiol*. 2005 Jan; 93(1):467-80.

Gispert S, Ricciardi F, Kurz A, Azizov M, Hoepken HH, Becker D, Voos W, Leuner K, Müller WE, Kudin AP, Kunz WS, Zimmermann A, Roeper J, Wenzel D, Jendrach M, García-Arencia M, Fernández-Ruiz J, Huber L, Rohrer H, Barrera M, Reichert AS, Rüb U, Chen A, Nussbaum RL, Auburger G. Parkinson phenotype in aged PINK1-deficient mice is accompanied by progressive mitochondrial dysfunction in absence of neurodegeneration. *PLoS One*. 2009 Jun 3; 4(6):e5777.

Gittis AH, Nelson AB, Thwin MT, Palop JJ, Kreitzer AC. Distinct roles of GABAergic interneurons in the regulation of striatal output pathways. *J Neurosci*. 2010 Feb 10; 30(6):2223-34.

Goffin D, Ali AB, Rampersaud N, Harkavyi A, Fuchs C, Whitton PS, Nairn AC, Jovanovic JN. Dopamine-dependent tuning of striatal inhibitory synaptogenesis. *J Neurosci*. 2010 Feb 24; 30(8):2935-50.

Graybiel AM, Pickel VM, Joh TH, Reis DJ, Ragsdale CW Jr. Direct demonstration of a correspondence between the dopamine islands and acetylcholinesterase patches in the developing striatum. *Proc Natl Acad Sci U S A*. 1981 Sep; 78(9):5871-5.

- Graybiel AM, Aosaki T, Flaherty AW, Kimura M. The basal ganglia and adaptive motor control. *Science*. 1994 Sep 23; 265(5180):1826-31.
- Grillner S, Hellgren J, Ménard A, Saitoh K, Wikström MA. Mechanisms for selection of basic motor programs--roles for the striatum and pallidum. *Trends Neurosci*. 2005 Jul; 28(7):364-70.
- Gustafson N, Gireesh-Dharmaraj E, Czubyko U, Blackwell KT, Plenz D. A comparative voltage and current-clamp analysis of feedback and feedforward synaptic transmission in the striatal microcircuit in vitro. *J Neurophysiol*. 2006 Feb; 95(2):737-52.
- Hamani C, Saint-Cyr JA, Fraser J, Kaplitt M, Lozano AM. The subthalamic nucleus in the context of movement disorders. *Brain*. 2004 Jan; 127(Pt 1):4-20.
- Hamasaki T, Goto S, Nishikawa S, Ushio Y. Early-generated preplate neurons in the developing telencephalon: inward migration into the developing striatum. *Cereb Cortex*. 2001 May; 11(5):474-84.
- Hamasaki T, Goto S, Nishikawa S, Ushio Y. Neuronal cell migration for the developmental formation of the mammalian striatum. *Brain Res Brain Res Rev*. 2003 Jan; 41(1):1-12.
- Hurst RS, Cepeda C, Shumate LW, Levine MS. Delayed postnatal development of NMDA receptor function in medium-sized neurons of the rat striatum. *Dev Neurosci*. 2001; 23(2):122-34.
- Ibáñez-Sandoval O, Tecuapetla F, Unal B, Shah F, Koós T, Tepper JM. Electrophysiological and morphological characteristics and synaptic connectivity of tyrosine hydroxylase-expressing neurons in adult mouse striatum. *J Neurosci*. 2010 May 19; 30(20):6999-7016.
- Ingham CA, Hood SH, Taggart P, Arbuthnott GW. Plasticity of synapses in the rat neostriatum after unilateral lesion of the nigrostriatal dopaminergic pathway. *J Neurosci*. 1998 Jun 15; 18(12):4732-43.
- Jaeger D, Kita H, Wilson CJ. Surround inhibition among projection neurons is weak or nonexistent in the rat neostriatum. *J Neurophysiol*. 1994 Nov; 72(5):2555-8.
- Jankovic J. Parkinson's disease: clinical features and diagnosis. *J Neurol Neurosurg Psychiatry*. 2008 Apr; 79(4):368-76.
- Kakita A, Goldman JE. Patterns and dynamics of SVZ cell migration in the postnatal forebrain: monitoring living progenitors in slice preparations. *Neuron*. 1999 Jul;23(3):461-72.
- Kasyanov AM, Safiulina VF, Voronin LL, Cherubini E. GABA-mediated giant depolarizing potentials as coincidence detectors for enhancing synaptic efficacy in the developing hippocampus. *Proc Natl Acad Sci U S A*. 2004 Mar 16; 101(11):3967-72.
- Kawaguchi Y, Wilson CJ, Emson PC. Intracellular recording of identified neostriatal patch and matrix spiny cells in a slice preparation preserving cortical inputs. *J Neurophysiol*. 1989 Nov; 62(5):1052-68.
- Kawaguchi Y, Wilson CJ, Emson PC. Projection subtypes of rat neostriatal matrix cells revealed by intracellular injection of biocytin. *J Neurosci*. 1990 Oct; 10(10):3421-38.
- Kawaguchi Y, Wilson CJ, Augood SJ, Emson PC. Striatal interneurons: chemical, physiological and morphological characterization. *Trends Neurosci*. 1995 Dec;18(12):527-35. Review. Erratum in: *Trends Neurosci* 1996 Apr; 19(4):143
- Kawaguchi Y. Neostriatal cell subtypes and their functional roles. *Neurosci Res*. 1997 Jan; 27(1):1-8. Review.
- Kemp JM, Powell TP. The synaptic organization of the caudate nucleus. *Philos Trans R Soc Lond B Biol Sci*. 1971 Sep 30; 262(845):403-12.
- Kessler JA. Differential regulation of cholinergic and peptidergic development in the rat striatum in culture. *Dev Biol*. 1986 Jan; 113(1):77-89.

- Kim DS, Froelick GJ, Palmiter RD. Dopamine-dependent desensitization of dopaminergic signaling in the developing mouse striatum. *J Neurosci*. 2002 Nov 15; 22(22):9841-9.
- Kita H. Glutamatergic and GABAergic postsynaptic responses of striatal spiny neurons to intrastriatal and cortical stimulation recorded in slice preparations. *Neuroscience*. 1996 Feb; 70(4):925-40.
- Kitada T, Pisani A, Porter DR, Yamaguchi H, Tscherter A, Martella G, Bonsi P, Zhang C, Pothos EN, Shen J. Impaired dopamine release and synaptic plasticity in the striatum of PINK1-deficient mice. *Proc Natl Acad Sci U S A*. 2007 Jul 3;104(27):11441-6.
- Kitai ST, Surmeier DJ. Cholinergic and dopaminergic modulation of potassium conductances in neostriatal neurons. *Adv Neurol*. 1993; 60:40-52.
- Koós T, Tepper JM. Inhibitory control of neostriatal projection neurons by GABAergic interneurons. *Nat Neurosci*. 1999 May; 2(5):467-72.
- Koós T, Tepper JM. Dual cholinergic control of fast-spiking interneurons in the neostriatum. *J Neurosci*. 2002 Jan 15; 22(2):529-35.
- Koos T, Tepper JM, Wilson CJ. Comparison of IPSCs evoked by spiny and fast-spiking neurons in the neostriatum. *J Neurosci*. 2004 Sep 8; 24(36):7916-22.
- Kowall NW, Hantraye P, Brouillet E, Beal MF, McKee AC, Ferrante RJ. MPTP induces alpha-synuclein aggregation in the substantia nigra of baboons. *Neuroreport*. 2000 Jan 17; 11(1):211-3.
- Krysko DV, Leybaert L, Vandenabeele P, D'Herde K. Gap junctions and the propagation of cell survival and cell death signals. *Apoptosis*. 2005 May; 10(3):459-69.
- Kurz A, Double KL, Lastres-Becker I, Tozzi A, Tantucci M, Bockhart V, Bonin M, García-Arencibia M, Nuber S, Schlaudraff F, Liss B, Fernández-Ruiz J, Gerlach M, Wüllner U, Lüddens H, Calabresi P, Auburger G, Gispert S. A53T-alpha-synuclein overexpression impairs dopamine signaling and striatal synaptic plasticity in old mice. *PLoS One*. 2010 Jul 7; 5(7):e11464.
- Kravitz AV, Freeze BS, Parker PR, Kay K, Thwin MT, Deisseroth K, Kreitzer AC. Regulation of parkinsonian motor behaviours by optogenetic control of basal ganglia circuitry. *Nature*. 2010 Jul 29; 466(7306):622-6.
- Kreitzer AC. Physiology and pharmacology of striatal neurons. *Annu Rev Neurosci*. 2009; 32:127-47.
- Krushel LA, Fishell G, van der Kooy D. Pattern formation in the mammalian forebrain: striatal patch and matrix neurons intermix prior to compartment formation. *Eur J Neurosci*. 1995 Jun 1; 7(6):1210-9.
- Krysko DV, Leybaert L, Vandenabeele P, D'Herde K. Gap junctions and the propagation of cell survival and cell death signals. *Apoptosis*. 2005 May; 10(3):459-69.
- Langston JW, Langston EB, Irwin I. MPTP-induced parkinsonism in human and non-human primates--clinical and experimental aspects. *Acta Neurol Scand Suppl*. 1984; 100:49-54.
- Lapper SR, Bolam JP. Input from the frontal cortex and the parafascicular nucleus to cholinergic interneurons in the dorsal striatum of the rat. *Neuroscience*. 1992 Dec; 51(3):533-45.
- Lau WK, Lui PW, Wong CK, Chan YS, Yung KK. Differential expression of N-methyl-D-aspartate receptor subunit messenger ribonucleic acids and immunoreactivity in the rat neostriatum during postnatal development. *Neurochem Int*. 2003 Jul; 43(1):47-65.
- Levine MS, Cepeda C, André VM. Location, location, location: contrasting roles of synaptic and extrasynaptic NMDA receptors in Huntington's disease. *Neuron*. 2010 Jan 28; 65(2):145-7.

- Liu JK, Ghattas I, Liu S, Chen S, Rubenstein JL. Dlx genes encode DNA-binding proteins that are expressed in an overlapping and sequential pattern during basal ganglia differentiation. *Dev Dyn*. 1997 Dec;210(4):498-512.
- Logan SM, Partridge JG, Matta JA, Buonanno A, Vicini S. Long-lasting NMDA receptor-mediated EPSCs in mouse striatal medium spiny neurons. *J Neurophysiol*. 2007 Nov; 98(5):2693-704.
- Magill PJ, Bolam JP, Bevan MD. Dopamine regulates the impact of the cerebral cortex on the subthalamic nucleus-globus pallidus network. *Neuroscience*. 2001; 106(2):313-30.
- Mahon S, Deniau JM, Charpier S. Various synaptic activities and firing patterns in cortico-striatal and striatal neurons in vivo. *J Physiol Paris*. 2003 Jul-Nov; 97(4-6):557-66.
- Mallet N, Ballion B, Le Moine C, Gonon F. Cortical inputs and GABA interneurons imbalance projection neurons in the striatum of parkinsonian rats. *J Neurosci*. 2006 Apr 5; 26(14):3875-84.
- Marin O, Anderson SA, Rubenstein JL. Origin and molecular specification of striatal interneurons. *J Neurosci*. 2000 Aug 15; 20(16):6063-76.
- Marín O, Rubenstein JL. A long, remarkable journey: tangential migration in the telencephalon. *Nat Rev Neurosci*. 2001 Nov; 2(11):780-90.
- Marín O, Rubenstein JL. Cell migration in the forebrain. *Annu Rev Neurosci*. 2003; 26:441-83.
- Masliyah E, Rockenstein E, Veinbergs I, Mallory M, Hashimoto M, Takeda A, Sagara Y, Sisk A, Mucke L. Dopaminergic loss and inclusion body formation in alpha-synuclein mice: implications for neurodegenerative disorders. *Science*. 2000 Feb 18; 287(5456):1265-9.
- Mason HA, Rakowiecki SM, Raftopoulou M, Nery S, Huang Y, Gridley T, Fishell G. Notch signaling coordinates the patterning of striatal compartments. *Development*. 2005 Oct; 132(19):4247-58.
- Meister M, Wong RO, Baylor DA, Shatz CJ. Synchronous bursts of action potentials in ganglion cells of the developing mammalian retina. *Science*. 1991 May 17; 252(5008):939-43.
- Misgeld U, Dodt HU, Frotscher M. Late development of intrinsic excitation in the rat neostriatum: an in vitro study. *Brain Res*. 1986 Jun; 392(1-2):59-67.
- Monyer H, Burnashev N, Laurie DJ, Sakmann B, Seeburg PH. Developmental and regional expression in the rat brain and functional properties of four NMDA receptors. *Neuron*. 1994 Mar; 12(3):529-40.
- Moon Edley S, Herkenham M. Comparative development of striatal opiate receptors and dopamine revealed by autoradiography and histofluorescence. *Brain Res*. 1984 Jul 2; 305(1):27-42.
- Mori T, Yuxing Z, Takaki H, Takeuchi M, Iseki K, Hagino S, Kitanaka J, Takemura M, Misawa H, Ikawa M, Okabe M, Wanaka A. The LIM homeobox gene, L3/Lhx8, is necessary for proper development of basal forebrain cholinergic neurons. *Eur J Neurosci*. 2004 Jun; 19(12):3129-41.
- Naeff B, Schlumpf M, Lichtensteiger W. Pre- and postnatal development of high-affinity [3H]nicotine binding sites in rat brain regions: an autoradiographic study. *Brain Res Dev Brain Res*. 1992 Aug 21; 68(2):163-74.
- Nansen EA, Jokel ES, Lobo MK, Micevych PE, Ariano MA, Levine MS. Striatal ionotropic glutamate receptor ontogeny in the rat. *Dev Neurosci*. 2000; 22(4):329-40.
- Neal BS, Joyce JN. Neonatal 6-OHDA lesions differentially affect striatal D1 and D2 receptors. *Synapse*. 1992 May; 11(1):35-46.
- Nery S, Fishell G, Corbin JG. The caudal ganglionic eminence is a source of distinct cortical and subcortical cell populations. *Nat Neurosci*. 2002 Dec;5(12):1279-87.

- Nicola SM, Surmeier J, Malenka RC Dopaminergic modulation of neuronal excitability in the striatum and nucleus accumbens. *Annu Rev Neurosci.* 2000; 23:185-215.
- Nisenbaum ES, Wilson CJ. Potassium currents responsible for inward and outward rectification in rat neostriatal spiny projection neurons. *J Neurosci.* 1995 Jun; 15(6):4449-63.
- Nóbrega-Pereira S, Kessar N, Du T, Kimura S, Anderson SA, Marín O. Postmitotic Nkx2-1 controls the migration of telencephalic interneurons by direct repression of guidance receptors. *Neuron.* 2008 Sep 11; 59(5):733-45.
- Nóbrega-Pereira S, Marín O. Transcriptional control of neuronal migration in the developing mouse brain. *Cereb Cortex.* 2009 Jul; 19 Suppl 1:i107-13. Review.
- Obeso JA, Rodríguez-Oroz MC, Benitez-Temino B, Blesa FJ, Guridi J, Marin C, Rodriguez M. Functional organization of the basal ganglia: therapeutic implications for Parkinson's disease. *Mov Disord.* 2008; 23 Suppl 3:S548-59.
- Ohtani N, Goto T, Waeber C, Bhide PG. Dopamine modulates cell cycle in the lateral ganglionic eminence. *J Neurosci.* 2003 Apr 1; 23(7):2840-50.
- Olsson M, Campbell K, Victorin K, Björklund A. Projection neurons in fetal striatal transplants are predominantly derived from the lateral ganglionic eminence. *Neuroscience.* 1995 Dec; 69(4):1169-82.
- Olsson M, Björklund A, Campbell K. Early specification of striatal projection neurons and interneuronal subtypes in the lateral and medial ganglionic eminence. *Neuroscience.* 1998 Jun; 84(3):867-76.
- Onn SP, Balzer JR, Sidney JP, Stricker EM, Zigmond MJ, Berger TW. Lesions of the dopaminergic nigrostriatal system in neonatal rats: effects on the electrophysiological activity of striatal neurons recorded during adulthood. *Brain Res.* 1990 Jun 4; 518(1-2):274-8.
- Onn SP, Grace AA. Alterations in electrophysiological activity and dye coupling of striatal spiny and aspiny neurons in dopamine-denervated rat striatum recorded in vivo. *Synapse.* 1999 Jul; 33(1):1-15.
- Owens DF, Kriegstein AR. Patterns of intracellular calcium fluctuation in precursor cells of the neocortical ventricular zone. *J Neurosci.* 1998 Jul 15; 18(14):5374-88.
- Pakhotin P, Bracci E. Cholinergic interneurons control the excitatory input to the striatum. *J Neurosci.* 2007 Jan 10; 27(2):391-400.
- Pang Z, Ling GY, Gajendiran M, Xu ZC. Enhanced excitatory synaptic transmission in spiny neurons of rat striatum after unilateral dopamine denervation. *Neurosci Lett.* 2001 Aug 10; 308(3):201-5.
- Partridge JG, Tang KC, Lovinger DM. Regional and postnatal heterogeneity of activity-dependent long-term changes in synaptic efficacy in the dorsal striatum. *J Neurophysiol.* 2000 Sep; 84(3):1422-9.
- Passante L, Gaspard N, Degraeve M, Frisén J, Kullander K, De Maertelaer V, Vanderhaeghen P. Temporal regulation of ephrin/Eph signalling is required for the spatial patterning of the mammalian striatum. *Development.* 2008 Oct; 135(19):3281-90.
- Pert CB, Kuhar MJ, Snyder SH. Opiate receptor: autoradiographic localization in rat brain. *Proc Natl Acad Sci U S A.* 1976 Oct; 73(10):3729-33.
- Pezzi S, Checa N, Alberch J. The vulnerability of striatal projection neurons and interneurons to excitotoxicity is differentially regulated by dopamine during development. *Int J Dev Neurosci.* 2005 Jun; 23(4):343-9.
- Phelps PE, Barber RP, Vaughn JE. Generation patterns of four groups of cholinergic neurons in rat cervical spinal cord: a combined tritiated thymidine autoradiographic and choline acetyltransferase immunocytochemical study. *J Comp Neurol.* 1988 Jul 22; 273(4):459-72.

- Picconi B, Centonze D, Rossi S, Bernardi G, Calabresi P. Therapeutic doses of L-dopa reverse hypersensitivity of corticostriatal D2-dopamine receptors and glutamatergic overactivity in experimental parkinsonism. *Brain*. 2004 Jul; 127(Pt 7):1661-9
- Platel JC, Boisseau S, Dupuis A, Brocard J, Poupard A, Savasta M, Villaz M, Albrieux M. Na<sup>+</sup> channel-mediated Ca<sup>2+</sup> entry leads to glutamate secretion in mouse neocortical preplate. *Proc Natl Acad Sci U S A*. 2005 Dec 27; 102(52):19174-9.
- Plenz D. When inhibition goes incognito: feedback interaction between spiny projection neurons in striatal function. *Trends Neurosci*. 2003 Aug;26(8):436-43. Review.
- Plotkin JL, Wu N, Chesselet MF, Levine MS. Functional and molecular development of striatal fast-spiking GABAergic interneurons and their cortical inputs. *Eur J Neurosci*. 2005 Sep; 22(5):1097-108.
- Polymeropoulos MH, Lavedan C, Leroy E, Ide SE, Dehejia A, Dutra A, Pike B, Root H, Rubenstein J, Boyer R, Stenroos ES, Chandrasekharappa S, Athanassiadou A, Papapetropoulos T, Johnson WG, Lazzarini AM, Duvoisin RC, Di Iorio G, Golbe LI, Nussbaum RL. Mutation in the alpha-synuclein gene identified in families with Parkinson's disease. *Science*. 1997 Jun 27; 276(5321):2045-7.
- Popolo M, McCarthy DM, Bhide PG. Influence of dopamine on precursor cell proliferation and differentiation in the embryonic mouse telencephalon. *Dev Neurosci*. 2004 Mar-Aug; 26(2-4):229-44.
- Qiu M, Bulfone A, Ghattas I, Meneses JJ, Christensen L, Sharpe PT, Presley R, Pedersen RA, Rubenstein JL. Role of the Dlx homeobox genes in proximodistal patterning of the branchial arches: mutations of Dlx-1, Dlx-2, and Dlx-1 and -2 alter morphogenesis of proximal skeletal and soft tissue structures derived from the first and second arches. *Dev Biol*. 1997 May 15;185(2):165-84.
- Ramanathan S, Hanley JJ, Deniau JM, Bolam JP. Synaptic convergence of motor and somatosensory cortical afferents onto GABAergic interneurons in the rat striatum. *J Neurosci*. 2002 Sep 15; 22(18):8158-69.
- Rymar VV, Sasseville R, Luk KC, Sadikot AF. Neurogenesis and stereological morphometry of calretinin-immunoreactive GABAergic interneurons of the neostriatum. *J Comp Neurol*. 2004 Feb 9; 469(3):325-39.
- Sadikot AF, Sasseville R. Neurogenesis in the mammalian neostriatum and nucleus accumbens: parvalbumin-immunoreactive GABAergic interneurons. *J Comp Neurol*. 1997 Dec 15;389(2):193-211.
- Salin P, López IP, Kachidian P, Barroso-Chinea P, Rico AJ, Gómez-Bautista V, Coulon P, Kerkerian-Le Goff L, Lanciego JL. Changes to interneuron-driven striatal microcircuits in a rat model of Parkinson's disease. *Neurobiol Dis*. 2009 Jun; 34(3):545-52.
- Schlossmacher MG, Frosch MP, Gai WP, Medina M, Sharma N, Forno L, Ochiishi T, Shimura H, Sharon R, Hattori N, Langston JW, Mizuno Y, Hyman BT, Selkoe DJ, Kosik KS. Parkin localizes to the Lewy bodies of Parkinson disease and dementia with Lewy bodies. *Am J Pathol*. 2002 May; 160(5):1655-67.
- Semba K, Vincent SR, Fibiger HC. Different times of origin of choline acetyltransferase- and somatostatin-immunoreactive neurons in the rat striatum. *J Neurosci*. 1988 Oct; 8(10):3937-44.
- Schlossmacher MG, Frosch MP, Gai WP, Medina M, Sharma N, Forno L, Ochiishi T, Shimura H, Sharon R, Hattori N, Langston JW, Mizuno Y, Hyman BT, Selkoe DJ, Kosik KS. Parkin localizes to the Lewy bodies of Parkinson disease and dementia with Lewy bodies. *Am J Pathol*. 2002 May; 160(5):1655-67.
- Schramm NL, Egli RE, Winder DG. LTP in the mouse nucleus accumbens is developmentally regulated. *Synapse*. 2002 Sep 15; 45(4):213-9.
- Sharpe NA, Tepper JM. Postnatal development of excitatory synaptic input to the rat neostriatum: an electron microscopic study. *Neuroscience*. 1998 Jun; 84(4):1163-75.
- Shen J, Cookson MR. Mitochondria and dopamine: new insights into recessive parkinsonism. *Neuron*. 2004 Aug 5; 43(3):301-4.

- Shen W, Tian X, Day M, Ulrich S, Tkatch T, Nathanson NM, Surmeier DJ. Cholinergic modulation of Kir2 channels selectively elevates dendritic excitability in striatopallidal neurons. *Nat Neurosci.* 2007 Nov; 10(11):1458-66.
- Sheng M, Kim MJ. Postsynaptic signaling and plasticity mechanisms. *Science.* 2002 Oct 25; 298(5594):776-80.
- Shimamura K, Hartigan DJ, Martinez S, Puelles L, Rubenstein JL. Longitudinal organization of the anterior neural plate and neural tube. *Development.* 1995 Dec; 121(12):3923-33.
- Shuen JA, Chen M, Gloss B, Calakos N. *Drd1a*-tdTomato BAC transgenic mice for simultaneous visualization of medium spiny neurons in the direct and indirect pathways of the basal ganglia. *J Neurosci.* 2008 Mar 12; 28(11):2681-5.
- Silvestri L, Caputo V, Bellacchio E, Atorino L, Dallapiccola B, Valente EM, Casari G. Mitochondrial import and enzymatic activity of PINK1 mutants associated to recessive parkinsonism. *Hum Mol Genet.* 2005 Nov 15; 14(22):3477-92.
- Sipilä ST, Huttu K, Soltesz I, Voipio J, Kaila K. Depolarizing GABA acts on intrinsically bursting pyramidal neurons to drive giant depolarizing potentials in the immature hippocampus. *J Neurosci.* 2005 Jun 1; 25(22):5280-9.
- Smith Y, Kieval JZ. Anatomy of the dopamine system in the basal ganglia. *Trends Neurosci.* 2000 Oct; 23(10 Suppl):S28-33.
- Smith Y, Raju DV, Pare JF, Sidibe M. The thalamostriatal system: a highly specific network of the basal ganglia circuitry. *Trends Neurosci.* 2004 Sep; 27(9):520-7.
- Smith Y, Villalba R. Striatal and extrastriatal dopamine in the basal ganglia: an overview of its anatomical organization in normal and Parkinsonian brains. *Mov Disord.* 2008; 23 Suppl 3:S534-47.
- Snyder-Keller AM. Development of striatal compartmentalization following pre- or postnatal dopamine depletion. *J Neurosci.* 1991 Mar; 11(3):810-21.
- Söhl G, Maxeiner S, Willecke K. Expression and functions of neuronal gap junctions. *Nat Rev Neurosci.* 2005 Mar; 6(3):191-200.
- Solis O, Limón DI, Flores-Hernández J, Flores G. Alterations in dendritic morphology of the prefrontal cortical and striatum neurons in the unilateral 6-OHDA-rat model of Parkinson's disease. *Synapse.* 2007 Jun; 61(6):450-8.
- Spitzer NC. Electrical activity in early neuronal development. *Nature.* 2006 Dec 7; 444(7120):707-12.
- Standaert DG, Testa CM, Young AB, Penney JB Jr. Organization of N-methyl-D-aspartate glutamate receptor gene expression in the basal ganglia of the rat. *J Comp Neurol.* 1994 May 1; 343(1):1-16.
- Stefani A, Chen Q, Flores-Hernandez J, Jiao Y, Reiner A, Surmeier DJ. Physiological and molecular properties of AMPA/Kainate receptors expressed by striatal medium spiny neurons. *Dev Neurosci.* 1998; 20(2-3):242-52.
- Storch A, Ludolph AC, Schwarz J. Dopamine transporter: involvement in selective dopaminergic neurotoxicity and degeneration. *J Neural Transm.* 2004 Oct; 111(10-11):1267-86.
- Stühmer T, Anderson SA, Ekker M, Rubenstein JL. Ectopic expression of the *Dlx* genes induces glutamic acid decarboxylase and *Dlx* expression. *Development.* 2002 Jan; 129(1):245-52.
- Sturrock RR. A developmental study of the mouse neostriatum. *J Anat.* 1980 Mar; 130(Pt 2):243-61.
- Surmeier DJ, Song WJ, Yan Z. Coordinated expression of dopamine receptors in neostriatal medium spiny neurons. *J Neurosci.* 1996 Oct 15; 16(20):6579-91.

- Surmeier DJ, Ding J, Day M, Wang Z, Shen W. D1 and D2 dopamine-receptor modulation of striatal glutamatergic signaling in striatal medium spiny neurons. *Trends Neurosci.* 2007 May; 30(5):228-35.
- Sussel L, Marin O, Kimura S, Rubenstein JL. Loss of Nkx2.1 homeobox gene function results in a ventral to dorsal molecular respecification within the basal telencephalon: evidence for a transformation of the pallidum into the striatum. *Development.* 1999 Aug; 126(15):3359-70.
- Syed MM, Lee S, He S, Zhou ZJ. Spontaneous waves in the ventricular zone of developing mammalian retina. *J Neurophysiol.* 2004 May; 91(5):1999-2009.
- Taverna S, Ilijic E, Surmeier DJ. Recurrent collateral connections of striatal medium spiny neurons are disrupted in models of Parkinson's disease. *J Neurosci.* 2008 May 21; 28(21):5504-12.
- Tecuapetla F, Koós T, Tepper JM, Kabbani N, Yeckel MF. Differential dopaminergic modulation of neostriatal synaptic connections of striatopallidal axon collaterals. *J Neurosci.* 2009 Jul 15; 29(28):8977-90.
- Tepper JM, Bolam JP. Functional diversity and specificity of neostriatal interneurons. *Curr Opin Neurobiol.* 2004 Dec; 14(6):685-92.
- Tepper JM, Koós T, Wilson CJ. GABAergic microcircuits in the neostriatum. *Trends Neurosci.* 2004 Nov; 27(11):662-9.
- Tepper JM, Sharpe NA, Koós TZ, Trent F. Postnatal development of the rat neostriatum: electrophysiological, light- and electron-microscopic studies. *Dev Neurosci.* 1998; 20(2-3):125-45.
- Tepper JM, Trent F. In vivo studies of the postnatal development of rat neostriatal neurons. *Prog Brain Res.* 1993; 99:35-50.
- Tepper JM, Wilson CJ, Koós T. Feedforward and feedback inhibition in neostriatal GABAergic spiny neurons. *Brain Res Rev.* 2008 Aug; 58(2):272-81.
- Tisch S, Silberstein P, Limousin-Dowsey P, Jahanshahi M. The basal ganglia: anatomy, physiology, and pharmacology. *Psychiatr Clin North Am.* 2004 Dec; 27(4):757-99. Review.
- Tokuno H, Chiken S, Kametani K, Moriizumi T. Efferent projections from the striatal patch compartment: anterograde degeneration after selective ablation of neurons expressing mu-opioid receptor in rats. *Neurosci Lett.* 2002 Oct 25; 332(1):5-8.
- Torch A, Ludolph AC, Schwarz J. Dopamine transporter: involvement in selective dopaminergic neurotoxicity and degeneration. *J Neural Transm.* 2004 Oct; 111(10-11):1267-86.
- Tunstall MJ, Oorschot DE, Kean A, Wickens JR. Inhibitory interactions between spiny projection neurons in the rat striatum. *J Neurophysiol.* 2002 Sep; 88(3):1263-9.
- Tseng KY, Kasanetz F, Kargieman L, Riquelme LA, Murer MG. Cortical slow oscillatory activity is reflected in the membrane potential and spike trains of striatal neurons in rats with chronic nigrostriatal lesions. *J Neurosci.* 2001 Aug 15; 21(16):6430-9.
- Uryu K, Butler AK, Chesselet MF. Synaptogenesis and ultrastructural localization of the polysialylated neural cell adhesion molecule in the developing striatum. *J Comp Neurol.* 1999 Mar 8; 405(2):216-32.
- Valente EM, Abou-Sleiman PM, Caputo V, Muqit MM, Harvey K, Gispert S, Ali Z, Del Turco D, Bentivoglio AR, Healy DG, Albanese A, Nussbaum R, González-Maldonado R, Deller T, Salvi S, Cortelli P, Gilks WP, Latchman DS, Harvey RJ, Dallapiccola B, Auburger G, Wood NW. Hereditary early-onset Parkinson's disease caused by mutations in PINK1. *Science.* 2004 May 21; 304(5674):1158-60.
- Vandecasteele M, Deniau JM, Glowinski J, Venance L. Electrical synapses in basal ganglia. *Rev Neurosci.* 2007; 18(1):15-35.

- Van der Kooy D, Fishell G. Neuronal birthdate underlies the development of striatal compartments. *Brain Res.* 1987 Jan 13; 401(1):155-61.
- Van der Kooy D, Fishell G. Embryonic lesions of the substantia nigra prevent the patchy expression of opiate receptors, but not the segregation of patch and matrix compartment neurons, in the developing rat striatum. *Brain Res Dev Brain Res.* 1992 Mar 20; 66(1):141-5.
- Van den Munckhof P, Gilbert F, Chamberland M, Lévesque D, Drouin J. Striatal neuroadaptation and rescue of locomotor deficit by L-dopa in aphakia mice, a model of Parkinson's disease. *J Neurochem.* 2006 Jan; 96(1):160-70.
- Venance L, Glowinski J, Giaume C. Electrical and chemical transmission between striatal GABAergic output neurones in rat brain slices. *J Physiol.* 2004 Aug 15; 559(Pt 1):215-30.
- Vergara R, Rick C, Hernández-López S, Laville JA, Guzman JN, Galarraga E, Surmeier DJ, Bargas J. Spontaneous voltage oscillations in striatal projection neurons in a rat corticostriatal slice. *J Physiol.* 2003 Nov 15; 553(Pt 1):169-82.
- Vila M, Przedborski S. Genetic clues to the pathogenesis of Parkinson's disease. *Nat Med.* 2004 Jul; 10 Suppl: S58-62.
- Vinay L, Brocard F, Clarac F, Norreel JC, Pearlstein E, Pflieger JF. Development of posture and locomotion: an interplay of endogenously generated activities and neurotrophic actions by descending pathways. *Brain Res Brain Res Rev.* 2002 Oct; 40(1-3):118-29.
- Wenzel A, Fritschy JM, Mohler H, Benke D. NMDA receptor heterogeneity during postnatal development of the rat brain: differential expression of the NR2A, NR2B, and NR2C subunit proteins. *J Neurochem.* 1997 Feb; 68(2):469-78.
- Wichterle H, Garcia-Verdugo JM, Herrera DG, Alvarez-Buylla A. Young neurons from medial ganglionic eminence disperse in adult and embryonic brain. *Nat Neurosci.* 1999 May; 2(5):461-6.
- Wilson CJ. GABAergic inhibition in the neostriatum. *Prog Brain Res.* 2007; 160:91-110. Review.
- Wilson CJ, Groves PM. Fine structure and synaptic connections of the common spiny neuron of the rat neostriatum: a study employing intracellular inject of horseradish peroxidase. *J Comp Neurol.* 1980 Dec 1; 194(3):599-615.
- Wilson CJ, Groves PM, Kitai ST, Linder JC. Three-dimensional structure of dendritic spines in the rat neostriatum. *J Neurosci.* 1983 Feb; 3(2):383-8.
- Wilson CJ, Kawaguchi Y. The origins of two-state spontaneous membrane potential fluctuations of neostriatal spiny neurons. *J Neurosci.* 1996 Apr 1; 16(7):2397-410.
- Winzer-Serhan UH, Chen Y, Leslie FM. Expression of opioid peptides and receptors in striatum and substantia nigra during rat brain development. *J Chem Neuroanat.* 2003 Aug; 26(1):17-36.
- Wüllner U, Standaert DG, Testa CM, Penney JB, Young AB. Differential expression of kainate receptors in the basal ganglia of the developing and adult rat brain. *Brain Res.* 1997 Sep 12; 768 (1-2):215-23.
- Yan Z, Song WJ, Surmeier J. D2 dopamine receptors reduce N-type Ca<sup>2+</sup> currents in rat neostriatal cholinergic interneurons through a membrane-delimited, protein-kinase-C-insensitive pathway. *J Neurophysiol.* 1997 Feb; 77(2):1003-15.
- Yin HH, Knowlton BJ. The role of the basal ganglia in habit formation. *Nat Rev Neurosci.* 2006 Jun; 7(6):464-76.
- Zhang L, Warren RA. Postnatal development of excitatory postsynaptic currents in nucleus accumbens medium spiny neurons. *Neuroscience.* 2008 Jul 17; 154(4):1440-9.

Zhao Y, Marín O, Hermes E, Powell A, Flames N, Palkovits M, Rubenstein JL, Westphal H. The LIM-homeobox gene Lhx8 is required for the development of many cholinergic neurons in the mouse forebrain. *Proc Natl Acad Sci U S A*. 2003 Jul 22; 100(15):9005-10.

Zhou FM, Wilson CJ, Dani JA. Cholinergic interneuron characteristics and nicotinic properties in the striatum. *J Neurobiol*. 2002 Dec; 53(4):590-605.

Zhu Y, Li H, Zhou L, Wu JY, Rao Y. Cellular and molecular guidance of GABAergic neuronal migration from an extracortical origin to the neocortex. *Neuron*. 1999 Jul; 23(3):473-85.